

Dissertation der Fakultät für Biologie
der Ludwig-Maximilians-Universität München

Cysteine protease inhibitors as novel therapeutics for the
prevention of primary graft dysfunction after lung
transplantation



Salome Raffaella Tosca Sofia Rehm

aus

München

2019

Dissertation eingereicht am	08.08.2019
1. Gutachter:	Prof. Dr. Elisabeth Weiß
2. Gutachter:	PD. Dr. Joseph Mautner
Mündliche Prüfung am	20.01.2020

„Nothing in life is to be feared, it is only to be understood.

Now it's the time to understand more, so that we fear less“

Marie Curie

Table of contents

Summary	1
1. Introduction	3
1.1 General introduction	3
1.1.1 Lung transplantation	3
1.1.2 Ischemia-reperfusion injury and primary graft dysfunction	3
1.1.3 <i>Ex vivo</i> lung perfusion	6
1.1.4 Cysteine proteases	6
1.2 CysC-Alb in LTx – Introduction	12
1.2.1 Albumin	12
1.2.2 FcRn-mediated recycling pathway	12
1.2.3 Albumin therapeutics	14
1.2.4 Cystatin C – endogenous inhibitor of cysteine proteases	14
1.3 CatC inhibition in LTx – Introduction	16
1.3.1 Neutrophil granulocytes	16
1.3.2 Neutrophil serine proteases	17
1.3.3 Serine protease biosynthesis	17
1.3.4 Pathophysiological function of NSPs	18
1.3.5 Role of neutrophils in I/R injury	19
1.3.6 CatC – a therapeutic target	19
1.3.7 ICatC – a potent nitrile CatC inhibitor	20
1.4 Objectives of this dissertation	21
2. Materials and methods	24
2.1 List of materials	24
2.1.1 Chemicals and Consumables	24

2.1.2 Laboratory equipment	24
2.1.3 Oligonucleotides	26
2.1.4 Plasmids	27
2.1.5 <i>E.coli</i> bacterial strains	27
2.1.6 Recombinant and purified proteins.....	27
2.1.7 Antibodies	28
2.1.8 Förster/Fluorescence resonance energy transfer (FRET) substrates	29
2.2 Molecular biological methods	29
2.2.1 Polymerase chain reaction (PCR)	29
2.2.2 Restriction enzyme digest	30
2.2.3 Agarose gel electrophoresis	31
2.2.4 DNA purification.....	31
2.2.5 Determination of DNA concentration	32
2.2.6 Vector dephosphorylation	32
2.2.7 DNA Ligation.....	32
2.2.8 Preparation of CaCl ₂ -competent bacteria.....	32
2.2.9 Transformation of CaCl ₂ -competent bacteria.....	33
2.2.10 Plasmid DNA purification from bacteria	34
2.2.11 DNA Sequencing.....	34
2.3 Recombinant protein expression	34
2.3.1 HEK cell transfection	34
2.4 Protein analysis.....	35
2.4.1 Purification of recombinant proteins by nickel-affinity chromatography.....	35
2.4.2 Purification of recombinant protein by HiTrap TM Blue HP affinity chromatography	36
2.4.3 Determination of protein concentration	36
2.4.4 Sodium dodecyl sulfate - polyacrylamide gel electrophoresis (SDS-PAGE).....	37

2.4.5 Protein detection	38
2.4.6 Enzymatic activity measurement.....	39
2.5 Mouse model analysis	41
2.5.1 Mouse strains.....	41
2.5.2 Study approval	41
2.5.3 Orthotopic lung transplantation model.....	41
2.5.4 <i>Ex vivo</i> lung perfusion (EVLP)	42
2.5.5 Allograft tissue sample collection (blood gas, bronchoalveolar lavage)	44
2.5.6 Isolation of polymorphonuclear neutrophils (PMNs) from the bone marrow	44
2.5.7 Preparation lung lysates for western blot analysis.....	45
2.5.8 Lung tissue preparation for staining of lung sections.....	45
2.6 Cell biological methods.....	46
2.6.1 Cell lines	46
2.6.2 Culturing of HEK 293 EBNA1 and RAW264.7 cells	46
2.6.3 Determination of cell count and viability	46
2.6.4 Live cell imaging of RAW264.7 cells.....	47
2.6.5 <i>In vitro</i> model of cold ischemia and simulated EVLP/Reperfusion	47
2.6.6 Apoptosis.....	48
2.6.7 Cell viability	48
2.6.8 Preparation of total cell lysates	48
2.7 Immunological methods.....	49
2.7.1 Immunoblotting	49
2.7.2 Enzyme-linked immunosorbent assay (ELISA)	50
2.7.3 Immunological staining of lung tissue	51
2.7.4 RNA analysis	54
2.8 Microscopy.....	54

2.9 Statistics	54
3. Results	55
3.1 CysC-Alb in LTx - Results	55
3.1.1 Cloning of the fusion protein CysC-Alb	55
3.1.2 Production of CysC-Alb and Alb in HEK 293E cells	55
3.1.3 Production of further CysC variants.....	57
3.1.4 Functional analysis of CysC-Alb.....	58
3.1.5 CysC-Alb graft preservation in a murine model of LTx	64
3.1.6 In vitro model of CS and simulated EVLP/Reperfusion	71
3.2 CatC inhibition in LTx - Results.....	79
3.2.1 CatC inhibition leads to reduced NSP activity in the bone marrow	79
3.2.2 ICatC pretreatment improves PGD and reduces the inflammatory response.....	81
3.2.3 Presence of NSP positive neutrophils in the lung	84
4. Discussion	87
4.1 CysC-Alb in LTx – Discussion	87
4.1.1 Development of a highly potent cysteine protease inhibitor	87
4.1.2 Effect of CysC-Alb on lung graft quality	89
4.1.3 CysC-Alb protects lung cells from CatB mediated damage.....	91
4.1.4 CatB is involved in the regulation of TACE.....	92
4.1.5 Limitations.....	94
4.2 CatC inhibition in LTx - Discussion	97
4.2.1 Effects of eliminated NSP activity on LTx outcome	97
4.2.2 CatC inhibition severely reduces NSP activity in the BM and lung.....	98
4.2.3 Clinical potential of our translational approach	100
4.2.4 Limitations.....	101
5. Reference list	103

6. Abbreviations.....	119
7. Appendix.....	123
7.1 Vector map	123
7.2 Sequences of expressed proteins	124
7.2.1 pTT5-Alb	124
7.2.2 pTT5-CysC-Alb	126
7.2.3 pTT5-CysC-Alb-Ruby.....	128
7.2.4 pTT5-CysC-Ruby	131
8. Publications and international meetings	133
8.1 Publications.....	133
8.2 Presentations at international conferences	134
8.2.1 Oral presentations	134
8.2.2 Poster presentation	134
9. Curriculum vitae	135
10. Acknowledgement.....	136

Summary

Lung transplantation (LTx) is lifesaving for patients with end-stage pulmonary diseases, when other therapeutic strategies have failed. Unfortunately, the mortality rate of patients on the LTx waiting list is quite high due to the low percentage of acceptable donor lungs. Additionally, LTx outcomes are harmed by the development of primary graft dysfunction (PGD) which is the leading cause for early mortality and morbidity. No effective treatment approach exists to date. Cysteine proteases play a substantial role in the complex biological pathways which are activated during cold storage and reperfusion of the transplant and thereby they contribute directly or indirectly to the early damage of lung transplants. In order to explore novel treatment options to prevent early lung transplant damage and dysfunction we used a clinical relevant murine model of orthotropic LTx to mimic the induction of ischemia reperfusion injury after extended graft storage in the cold.

In the first project we developed a highly cell permeable, cysteine protease inhibitor, termed CysC-Alb, with increased circulatory half-life. This inhibitor was designed and produced to improve the storage condition of donor lungs adding CysC-Alb to the preservation solution during cold storage and *ex vivo* lung perfusion (EVLP), which could allow extended storage and better preservation. We found that ischemic storage times of lung transplants can be extended to 18 h with improved transplant function after transplantation when CysC-Alb is added to the preservation solution. Moreover, TNF- α release and apoptosis of lung cells were reduced after the preservation time in the CysC-Alb group. Using an *in vitro* model of cold storage and simulated EVLP/Reperfusion, we recognized that not only the activity of cathepsin B (CatB), but also the activity of TNF- α

converting enzyme (TACE), one of the main TNF- α sheddases, are significantly lower after CysC-Alb treatment. This suggests that CatB is involved in the regulation of TACE either during maturation steps or on the cell surface.

In the second project, we anticipated that patients on the LTx waiting list can be protected from neutrophil mediated inflammation and damage of the lung transplant after LTx through the preoperative treatment with a cathepsin C inhibitor (ICatC). Neutrophil serine proteases (NSPs) are main triggers of ischemia reperfusion injury after transplantation. The cysteine protease, cathepsin C acts as the key activator of NSPs during neutrophil maturation in the bone marrow. Pretreatment of recipient mice with ICatC significantly reduced serine protease activity in bone marrow neutrophils, diminished the inflammatory response and improved gas exchange after lung LTx compared to the control group. We conclude that the elimination of NSP activity by the pretreatment with ICatC reduces the early reperfusion-induced injury of transplanted lungs, which makes it a promising new therapeutic strategy to prevent PGD.

1. Introduction

1.1 General introduction

1.1.1 Lung transplantation

Lung transplantation (LTx) is the final treatment option for patients suffering from end-stage pulmonary disease, like chronic obstructive pulmonary disease (COPD, 32%), idiopathic pulmonary fibrosis (IPF, 24%) or cystic fibrosis (17%) (1). The total number of lung transplantations performed worldwide is approximately 4000 per year with a majority of bilateral transplantations and is still increasing every year. Despite significant improvements, the long-term outcome of LTx remains uncertain with a 5 year survival of 53%, and for this reason has the worst short and long term prognosis amongst all organ transplantations (2). Development of primary graft dysfunction (PGD) is the leading cause of early morbidity and mortality after LTx, resulting in a one year survival of approximately 80 %. It is a consequence of ischemia reperfusion-injury, and occurs within the first 72 hours after reperfusion (3-5).

1.1.2 Ischemia-reperfusion injury and primary graft dysfunction

Ischemia is defined as a deficiency of oxygen caused by the restriction of the blood flow (6). During reperfusion, the blood supply returns to the ischemic tissue, which may induce and exacerbate tissue injury as a consequence of the absence of oxygen and nutrients during ischemia. This process is termed ischemia-reperfusion (I/R) injury, and is associated with increased permeability of capillaries, cell death programs, activation of the complement system, cytokine release and neutrophil recruitment (7-10). Moreover, it is identified as the key element of PGD, affecting an estimated 10 to 25 % of lung

transplants (6). Patients who survive after PGD have an impaired lung function and an increased chance of developing bronchiolitis obliterans syndrome (BOS), the manifestation of chronic lung rejection (11).

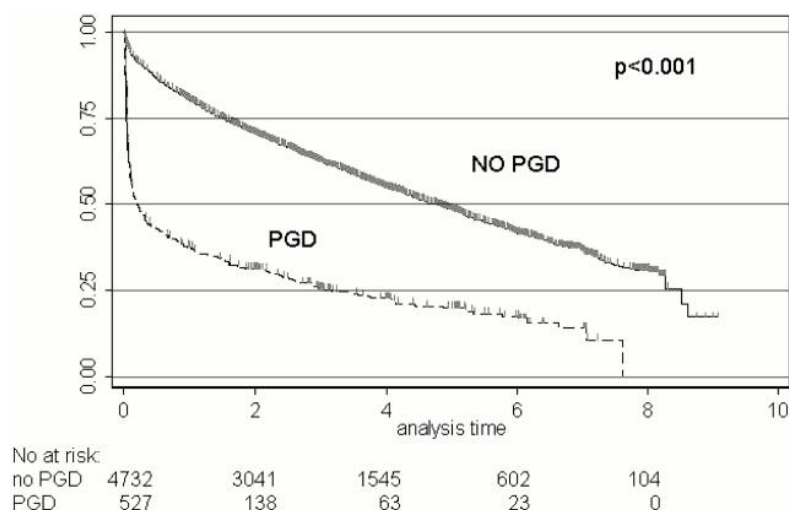


Figure 1: Effect of primary graft dysfunction on the survival after LTx. Overall survival of LTx patients with and without PGD. Analysis time is years. The number at risk appears along the x-axis. The log-rank p-value for the comparison of PGD and no PGD is $p < 0.001$. From the American Thoracic Society (3).

1.1.2.1 Cold ischemia

One of the most common accepted methods utilized for the storage of organs prior to transplantation is hypothermic storage. Under this condition, the organ is kept at temperatures below physiological temperatures to suppress organ metabolism (12, 13). Lung transplants are generally considered acceptable for transplantation after static storage at 4°C for up to six hours. This method involves whole organ perfusion with the standard preservation solution, Perfadex. Although hypothermic storage protects the organ for some time, several events can occur, leading to the activation of inflammatory mediators that are highly deleterious to the organ during reperfusion. Briefly, during the course of cold storage (CS) metabolic rates of individual cells are slowed down,

intracellular ATP levels steadily decline, and ATPase dependent- transmembrane ion pumps show low activity. Consequently, intracellular and mitochondrial calcium levels increase, triggering cell swelling and cell death by necrotic, necroptotic, apoptotic, and autophagic mechanisms (14, 15). This process is also associated with the formation of reactive oxygen species (ROS) and lipid peroxidation (16). Prolonged storage times are correlated with a higher risk of vascular damage and PGD.

1.1.2.2 Consequences of reperfusion

Although oxygen is restored after ischemia, reperfusion itself has detrimental consequences exacerbating tissue injury. It was first reported in the 1960s that the predicted beneficial effect of reperfusion is challenged by a paradoxical enhancement of the injury response following reperfusion of ischemic tissue (17). The mechanism underlying reperfusion injury is complex and involves upregulation of adhesion molecules (e.g. integrins) on the cell surface, release of pro-inflammatory cytokines and leukocyte activation. Pulmonary intravascular non-classical monocytes (passenger monocytes) from the donor (early phase of reperfusion) and macrophages that are carried to the lung with the newly restored blood flow (later phase of reperfusion) release inflammatory cytokines, which are pivotal for the further recruitment of recipient neutrophils and leukocytes into the lung. Activated neutrophils locally secrete a wide range of pro-inflammatory mediators, ROS and proteolytic enzymes (18-20), irreversibly damaging lung tissue. Clear evidence of the involvement of neutrophils has been revealed in preclinical and clinical studies in which neutrophil depletion was protective against I/R injury (21-23). In a more recent approach, neutrophil influx was attenuated, when non-classical monocytes were depleted in murine donor lung transplants (24).

Thus, neutrophils play a major role in I/R injury after reperfusion, representing a potentially important therapeutic target for reducing PGD.

1.1.3 *Ex vivo* lung perfusion

Donor lung shortage has been the main reason for the increasing mortality of patients on the waiting list. Donor lungs are often rejected for transplantation since they are exposed to various stress and injury before and during brain death such as thoracic trauma, ventilator-associated pneumonia and barotrauma. Nevertheless, about 40% of these lungs can be considered appropriate for transplantation (25). In the last decade, *ex vivo* lung perfusion (EVLP) was shown to safely increase the donor lung pool. During EVLP, donor lungs are ventilated and held at body temperature (37 °C), which keeps the lungs viable and metabolic active. During this time period, lungs can be examined, reassessed and reconditioned by treatment in the normothermic state (26). The results from the first prospective clinical trial in 2011 have shown that EVLP is able to reconstitute donor lungs with inferior quality so that the LTx outcome (PGD development) is similar to standard criteria donor lungs (27). To date, three different protocols for the EVLP procedure exist, with the Toronto protocol being the most commonly used protocol. In principle, the lung undergoes a cold perfusion before it is harvested and is transported to the recipient hospital in static cold storage on ice. The lung is then connected to the *ex vivo* device and assessed.

1.1.4 Cysteine proteases

Proteases are peptide bond-cleaving enzymes. This large family of proteolytic enzymes can be further grouped according to 1) the position of the cleavage site in the polypeptide chain of the substrate (exopeptidases and endopeptidases), 2) which

terminus of the substrate is involved in the cleavage (aminopeptidase and carboxypeptidase), and 3) according to the active site region residues (aspartate, metallo, serine, cysteine proteases). Cysteine proteases are either exo- or endopeptidases, which use the cysteine residue in the active site for hydrolysis.

1.1.4.1 Structure and occurrence of cysteine proteases

Cysteine proteases are distributed among most of the living organisms, from bacteria and viruses to fungi and mammals (28). The most intensively investigated and largest family of cysteine proteases is the superfamily of papain-like cysteine proteases, which comprise calpains and lysosomal cathepsins in mammals (29). Lysosomal cathepsins share a high sequence similarity with papain, a plant protease isolated from a papaya, which is the prototype for all cysteine proteases. The highest sequence similarity of all cathepsins is found in active site which is formed by cysteine (Cys-25), histidine (His-159) and asparagine (Asn-157) residues. All cathepsins are synthesized as inactive precursor enzymes with a 15-21 residue long signal peptide, a propeptide domain consisting 41 and 251 amino acid residues, and a mature domain of 214 to 260 amino acids. The propeptide domain prevents premature proteolysis until it is cleaved by other enzymes or self-processing (30). In addition, lysosomal cathepsins possess putative *N*-linked mannose-6-phosphate glycosylation sites that are used to target proteases into lysosomes. For many years these enzymes were believed to have redundant “house-keeping functions” and as such have not been considered to have any value as drug target. However, over the past decades large progress was made in identifying new members and understanding the physiological roles of cathepsins. It has become clear that cathepsins have a multi-faceted role in several physiological processes including

extracellular matrix remodeling, antigen presentation and processing events (31). As such they are also involved in many pathological conditions and represent promising drug targets for cancer (32), arthritis, osteoporosis (33), Alzheimer's disease and a variety of parasitic infections (34) .

1.1.4.2 Protease nomenclature

The specificity of proteases is determined by the amino acid sequence of substrates cleaved by the protease. To guarantee successful substrate cleavage, a close interaction between the substrate sequence that is cleaved (scissile bond) and the active site cleft of the protease is necessary. Schechter and Berger introduced a nomenclature to describe the interaction of a protease and its substrate (35). All protease subsites and substrate residues are numbered and named with regard to the location of the scissile bond. Consequently, the N-terminal substrate residues of the scissile bond are referred to as P₃, P₂, P₁ etc. and the residues on the C-terminal side P₁', P₂', P₃' etc. Accordingly, the protease subsites that interact with the substrate residues are called S₃, S₂, S₁ etc. on the N-terminal side and S₁', S₂', S₃' etc. on the C-terminal side. The scissile bond is located between P₁ and P₁' as indicated in Figure 2.

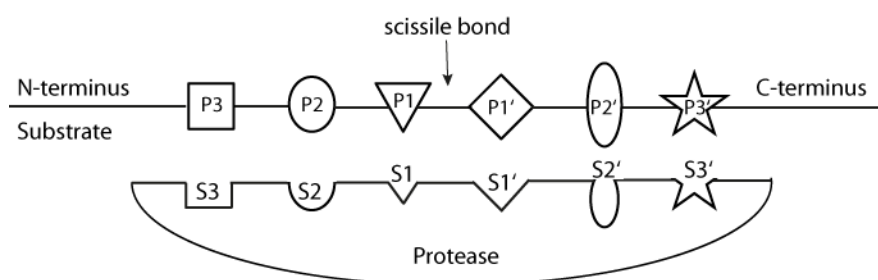


Figure 2: Schechter and Berger nomenclature. Protease subsites are designed as S₁, S₂, S₃, S₁', S₂' and S₃' and the amino acid residues of the substrate are named P₁, P₂, P₃, P₁', P₂' and P₃' respectively. Cleavage of the substrate occurs at the scissile bond between P₁ and P₁'.

1.1.4.3 Cysteine protease hydrolysis

Cysteine proteases catalyze peptide bond hydrolysis through nucleophilic reaction of the cysteine thiol with the substrate carbon carbonyl. The first step of the reaction involves formation of a non-covalent enzyme-substrate complex. Once this complex is formed and stabilized with hydrogen bonds, the negative charged SH group of the cysteine thiol enables a nucleophilic attack on the scissile bond of the substrate carbonyl carbon, producing the first tetrahedral intermediate. This intermediate is generally stabilized by hydrogen bonding through the interaction with the oxyanion hole in the active site. Acylation of the enzyme occurs through the protonation of the amine group under the release of the first product. This step is followed by the hydrolysis of the acyl-enzyme complex of the carbon carbonyl by a water molecule (deacylation), forming the second tetrahedral intermediate, which finally dissociates into the cleaved substrate and the active enzyme (Figure 3).

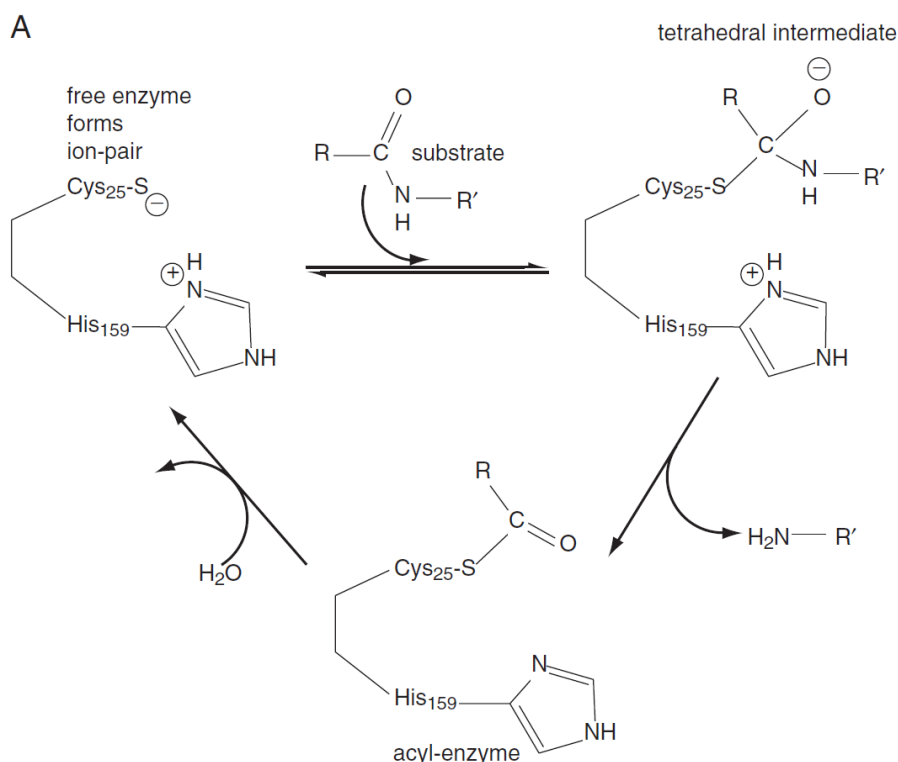


Figure 3: Mechanism of hydrolysis by cysteine proteases. The thiol group of the cysteine protease attacks the carbon carbonyl of the substrate and forms the tetrahedral intermediate which resolves in an acyl-enzyme complex with the release of the first product. The active enzyme is then regenerated through the nucleophilic attack of a water molecule (30).

1.1.4.4 Inhibitors of cysteine proteases

For many types of proteases, activity is regulated by the balance of the amounts of active proteases and inhibitors. Active site directed inhibitors can be divided into covalent/non-covalent and reversible/irreversible inhibitors. Irreversible inhibition always includes covalent binding of the inhibitor; whereas reversible inhibition mostly involves non-covalent binding, but not in all cases. The most abundant family of endogenous cysteine protease inhibitors are cystatins: the intracellular cystatin A and B are commonly called stefin A and B; the circulating kininogens; and the extracellular cystatin C (36, 37). All of them are low molecular weight peptide inhibitors, which bind tight and almost

irreversibly by interacting on multiple sites with the active cysteine protease. Synthetic cysteine protease inhibitors can be either low or high molecular weight inhibitors and typically display common structural similarities. They include an at least two amino-acid peptide sequence to achieve high protease affinity and substitutable electrophilic groups to irreversibly react with the cysteine residue of the active site. Many different synthetic inhibitors have been developed, which can be classified into peptidyl nitriles and aldehydes, epoxides, aziridines and many more (28).

1.2 CysC-Alb in LTx – Introduction

1.2.1 Albumin

Alb is the most abundant plasma protein in the body with a size of 67 kDa (41). It consists of three homologous domains, which function together to give Alb its unique binding properties. Hence, Alb transports a lot of endogenous and exogenous compounds, such as fatty acids, steroids and ions. Additionally, it is responsible for the stabilization of the colloidal osmotic pressure and plays a major role in pH buffering of serum (42). It is predominately synthesized by hepatocytes in the liver, from which it is continuously secreted, and degraded at a rate of 14 g per day (43). The circulatory half-life of Alb is 21 days in humans (mice), and is strongly dependent on the interaction with the cellular expressed neonatal Fc receptor (FcRn). The FcRn-mediated recycling mechanism protects Alb from lysosomal degradation and thereby increases its serum half-life. This feature is unique for Alb and IgG, which both bind to distinct and non-interactive binding sites of FcRn in a strictly pH-dependent manner, with binding at acidic pH (pH 6) and release or no binding at neutral pH (7,4) (44). The FcRn is a heterotrimeric receptor, comprising of a major histocompatibility class I (MHC-I) heavy α -chain and a non-covalent associated β -microglobulin light chain (45). It was shown, that domain III of Alb is required for binding to the neonatal Fc receptor (FcRn), as well as three conserved histidine residues (H464, H510 and H535), which become positively charged at acidic pH (46).

1.2.2 FcRn-mediated recycling pathway

The pH dependence of the interaction is crucial for the FcRn-mediated rescue of its ligands from lysosomal degradation. Initially, extracellular Alb is pinocytosed at neutral

pH. Upon acidification of the early endosome Alb binds to the FcRn membrane protein, which results into the recycling of Alb back to the cell surface where FcRn-bound Alb is exposed due to neutral pH of the plasma. In contrast, non FcRn-bound proteins are sorted to late endosomes and subsequently to lysosomes where they are degraded (44, 47, 48). The FcRn-mediated recycling mechanism exists in almost all cell-types.

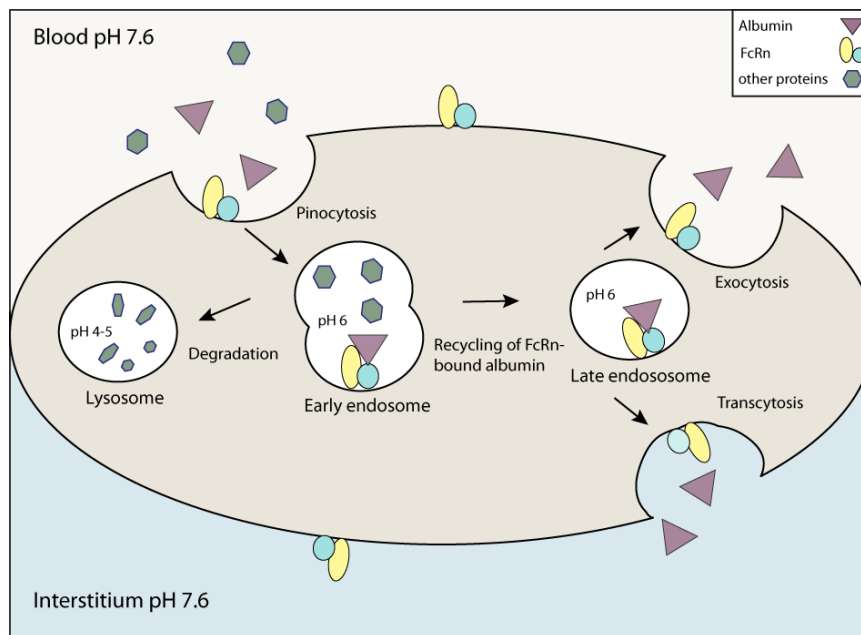


Figure 4: The FcRn-mediated recycling mechanism. Schematic representation for FcRn-mediated albumin recycling using an endothelial cell as example. Upon pinocytosis, albumin binds to membrane-bound FcRn at the slightly acidic pH (~ pH 6) of the endosome. Other non FcRn-bound proteins are sorted to lysosomes for degradation. The FcRn-albumin complex is either recycled back to the apical membrane (exocytosis) or from the apical to the basolateral membrane (transcytosis), where albumin is released due to the weak affinity to FcRn at neutral pH (pH 7.6).

1.2.3 Albumin therapeutics

The therapeutic efficiency of small drug molecules, especially biopharmaceuticals is hampered by their short half-life as they are rapidly cleared by the kidney or liver due to their low molecular mass. Consequently, strategies to extend serum half-life of pharmaceuticals have been extensively explored. Attachment of pharmaceuticals to Alb to increase their size in order to prevent kidney clearance and using its FcRn-mediated recycling mechanism has been shown to be a promising purpose. Various molecules have been joined to Alb either non-covalently or covalently by conjugation or genetic fusion primarily to treat diabetes, cancer, rheumatic arthritis and infectious disease (49-53). Beside its unique recycling mechanism, there are several other advantages of Alb as a drug carrier: 1) as an endogenous protein it is native to the body; 2) it is stable over a wide pH range, therefore unaltered by denaturing agents and solvents at moderate concentrations (41); 3) it is readily available as it is the most abundant plasma protein.

1.2.4 Cystatin C – endogenous inhibitor of cysteine proteases

Cystatin C (CysC) is a member of the cystatin superfamily of cysteine protease inhibitors. It is considered to be the physiologically most important endogenous inhibitor of cysteine cathepsins from the papain family, such as CatB, CatL, CatS and CatH, as well as the asparaginyl endopeptidase legumain (54). Physiologically, the role of CysC is the protection of the organism from extracellular proteases released or leaked from lysosomes e.g. from damaged or tumor cells. CysC is a single-domain protein with a signal peptide, hence being secreted and therefore be found extracellular. It is expressed in all nucleated cells and secreted at a constant rate. Due to its small size of 13 kDa and basic pI (~9.0), it is quickly filtered by the glomerulus (55). The interaction of CysC and chicken

papain as an example for CysC-protease inhibition has been intensively investigated. Three regions of the CysC 122-amino acid polypeptide chain have been implicated in the formation of the reversible enzyme-inhibitor complex. The most critical region for the tight enzyme-binding property of CysC is the N-terminal tri-peptide sequence L⁹-V¹⁰-G¹¹ which interacts with the cysteine protease pockets S³ S² S¹ respectively. Hereby, it was shown that L⁹ is the discriminating residue for binding to CatS, CatB and CatL. Together with the two other regions, the evolutionary conserved Q⁵⁵-I-V-A-G⁵⁹ and the C-terminal P₁₀₅-W¹⁰⁶, they form a wedge-shaped structure occluding the protease substrate-binding sites, thus inhibiting them (56).

1.3 CatC inhibition in LTx – Introduction

1.3.1 Neutrophil granulocytes

Neutrophil granulocytes are derived from myeloid cells and account for 40-70% of circulating leukocytes in the blood. They are named according to their high content of dense packed granules in the cytoplasm. One of their unique characteristics is the segmented nucleus, for which they are also called polymorphonuclear cells (PMNs). Neutrophil granulocytes, in the following just called neutrophils are among the first cells to be recruited to sites of inflammation. Neutrophils reach the inflammatory site via the blood and transmigrate through the endothelial wall into the tissue via a multistep process, which involves rolling, adhesion, firm attachment and diapedesis (97). The primary function of neutrophils at the inflammatory site is host defense with the help of their antimicrobial cocktail that includes oxidants, proteases and cationic peptides. These microbial compounds are stored in three different classes of granules: primary (azurophilic), secondary (specific) and tertiary (gelatinase) granules. They are formed sequentially during different stages of granulocyte development in the BM and therefore differ in their contents (98).

Pathogens are phagocytosed by neutrophils and the resulting phagosomes fuse with neutrophil cytoplasmatic granules to form phagolysosomes. Engulfed pathogens can be destroyed in several ways, e.g. by the production of ROS, antimicrobial proteins from the lysosomes or proteases like neutrophil serine proteases (NSPs) (99). Furthermore, neutrophil activation can lead to the formation of extracellular traps (NETs), a network of extracellular DNA fibers, which are decorated with antimicrobial enzymes and peptides in order to kill pathogens (100). Under pathological conditions, antimicrobial compounds

are released in an uncontrolled way into the extracellular space where they paradoxically can damage host tissue.

1.3.2 Neutrophil serine proteases

The NSPs, neutrophil elastase (NE), cathepsin G (CatG), proteinase 3 (PR3) and the recently discovered neutrophil serine protease 4 (NSP4) belong to the trypsin/chymotrypsin proteases and are stored in azurophilic granules. They acquire catalytic activity at the neutral pH of phagolysosomes (101, 102). The genes for NE (ELA2, ELANE) and PR3 (PRTN3) and NSP4 form a tight linked cluster on chromosome 19 in humans and on chromosome 10 in mice. By contrast, the gene encoding CatG is located within a separate cluster on syntenic regions of human and mouse chromosome 14, containing also the genes for chymase, granzyme H and granzyme B (103). All human and mouse NSPs contain an active center with the catalytic triad His⁵⁷, Asp¹⁰² and Ser¹⁹⁵ (104). Besides their proteolytic properties, evidence indicates that NSPs play an important role in inflammation (102, 105).

1.3.3 Serine protease biosynthesis

NSPs are synthesized as inactive precursor (zymogens) during the promyelocytic stage of neutrophils in the BM. After cleavage of the two N-terminal amino-residues by dipeptidylpeptidase I (DPPI) also known as cathepsin C (CatC), NSPs are in their enzymatically active conformation (106-108). The now accessible Ile¹⁶ is able to interact with Asp¹⁹⁴, which results in a conformational change unveiling the active site. Mature NSPs are stored in azurophilic granules of neutrophils until their regulated secretion in response to several stimuli.

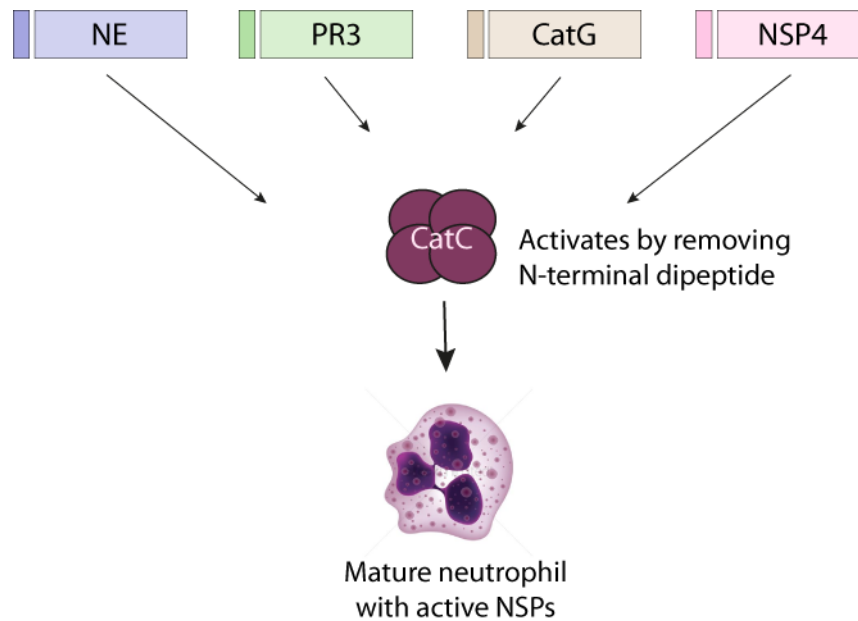


Figure 5: Neutrophil serine protease maturation. CatC plays a key role in the activation of the NSPs, CatG, PR3 and NE in the BM. Active NSPs are stored in azurophile granules in neutrophils. Adapted from (109).

1.3.4 Pathophysiological function of NSPs

NSPs are important modulators of the innate immunity; however, uncontrolled neutrophil activation and subsequent NSP release participate in the pathogenesis of inflammatory diseases. Examples are autoimmune disorders and chronic inflammatory diseases like granulomatosis with polyangiitis, lupus nephritis, cystic fibrosis and lung emphysema (110, 111). The disruption of the balance between proteases and their inhibitors is a major feature of these diseases. Hence, a tight regulation of NSP activity is necessary to maintain a healthy homeostasis. Under physiological conditions, NE and PR3 activities are antagonized by AAT, elafin, monocyte neutrophil elastase inhibitor, secretory leucocyte protease inhibitor and α 2-macroglobulin. CG is inactivated by monocyte neutrophil elastase inhibitor, secretory leucocyte protease inhibitor, AAT and

additionally anti-chymotrypsin (112). Based on their highly important role in inflammatory processes, NSPs represent an attractive therapeutic target.

1.3.5 Role of neutrophils in I/R injury

Neutrophils are known to play a major role in the development of I/R injury after organ transplantation. During reperfusion, neutrophils are the primary effector cells recruited to the allograft by the neutrophil chemoattractants IL-8 and CXCL2 (113, 114). Upon arrival in the tissue, neutrophils secrete toxic free radicals and NSPs that can irreversibly damage the transplant tissue and therefore also impair tissue function. In several preclinical and clinical studies it was demonstrated that neutrophil depletion was protective against tissue damage after organ transplantation (21-23). Pharmacological targeting of NE strongly reduced inflammatory processes in a series of experimental and clinical settings, and NE inhibitors are considered for various therapeutic applications (115-118). However, the mechanisms of NSP function in this process are poorly understood. So far, it is known that NE promotes epithelial and endothelial permeability by alteration of the actin skeleton and by proteolytic cleavage of E-cadherin and endothelial VE-cadherin (119, 120). NSPs may also act through binding to cell surface receptors thereby inducing signal transduction pathways of inflammation and apoptosis in the lung (121-123). Nevertheless, through the broad spectrum of NSP actions and substrates it is hard to define their downstream mechanisms involved in the development and progression of I/R injury.

1.3.6 CatC – a therapeutic target

The cysteine protease, CatC, also known as dipeptidylpeptidase I (DPPI) belongs to the papain superfamily and acts as an N-terminal exopeptidase. As mentioned above, a key

function of CatC is the activation of NSP zymogens through the removal of their pro-peptide sequences. Homozygous loss of CatC function mutations in humans are the genetic cause of the rare Papillon-Lefevre syndrome (PLS, OMIM: 245000) primarily occurring in consanguineous families. The symptoms are quite variable, but not life-threatening (124, 125). Over the last years, CatC came into focus of attention as a therapeutic target for various NSP-driven inflammatory diseases. It was first shown in non-human primates that pharmacological inhibition of CatC results in the elimination of NSPs protein levels and activity in peripheral blood and BAL neutrophils attracted to the lung by intratracheal lipopolysaccharide (LPS) instillation (126). Two different small molecule CatC inhibitors (AZD7986 and GSK2793660) have been evaluated in a phase 1 clinical trials with healthy humans. One drug candidate (AZD7986) successfully reduced NE activity in human blood neutrophils in a dosage-dependent manner, while the other one only inhibited CatC activity, but not the downstream activities from NSPs (127, 128). Further therapeutic trials will be undertaken on the basis of these positive safety results.

1.3.7 ICatC – a potent nitrile CatC inhibitor

Several potent and selective CatC inhibitors have been described in literature (129, 130). However, most of them are associated with poor metabolic stability based on their peptidic and electrophilic nature, as well as cytotoxicity. In the last years dipeptidyl nitriles have emerged due to their strong inhibitory activity against human CatC, which show no cytotoxic effects and effectively block downstream elastase-like NSPs (131, 132). The warhead in cyclonitrile inhibitors targeting CatC is the nitrile group that binds covalently to the nucleophilic cysteine residue of the active site (133). The reversible cyclonitrile CatC inhibitor available to us ((S)-2-amino-N-((1S,2S)-1-cyano-2-(4'-(4-

methylpiperazin-1-ylsulfonyl)biphenyl-4-yl)cyclopropyl) butanamide) was first described as XPZ-01 by Unizyme Laboratories (134) and will hereinafter be referred to as ICatC. It was identified as a potent inhibitor of human and rodent CatC and was successfully used to reduce BM NSP activity which resulted in anti-arthritic activity in a mouse model of rheumatoid arthritis (134). The inhibitor (ICatC) used in this study was available to us for our mouse LTx study.

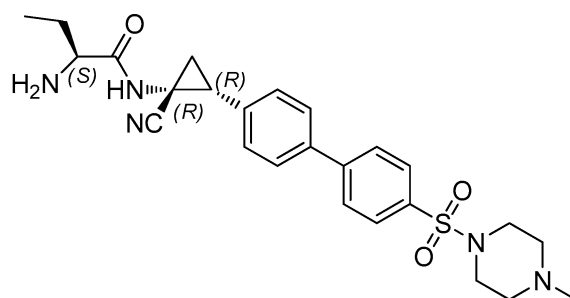


Figure 6: Chemical structure of ICatC. ICatC, (S)-2-amino-N-((1R,2R)-1-cyano-2-(4'-(4-methylpiperazin-1-ylsulfonyl)biphenyl-4-yl)cyclopropyl)butanamide was synthesized by Brice Korkmaz, Tour, France. The inhibitory potency and selectivity were determined on recombinant human CatC. $IC_{50} = 0.015 \pm 0.001$.

1.4 Objectives of this dissertation

LTx faces two major challenges; the first one is the ischemic storage of the donor organ, during which the blood and oxygen supply is disrupted. The second challenge is reperfusion, when the blood flow is restored back to the ischemic tissue. Both contribute to PGD, which has been associated with acute and chronic lung rejection. To date, no effective treatment approach exists. Therefore the objective of this dissertation was to develop new treatment options in order to prevent the immediate inflammatory response in the recipient lung after LTx and to increase the donor organ pool suitable for

transplantation. Using cysteine protease inhibitors, two different approaches were chosen:

The first pre-clinical study was conducted to reduce early tissue damage which is caused by lysosomal leakiness, cell death and lysosomal cathepsin release into the extracellular space during CS and EVLP. We hypothesized that cathepsins can be neutralized with a cysteine protease inhibitor added to the preservation solution and thereby protect lung cells and preserve lung function by preventing tissue-damage during cold graft storage and reperfusion. We further intended to increase the donor organ pool by allowing longer storage times. The endogenous inhibitor, CysC, has been shown to effectively reduce the cysteine protease pool, more specifically cathepsin S, B and L (CatS, CatB, CatL). Unfortunately the direct use of this natural low-molecular mass inhibitor has been harmed by a short half-life period and poor accessibility of the recombinant product to diseased areas. Hence, new fusion proteins consisting of Alb and CysC were developed by us to create more effective inhibitors. For proof of concept experiments, a clinical relevant lung preservation protocol was set up, including extended CS and EVLP. Perfadex was supplemented with CysC-Alb (0.4 µg/ml) for extended CS (18h) and EVLP at 37°C (2h) prior to the usage of a murine orthotropic LTx model (Figure 6 established by (39)). Using this model the anticipated enhancement of the lung function and the protection of lung cells after adding CysC-Alb to Perfadex was investigated. To assess possible mechanisms of lysosomal cathepsin mediated tissue damage after CS and EVLP more in detail, an *in vitro* model of cold ischemia and simulated EVLP/Reperfusion was developed.

In the second part of this dissertation, we considered the use of CatC inhibitors for the pre-operative treatment of patients on the waiting list for LTx surgery. The aim of this preclinical study was to examine if the immediate inflammatory response triggered by NSPs after reperfusion can be prevented by the pre-treatment of recipient mice with a CatC inhibitor. In detail, we investigated whether NSP maturation in the BM could be blocked by a CatC inhibitor and determined the effect on lung graft function and quality after LTx.

To initiate proof of concept experiments, we used the murine orthotopic LTx model which was used in our previous study. Recipient mice were treated with a CatC inhibitor, ICatC, twice daily for 10 days prior to LTx. We used a reversible cyclonitrile CatC inhibitor ICatC, which was first described as XPZ-01 by Unizyme Laboratories.

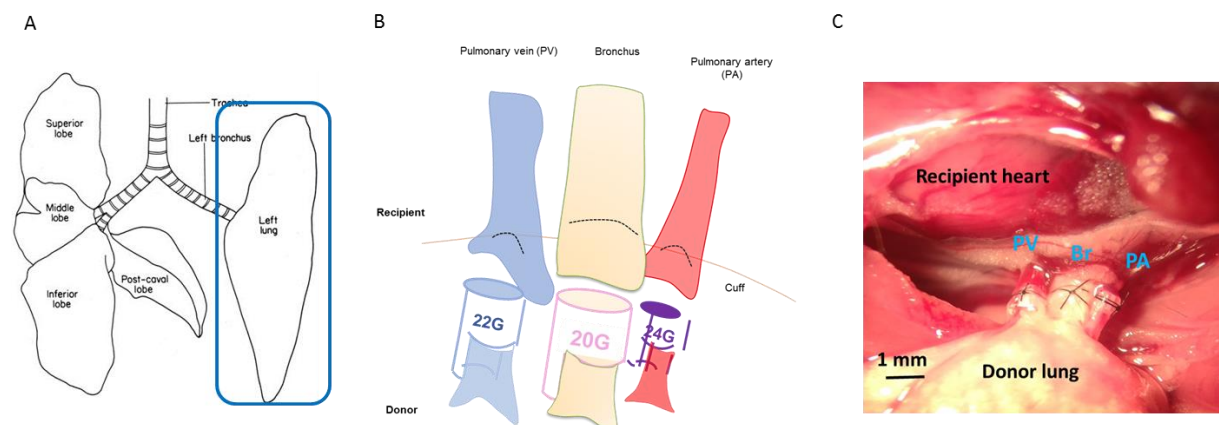


Figure 7 Mouse model of orthotopic lung transplantation. (A) Model of a murine lung: the right lung consists of four lobes and the left lung only of one lobe. (B) Principle of left LTx in the mouse: first the pulmonary artery (PA, red) is attached to the recipient, then the pulmonary vein (PV, blue), and finally the bronchus (Br, orange). (C) Picture of left donor lung attached to the recipient during surgery (taken by Natalia Smirnova).

2. Materials and methods

2.1 List of materials

2.1.1 Chemicals and Consumables

Chemicals were purchased from the companies BD Biosciences (Franklin Lakes, NJ, USA), Bio-Rad Laboratories (Hercules, CA, USA), Biozym (Hessisch Oldendorf, Germany), Life Technologies (Carlsbad, CA, USA), Merck (Darmstadt, Germany), PAA Laboratories GmbH (Pasching, Austria), GE Healthcare (Little Chalfont, Buckinghamshire, UK), Qiagen (Hilden, Deutschland), Roth (Karlsruhe, Germany), and Sigma-Aldrich (St Louis, MO, USA), unless mentioned otherwise. Restriction enzymes and T4 deoxyribonucleic acid (DNA) ligase were purchased from New England Biolabs (Ipswich, MA, USA) and Thermo Fisher Scientific (Waltham, MA, USA). Consumables such as pipette tips, centrifuge tubes, reaction tubes, and microwell plates were procured from Biozym (Hessisch Oldendorf, Germany), Eppendorf (Hamburg, Germany), BD Biosciences and Nunc/Thermo Fisher Scientific (Waltham, MA, USA). Cell culture flasks and dishes were obtained from Corning (Corning, NY, USA) and BD Biosciences.

2.1.2 Laboratory equipment

Device designation	Supplier
Autoclave	Varioklav, H+P Labortechnik, Oberschleissheim, Germany
Axio Imager. Z1	Carl Zeiss, Göttingen, Germany
Balances	PM 4800 Delta Range, Mettler-Toledo, Columbus, OH, USA 2001 MP2, Sartorius,

	Göttingen, Deutschland
Centrifuge	5417R, Eppendorf 5417C, Eppendorf Rotanta 460R, Hettich, Tuttlingen, Germany
Detection sytem Chemidoc	Biorad, Munich, Germany
Gel electrophoresis chambers/ power supplies	Bio-Rad, Amersham-Pharmacia, MPI workshop
Incubation shaker	HT Multitron, Infors, Bottmingen, Switzerland
Incubator	BBD6220, Heraeus, Thermo Scientific, Waltham, USA
Icemachine	Ziegra, Isernhagen, Germany
Magnetic stirrer	MR3003, Heidolph, Kelheim, Germany
Microplate reader	FLUOStar Optima, BMG Labtech, Offenburg, Germany
Microscope	Leica DM IL, Leica Microsystems, Wetzlar, Germany
NanoDrop 2000c	Peqlab Biotechnology GmbH, Erlangen, Germany
pH-meter	Inolab pH Level 1, WTW, Weilheim, Germany
PCR cyclcr	T3 Thermocycler, Biometra, Göttingen, Germany
Semidry blotter	Biometra, Göttingen, Germany
Shaker	130 basic, IKA KS

Spectrophotometer	ND-1000, peqlab, Erlangen, Germany
Thermoblock	Thermoblock
Water bath incubator	MA6, Lauda, Lauda-Königshofen, Germany
Water preparation	Milli Q Advantage, Millipore, Billerica, MA, USA

2.1.3 Oligonucleotides

Oligonucleotides were synthesized by Eurofins Genomics (Ebersberg, Germany).

Name	Sequence	Application
DJ3710	5'-CGGGGTACCAGGTTCCACcGGTGAAGCACACAAGAGTGA-3'	cloning
DJ3729	5'-GATGTCCGGAGGCTAACGCGTCTTTGCATCTAGTGACAAG-3'	cloning
DJ3765	5'-TGGGTACCTGGCTCAACCGGACCTAGGATGCTGGGGGCT-3'	cloning
DJ3766	5'-GACTCTTGGTGCACGTGGT-3'	cloning
DJ3767	5'-TGGGTACCTGGCTCAACCGGACTGCTGGGGGCTCCCGAGGA-3'	cloning
TNFa-2f	5'-CACCACGCTCTTCTGTCT-3'	real-time PCR
TNFa-2r	5'-GGCTACAGGCTTACTC-3'	real-time PCR
IL-10-1f	5'-TCTGTCTAGGTCCTGGAGTC-3'	real-time PCR
IL-10-1r	5'-GGAGCAGGTGAAGAGTGA-3'	real-time PCR
IL-1α-1f	5'-AGCGTCCAAGGAGAAGAC-3'	real-time PCR
IL-1α-1r	5'-CTGTCATAGAGGGCAGTCC-3'	real-time PCR
IL-1βf	5'-CAACAAACAAGTATTCTCCATG-3'	real-time PCR
IL-1βr	5'-GATCCACACTCTCCAGCTGCA-3'	real-time PCR

2.1.4 Plasmids

Plasmid	Origin
pTT5	NRC Biotechnology Research Institute, Ottawa, USA
pTT5_MIP-2(5-73)_RUBY_H6	Therese Dau, AG Jenne
pTT5_Ruby_Alb_CysC	Salome Rehm, AG Jenne
pTT5_Ruby_CysC	Salome Rehm, AG Jenne
pTT5_Alb_CysC	Salome Rehm, AG Jenne

Vector maps can be found in the Appendix 7.1.

2.1.5 *E.coli* bacterial strains

Strain	Genotype	Provider
DH5 α	F– Φ 80 <i>lacZ</i> Δ M15 Δ (<i>lacZYA-argF</i>) U169 <i>recA1 endA1 hsdR17</i> (rK–, mK+) <i>phoA supE44</i> λ – <i>thi-1 gyrA96 relA1</i>	18265017, Thermo Fisher Scientific

2.1.6 Recombinant and purified proteins

Protein	Origin
CystatinC-albumin	Salome Rehm, Jenne Lab
CystatinC-albumin-ruby	Salome Rehm, Jenne Lab
CystatinC-ruby	Salome Rehm, Jenne Lab
Cystatin C	R&D systems
Cathepsin B	R&D systems

2. Materials and methods

Cathespin S	R&D systems
-------------	-------------

2.1.7 Antibodies

Primary antibodies

Antigen	Species	Klone	Provider	Catalog No.
Mouse PR3	Goat		AG Jenne	
Mouse NE	Rabbit		Abcam	ab68672
Mouse AAT	Rat	RM0527-3E39	Abcam	ab205152
Ly-6G	Rat	1A8	Biolegend	127602
Cystatin C	Rabbit	EPR4413	Abcam	ab109508

Secondary antibodies

Antigen	Species	Label	Provider	Catalog No.
Goat	mouse	HRP	Merck Millipore	AP186P
Rabbit	goat	HRP	Merck Millipore	12-348
Rat IgG+IgM	goat	HRP	Jackson Immuno Research	112-035-068

Other

Antigen	Label	Provider	Catalog No.
Avidin	Peroxidase	Invitrogen	434423

2.1.8 Förster/Fluorescence resonance energy transfer (FRET) substrates

Sequence	Cleaving proteases	Provider
TAMRA-GVRRVVQVQD-Dap (CF)	Mouse PR3	KH Wiesmüller, EMC Microcollection
Abz-GAVVASELR-Y-(NO ₂)-D	Mouse NE, mPR3	KH Wiesmüller, EMC Microcollection
Z-Arg-Arg-AMC	Human Cathepsin B	Bachem, 404789
Z-Val-Val-Arg-AMC	Human Cathepsin S	Bachem, 4016422

2.2 Molecular biological methods

2.2.1 Polymerase chain reaction (PCR)

PCR is a fast and easy method to amplify a specific DNA fragment from a larger DNA template. Two oligonucleotides, so called primers are required to flank the two ends of the DNA fragments. They contain a free 3'-OH at one end, ensuring the synthesis of the new strand in only one direction. The synthesis is carried out by a polymerase by adding and linking new nucleotides to the primers, thereby generating many copies of the amplicon. A typical PCR cycle consists of denaturation of the DNA double helix, annealing of the primers to the single strands and a final extension step in which the DNA polymerase extends the DNA fragments to their full length. The Phusion High Fidelity polymerase from Finnzymes (New England Biolabs) was used for all PCRs. The conditions used are described in the tables below.

Phusion PCR reaction (25 µl):

Component	Volume (µl)
template DNA	2-5ng
Phusion HF buffer	1x
dNTPs	200 µM
forward primer (10 µM)	0.5 µM
reverse primer (10 µM)	0.5 µM
Phusion DNA polymerase	0.2 µl
dH ₂ O	up to 25 µl

Phusion PCR program:

Step	Temperatures	Periods	Cycles
1	95°C	30 s	x25
2	98°C	10s	
3	60°C	30s	
4	72°C	60 s	
5	72°C	10 min	

2.2.2 Restriction enzyme digest

Restriction endonucleases are enzymes which cleave DNA at a specific recognition sequence. The DNA obtained from PCR was digested with one or two different restriction enzymes to produce linear fragments with non-complementary ends. One unit is defined as the amount of restriction enzyme needed to digest 1 µg of DNA in one hour at room temperature. The protocol was performed according to the manufacturers' instructions. Restriction enzymes were purchased from New England Biolabs.

2.2.3 Agarose gel electrophoresis

Due to their negatively charged sugar-phosphate backbone, DNA fragments can be separated in an agarose gel matrix in an electric field according to their size. Agarose gels were prepared with TAE buffer supplemented with SYBR Safe (Life Technologies, dilution 1: 10000) to visualize DNA by exposure to UV light (254-366 nm). Depending on the size of the DNA fragment, the percentage of the agarose in the gels ranged from 0.5 – 2 % (w/v).

DNA samples were mixed with 1x loading buffer and electrophoresis was performed with a constant voltage of 60 volt (small chambers) for 1 hour. As a molecular marker Gene Ruler DNA ladder (1kb, Fermentas, Thermo Fisher Scientific) was used. The fluorescence signal was detected with a Chemidoc imaging system (Bio-Rad).

Buffer/Solution	Composition
50 x TAE buffer	243 g Tris 100 ml 0.5 m EDTA pH 8.0 57.1 ml acetic acid up to 1 l dH ₂ O
10 x DNA loading dye	0.25% (w/v) bromphenol blue 0.25% (w/v) xylene cyanol 50% (w/v) glycerol

2.2.4 DNA purification

After PCR, or restriction digest, DNA was purified by gel extraction (QIAquick GelExtraction Kit, Qiagen) or with the QIAquick PCR Purification Kit (Qiagen) in accordance with the manufacturer's instructions. The final elution volume comprised 30-50 µL elution buffer or ddH₂O.

2.2.5 Determination of DNA concentration

DNA concentrations were determined by Nanodrop with absorption of 260 nm. The theoretical fundament for this measurement is described by the Beer-Lambert law (Absorption = (extinction coefficient) x (length of solution) x (concentration of solution)).

2.2.6 Vector dephosphorylation

To avoid religation of linearized plasmids with compatible ends, 5' phosphate groups from restricted vector DNA were removed by adding alkaline phosphatase (New England Biolabs) according to the manufacturer's protocol.

2.2.7 DNA Ligation

Ligation was performed adding 400 U/ μ l T4 DNA Ligase (New England Biolabs), 2 μ l ligase buffer (NEB) and H₂O up to a volume of 20 μ l. Restricted plasmid DNA and the DNA fragment were ligated in a molar ratio of 1:5 for 3 h at room temperature.

2.2.8 Preparation of CaCl₂-competent bacteria

5 ml of LB medium (Luria-Bertani-Broth) were inoculated with a single colony of *E.coli* DH5 α and grown without the addition of antibiotics in a 15 ml tube at 37 °C with shaking (250 rpm) overnight. On the next day 4 ml of the pre-culture were added to 400 ml fresh LB medium. The cells were incubated (37 °C, 250 rpm) until the OD₆₀₀ reached 0.4, which took approximately three hours. Then, the bacterial suspension was pre-cooled on ice in 50 ml tubes for 10 min. Subsequently, the suspensions were pelleted by centrifugation without break (7 minutes, 3000 rpm, 4 °C). For all remaining steps the cells were kept on ice and all flasks, pipette tips and tubes were pre-cooled at 4 °C. Cell pellets of 100 ml culture volume were resuspended in 10 ml ice-cold CaCl₂ buffer and centrifuged again (5

min, 2500 rpm, 4 °C, no brakes). Cell pellets were again resuspended in 10 ml ice-cold CaCl_2 buffer and incubated on ice for 30 min followed by centrifugation (5 min, 2500 rpm, 4 °C, no brakes). Bacteria pellets were resuspended in 2ml ice-cold CaCl_2 buffer and 150 μl aliquots were snap frozen in liquid nitrogen and stored at -80 °C.

Buffer/Solution	Composition
CaCl_2 buffer	60 mM CaCl_2 5% (w/v) Glycerol 10 mM PIPES pH 7
LB medium	1% (w/v) Bacto tryptone 0.5% (w/v) Yeast extract 1% (w/v) NaCl pH 7.5, autoclaved
LB agar plates	1x LB medium 1.5% (w/v) Bacto agar, autoclaved

2.2.9 Transformation of CaCl_2 -competent bacteria

First, competent *E. coli* DH5 α were thawed on ice for 10 min. 50 μl of thawed competent *E. coli* DH5 α cells were mixed with 3 μl ligation mix and incubated for 30 min on ice. This allows the plasmid DNA to attach to the cell wall of the bacteria. Then cells were heated for 90 s at 42 °C and subsequently cooled on ice for 10 min. The heat-shock permeabilizes the cell membrane for a short duration, so that the plasmid DNA can enter the cell. 250 μl warm LB medium was added followed by incubation for 1 hour at 37 °C in a shaking thermoblock. 200 μl of cell suspension was plated on LB agar plates containing 100 $\mu\text{g}/\text{ml}$ ampicillin. After overnight incubation at 37 °C colonies were picked.

2.2.10 Plasmid DNA purification from bacteria

Isolation of plasmid DNA from 5 ml *E.coli* overnight culture was carried out with the QIAprep Spin Miniprep Kit (Qiagen). For the purification of higher amounts of Plasmid DNA out of larger overnight cultures the PureYield™ Plasmid Maxiprep System (Promega) was utilized. Both kits were used according to the manufacturer's protocol. The purified and endotoxin free plasmid DNA was used for transfection of mammalian cells.

2.2.11 DNA Sequencing

DNA samples were sent to Eurofins MWG GmbH (Ebersberg, Germany) for sequence analysis.

2.3 Recombinant protein expression

2.3.1 HEK cell transfection

For the expression of albumin (Alb) and the fusion proteins CysC-Alb, CysC-Alb-Ruby and CysC-Ruby human embryonic kidney cell line (HEK) 293-EBNA cells were used. Before transfection HEK 293 cells were grown to a density of 1×10^6 cells /ml in Freestyle™ 293 expression medium (Invitrogen) with 0.01% (v/v) Pluronic® F-68 and 25 µg/ml Geneticin® G418. First, DNA (7.5 µg) and polyethyleneimine (PEI, 30 µl) were diluted separately in 500 µl OptiPro serum free medium (Invitrogen). After mixing both solutions together complexes are forming at room temperature within the next 20 min due to the cationic binding capacity of PEI to negatively charged DNA. The DNA/PEI mixture was added drop-by-drop to 15 ml (1×10^6 cells/ml) cell suspension. For stabilization of the recombinant protein Bacto TC Lactalbumin Hydrolystae (BD Bioscience) was added after

24 hours incubation at 37°C. Supernatants were harvest after 4 days by centrifugation (1500 rpm/10 min/4°C).

2.4 Protein analysis

2.4.1 Purification of recombinant proteins by nickel-affinity chromatography

Since CysC-Alb, CysC-Alb-Ruby and CysC-Ruby carry a his-tag, these proteins were purified by nickel-affinity chromatography. First, the cell culture supernatant was filtered through a 0.22 µm membrane (Millipore) to remove potential bacterial contamination. Then, the supernatant was dialyzed against Ni-NTA binding buffer at 4°C over night. Before the supernatant was applied, the HiTrap HP columns (GE Healthcare) were equilibrated with binding buffer. The column was washed with binding buffer, and bound proteins were eluted applying a linear imidazole gradient from 40 mM to 1 M imidazole in binding buffer. Fractions were collected and analyzed by SDS-PAGE and coomassie or silver staining to detect the protein of interest. The fractions that contained the protein of interest were pooled and concentrated. Imdidazol was removed by dialysis against the binding buffer.

Buffer	Composition
Binding buffer	20 mM Na ₂ HPO ₄ 300 mM NaCl pH 7.4
Elution buffer	20 mM Na ₂ HPO ₄ 300 mM NaCl Imidazole, gradient 1 M – 60 mM pH 7.4

2.4.2 Purification of recombinant protein by HiTrap™ Blue HP affinity chromatography

The recombinant wild-type Alb was purified by using its interaction with the dye Cibacron Blue F3G-A. The supernatant was applied to HiTrap™ Blue HP columns (GE Healthcare) and the purification was performed according to the manufacturer's protocol.

Buffer	Composition
Binding buffer	20 mM sodium phosphate pH 7
Elution buffer	20 mM sodium phosphate 2 M NaCl pH 7

2.4.3 Determination of protein concentration

The concentration of protein solutions was either assessed by a bicinchonic acid (BCA) assay carried out according to the manufacturer's instructions, or by spectrophotometrically measurement of absorbance at 280 nm. The concentration can be calculated using the Beer-Lambert law:

$$c = (A_{280} \times MW) / (\epsilon_{280} \times l)$$

(c = concentration; A = absorbtion;; MW = molecular weight; ϵ = extinction coefficient; l = length of solution)

The extinction coefficient of each protein was determined by using the ProtParam tool (<http://us.expasy.org/tools/protparam.htm>) inserting the protein sequence obtained from the UniProt database (<http://www.uniprot.org/>).

2.4.4 Sodium dodecyl sulfate - polyacrylamide gel electrophoresis (SDS-PAGE)

Protein lysates containing equal amounts of protein were size-fractionated by denaturing SDS-polyacrylamide gel electrophoresis (SDS-PAGE) in a discontinuous system with a 1.0 mm thick stacking and separating gel in 1x running buffer. Both, the samples and the gel contain the detergent SDS, which denatures the proteins. They unfold into their secondary structure and get negatively charged according to their size. Protein lysates were mixed with 5x loading buffer and boiled for 5 min at 95 °C before loading onto the gel. For analysis, 10 to 20 µl of sample and 5 µl of protein marker (Prestained Protein Marker, Broad Range, New England Biolabs) were loaded.

12 % polyacrylamide gel (8 gels)

	Stacking gel	Resolving gel
H ₂ O	13.6 ml	13,4 ml
1.5 M Tris HCl, pH 8.8		10 ml
1 M Tris HCl, pH 6.8	2.6 ml	
20 % SDS	100 µl	200 µl
30 % polyacrylamide	3.3 ml	16 ml
TEMED	200 µl	400 µl
10% APS	20 µl	16 µl

Buffer	Composition
10 × Running Buffer	250 mM Tris HCl 1.92 M Glycine 1 % (w/v) SDS
4 x Reducing Loading Buffer	200 mM Tris HCl, pH 6.8 40% (v/v) Glycerin 10% (w/v) SDS 30% (w/v) β-mercaptoethanol 0.2% (w/v) Bromphenol blue

2.4.5 Protein detection

2.4.5.1 Coomassie staining

After SDS-PAGE gels were incubated for 1 h in Coomassie staining solution to visualize the protein of interest. To remove unspecific staining the gel was incubated in Coomassie destaining solution until protein bands were visible. The gels were photographed with a Chemidoc imaging system (Bio-Rad).

Solution	Composition
Coomassie staining solution	0.25% (w/v) Coomassie Brilliant Blue 45% (v/v) Methanol 10% (v/v) Acetic acid
Coomassie destaining solution	45% (v/v) Methanol 10% (v/v) Acetic acid

2.4.5.2 Silver staining

For the detection of proteins by silver nitrate staining, gels were incubated in fixation solution for 1 h at room temperature while shaking. Subsequently, it was washed three times in 50% ethanol for 20 min and then the gel was incubated in thiosulfate solution for 1 min for sensitization. Then the gel was rinsed with tap water three times, incubated with silver nitrate solution for 20 min and developed until the bands became visible. The staining reaction was stopped in 50% methanol for 20 min. After the stopping solution was replaced with tap water, the gels were photographed with a Chemidoc imaging system (Bio-Rad).

Solution	Composition
Fixation solution	50% (v/v) Methanol 12% (v/v) Acetic acid 0.5 ml/l 37% Formaldehyde
Thiosulfate solution	0.2 g/l $\text{Na}_2\text{S}_2\text{O}_3 \times 5 \text{ H}_2\text{O}$
Silver nitrate solution	2 g/l AgNO_3 750 ml/l 37% Formaldehyde
Development solution	60 g/l Na_2CO_3 4 mg/ml $\text{Na}_2\text{SO}_3 \times 5 \text{ H}_2\text{O}$

2.4.6 Enzymatic activity measurement

Enzymatic activities were measured using Förster resonance energy transfer (FRET) with specific FRET-substrates. The substrates consist of a quencher and a fluorescence group. Once the peptide is cleaved internally, quencher and fluorescence group are separated and the hydrolysis rate of the FRET substrate by the protease is measured over time.

The TAMRA-FRET and AMC-FRET substrates were diluted in DMSO to reach a concentration of 100 μM .

Typical reaction:

Component	Volume	Final concentration
Activity assay buffer	40 μl	
Protease (1 μM)	5 μl	0.1 μM
Substrate (100 μM)	5 μl	10 μM

Buffer	Composition
Activity assay buffer	50 mM Tris 150 mM NaCl 0.01% Triton X-100 pH 8

2.4.6.1 Activity measurement assays

The enzymatic activities of the serine proteases, PR3 and NE, were determined using TAMRA-FRET or ABZ-FRET substrates. For the specific mouse PR3 substrate, TAMRA-GVRRVVQVQD-Dap (CF), fluorescence was measured at $\lambda_{\text{Ex}} = 485 \text{ nm}$ and $\lambda_{\text{Em}} = 520 \text{ nm}$. This substrate was synthesized by Oliver Schilling based on unpublished data. Activity measurements for NE were carried out with Abz-GAVVASELR-Y-(NO₂)-D and the fluorescence was obtained at $\lambda_{\text{Ex}} = 320 \text{ nm}$ and $\lambda_{\text{Em}} = 405 \text{ nm}$.

The enzymatic activity of CatB in mouse samples was measured using the mouse specific CatB substrate Z-Arg-Arg-AMC at $\lambda_{\text{Ex}} = 360 \text{ nm}$ and $\lambda_{\text{Em}} = 440 \text{ nm}$. The slope of the reaction curve was used to define the enzymatic activity in relative fluorescence units (RFU).

2.4.6.2 Assay for CysC-Alb and CysC inhibitory activity measurement

Inhibitory activities of CytC-Alb and CytC were tested in an activity assay using 0.1 μM recombinant human cathepsin S and B. The remaining activity of these proteases was determined using the CatS specific FRET-substrate Z-Val-Val.Arg-AMC and Z-Arg-Arg-AMC which is specific for CatB at 0.1 nM.

Buffer	Composition
Cathepsin activity assay buffer	Acetic acid 20 mM NaCl 150 mM DTT 1 mM EDTA 1 mM, pH 5.5

2.5 Mouse model analysis

2.5.1 Mouse strains

Pathogen-free C57BL/6J mice were obtained from Charles River. PR3/NE knockout animals (*Ela2^{-/-}Prtn3^{-/-}*) were established by Pfister *et al.* (38). Mice were backcrossed for more than ten generations with C57BL/6J mice. All animals were kept under normal housing conditions with constant temperature and humidity, a 12 hour light cycle, and food and water were allowed *ad libitum*.

2.5.2 Study approval

All animal experiments were conducted under strict governmental and international guidelines and were approved by the local government for the administrative region of Upper Bavaria (Project 55.2–1-54-2532-120-2015).

2.5.3 Orthotopic lung transplantation model

Orthotopic LTx was performed as described by Krupnick *et al.* with minor modifications (39). Male 8-12 weeks old C57BL/6J mice were utilized as donors and recipients. In brief, donors were anesthetized with a intraperitoneal injection of ketamine/xylazine. The pulmonary artery (PA), bronchus (BR) and pulmonary vein (PV) were separated with blunted forceps, prior to cuffing with, 24G, 20G and 22G cuffs, respectively. The left lung lobe was perfused intravenously with Perfadex (3 ml). Subsequently, it was perfused with

Perfadex alone or supplemented with 0.40 µg/ml CysC-Alb or Alb. The PA and PV were clamped with Biemer micro vessel clips (Bbraun), in order to keep the solution inside the blood vessels, and it was stored for 18 hours at 4°C before implantation. The recipient was anesthetized with a medetomidine/midazolam/fentanyl (1/0.05/0.02 mg/kg), intubated, and connected to a small animal ventilator (Harvard Apparatus), at a respiratory rate of 120 bpm and a tidal volume of 300 µL. The chest was incised on the left side between rib 3 and rib 4 and the native left lobe of the mouse lung retracted with a clamp. The hilar structures were carefully separated with blunted forceps. The donor lung graft, prepared 18 hours earlier, was perfused intravenously with Perfadex to rinse out the storage solution. After arrest of the blood and air flow towards the left lung, the cuffed graft PA, BR and PV were inserted into the recipient counterparts, and the connection was secured with 9-0 sutures. The native left lung was removed and the incision in the chest was closed with a 6-0 suture, after removing all potential air bubbles from the chest. After administration of antagonist the animal was extubated at the first signs of spontaneous breathing. After the operation, the recipients were allowed to recover at 30 °C and received buprenorphine (0.1 mg/kg). The mice were sacrificed four hours after transplantation for PGD assessment.

2.5.4 *Ex vivo* lung perfusion (EVLP)

In order to perform EVLP, three chambers were prepared; the inflow chamber (IC), the lung chamber (LC) and the outflow chamber (OC). All three chambers were filled with Perfadex and the IC was kept at 37°C on the water bath. The donor lung was harvest following intubation with a 20G cannula and perfusion through the pulmonary vein with a 26G cannula. Then the ventilation cannula was connected to the bronchus, the inflow

perfusion cannula to the pulmonary artery and the outflow cannula to the pulmonary vein. After putting the lung in the LC, the perfusion system was started by turning on the peristaltic pump (0.35ml/min) that is placed between the IC and the LC, and the ventilation system (80 strokes/min). Observed air bubbles in the pipeline were removed by using an air purge stopcock. The Perfadex solution containing either CysC-Alb or Alb was run through the lung scaffold for 2 h. A second peristaltic pump between the LC and the OC was turned on to collect the Perfusate in the OC overtime. In total 42 ml of Perfusate was collected in the OC after 2h EVLP.

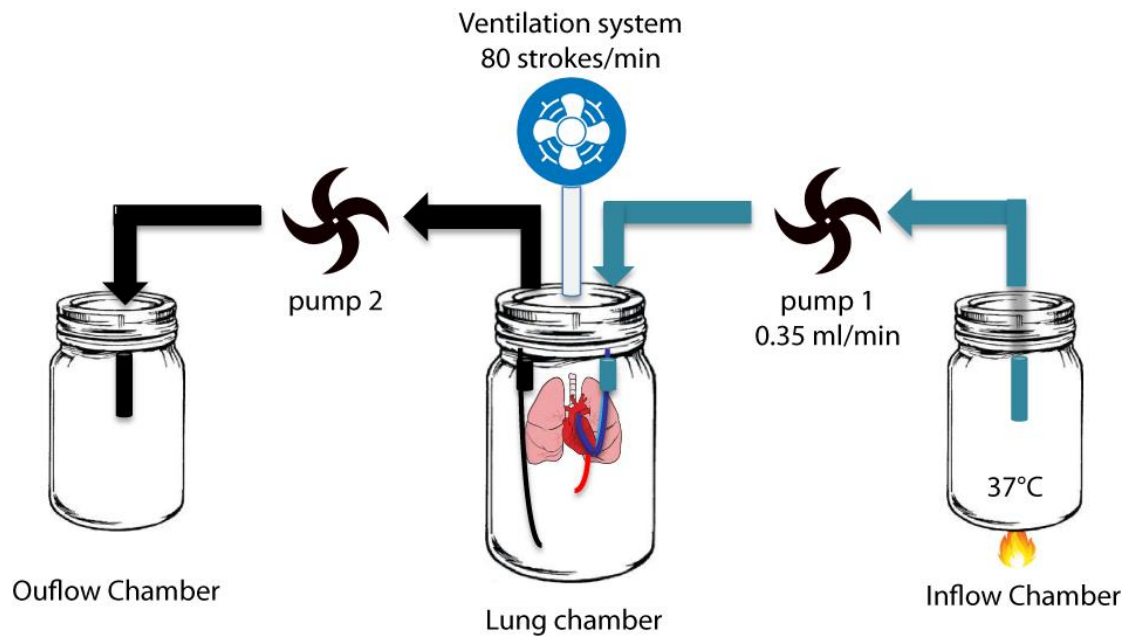


Figure 8: *Ex vivo* lung perfusion system. Once the lung is connected to a ventilation system (80 strokes/min) via the bronchus and the inflow and outflow cannulas via the pulmonary artery and vein, the lung is placed in a chamber containing Perfadex. Perfadex, which is kept at 37°C in the inflow chamber, reaches via a pump (0.35 ml/min) the lung through the pulmonary artery and is flushed out through the pulmonary vein in the lung chamber. The perfusate is then collected via a second pump in the outflow chamber. Perfadex contained 40 µg/ml CysC-Alb or Alb in our experimental setting.

2.5.5 Allograft tissue sample collection (blood gas, bronchoalveolar lavage)

The recipient was anesthetized with a mixture of medetomidine/midazolam/fentanyl (1/0.05/0.02 mg/kg) 4 hours after LTx. After intubation (300 μ l room air/120 strokes/min), a midline abdominal incision was executed and the chest opened to expose the lung and heart. The right bronchus and pulmonary vein were clamped for 5 min (75 μ l room air /120 strokes/min) to determine the oxygenation function of the transplanted left lung by measuring the pO₂ [%] of the blood from the left ventricle using a blood gas analyzer (ABL80 FLEX CO-OX analyzer, Radiometer). With the right bronchus still clamped, bronchoalveolar lavage (BAL) of the transplanted left lung was collected by instilling cold PBS (three times, 200 μ L) into the trachea. The BAL fluid (BALF) was obtained by centrifugation (400 g, 20 min, 4°C) and protein concentration was measured with the Pierce™ BCA Protein Assay Kit (catalog no. 23225, Thermofisher). 30.000 cells from the BAL cell pellet were used for a cytospin (200 x g, 6 min, 4°C) and stained with May Grünwald (1424, Merck) and Giemsa (Merck, 9204) solution in order to perform a differential cell count. The lower part of the lung was kept separately for protein analysis (snap freezing, storage at -80 °C) and the remaining upper part was utilized for histology (inflation with and storage in 4% PFA).

2.5.6 Isolation of polymorphonuclear neutrophils (PMNs) from the bone marrow

After sacrificing the mice, bone marrow (BM) leucocytes were isolated from both femurs. The BM was flushed out with 10 ml RPMI medium using a syringe with a 21-gauge cannula and send through a cell strainer. The suspension was carefully underplayed with 10 ml 62.1% Percoll (GE Healthcare) in 2 × HBSS and centrifuged at 500 ×g for 30 min. The cell pellet containing PMNs and erythrocytes was lysed with erythrocyte lysis buffer

(9 ml 0.16 M NH_4Cl + 1 ml 0.17 TrisHCl, pH 7.5). The remaining PMNs were washed with ice-cold PBS and resuspended in 1ml PBS for counting.

2.5.7 Preparation lung lysates for western blot analysis

Whole lung tissues from the transplanted left lungs were homogenized to fine tissue powders of each lung. The whole lung powder was lysed in cold RIPA buffer containing 1× phosphatase- and 1× proteinase inhibitor cocktail. Samples were left on ice for 15 min, followed by sonification for 5 min (×4). Cell debris and DNA were pelleted and removed by centrifugation (10 min, 20000 x, 4 °C). The total protein concentration was measured by Pierce™ BCA Protein Assay Kit (23225, Thermofisher).

Buffer	Composition
RIPA Buffer	Tris 50 mM NaCl 150 mM Deoxycholic acid 0.5% (w/v) SDS 0.1% (w/v) Nonident P-40 (Igepal) 0.5% (w/v) EDTA 1 mM pH 8.0

2.5.8 Lung tissue preparation for staining of lung sections

Left mouse lungs were inflated with 4% PFA through an intratracheal cannula at the time of sacrifice, the trachea was ligated, and the lungs were fixed in 4% PFA, at 4°C overnight, and transferred to 70% ethanol before paraffin-embedding. The grafts were subsequently embedded in agarose, and cut into 3 pieces, and then separated 3 mm from each other. The pieces were embedded in paraffin, and then sliced into 3 μm -thin sections with a microtome (Hyrax M55, Zeiss).

For immunofluorescence stainings, lungs were frozen after EVLP and embedded in optimal cutting temperature (O.C.T) compound (Scigen). 3 μm -thin sections were cut with a cryotome (CM3050, Leica).

2.6 Cell biological methods

2.6.1 Cell lines

The cell line HEK 293 EBNA1 was purchased from the NRC Biotechnology Research Institute (National Research Council in Montreal, Canada), and the murine macrophage-like cell line RAW264.7 derived from Balb/C mice from Sigma-Aldrich (Missouri, USA).

2.6.2 Culturing of HEK 293 EBNA1 and RAW264.7 cells

HEK 293 EBNA1 were seeded at 0.2×10^6 cells and cultured in FreestyleTM 293 expression medium (Invitrogen) with 0.01% (v/v) Pluronic[®] F-68 and 25 $\mu\text{g}/\text{ml}$ Geneticin[®] G418 in suspension. RAW264.7 were seeded at 2×10^5 cells and cultured in DMEM; F12, (+ 1% Pen/Strep, 10 % FCS) at 5% CO_2 , 37°C. Cells grown adherent and were dislodged from the flask with a cell scraper for subculturing.

2.6.3 Determination of cell count and viability

A hemocytometer (Neubauer improved) was used to count the number of viable cells. For this purpose 10 μl of cell suspension were mixed with 10 μl Trypan blue buffer and all viable cell were counted in the four quadrants. Dead cells have perforated membranes; Trypan blue can enter into the cytoplasm and stains these cells blue. The average number of cells in one quadrant (100 nl) was multiplied with the dilution factor and by 10^4 to determine the number of cells/ml.

Buffer	Composition
Trypan blue buffer	Trypan blue 0.1% (w/v) PBS pH 7.4

2.6.4 Live cell imaging of RAW264.7 cells

4×10^4 cells were seeded on 170 μm imaging dishes (Eppendorf) in culturing medium and cultured for 18 h. Adherent cells were washed with PBS for 5 min prior to staining. LysoTracker (1:1000), Hoechst (1:10000) and CysC-Ruby (40 $\mu\text{g}/\text{ml}$) or CysC-Alb-Ruby (40 $\mu\text{g}/\text{ml}$) were added to culturing medium without FCS and incubated for 2 hours at 37°C. Cells were washed 3 times with PBS for 5 min and immunofluorescence was examined with a confocal microscope (LSM 710, Zeiss). Fluorescence confocal microscopy were recorded under triple fluorescent mode in which cells were successively exposed to 647 nm, 460 nm and 568 nm.

2.6.5 *In vitro* model of cold ischemia and simulated EVLP/Reperfusion

In vitro modeling of cold ischemia and simulated EVLP/Reperfusion was developed as described by Casiraghi et al. with modifications mimicking our *in vivo* LTx model (40). RAW264.7 were seeded at a density of 2×10^5 and grown in culturing medium for 24h at 37°C. They underwent cold ischemia by replacing 37°C medium with 4°C Perfadex for 18h. To determine the effect of CysC-Alb, either CysC-Alb or Alb was supplemented to Perfadex. To imitate EVLP (2 h) and reperfusion (4 h) dishes were warmed up to 37°C for 6h. Perfadex supernatant and cells were collected for subsequent analysis.

2.6.6 Apoptosis

Apoptotic cell death was analyzed by terminal deoxynucleotidyl transferase-mediated dUTP nick end labeling using the Apoptosis Detection System (DeadEnd Fluorometric TUNEL, Promega). Cells in 24-well plates were treated according to the manufacturers' instructions. For quantitative analysis, the number of TUNEL positive nuclei in 24-well plates was counted.

2.6.7 Cell viability

Cell viability was analyzed by using a cell counting Kit (Cell Counting Kit-8, Biotool) that used the tetrazolium salt WST-8 to produce a water-soluble formazan dye by the dehydrogenases in the cells. For quantitative analysis, the absorbance was measured at 450 nm using a microplate reader.

2.6.8 Preparation of total cell lysates

For the lysis of PMN, cells were resuspended in cold RIPA (radioimmunoprecipitation assay) buffer ($12\ \mu\text{l}/10^6$ cells). After incubating on ice for 20 min the samples were centrifuged (10 min, 4 °C, 20 000 x g). Cell debris and DNA remained in the pellet, while the supernatant was transferred to a new tube.

RAW264.7 cells were washed 2× with PBS and scratched with RIPA containing 1× protease inhibitor cocktail and 1× phosphatase inhibitor (Roche). After incubation on ice for 30 min, lysate was centrifuged at 13000 rpm for 5 min and supernatant was transferred to a new tube.

2.7 Immunological methods

2.7.1 Immunoblotting

For immunoblotting, proteins were transferred onto a polyvinylidene difluoride (PVDF) membrane by semi-dry electro blotting. The membrane was shortly immersed in methanol and incubated for 5 min together with the gel in blotting buffer. The transfer was carried out between four sheets of transfer buffer soaked Whatman paper at 200 mA for 50 min. The membrane was then blocked with 5 % fat dried milk or 1 × RotiBlock® (Carl Roth) for 1 h at room temperature, followed by incubation with the primary antibody diluted in blocking buffer overnight at 4°C. After washing the membrane three times for 10 min with PBS-T at room temperature to remove unbound antibody, the membrane was incubated with a specific (second) antibody conjugated to a horseradish peroxidase (HRP). After incubation for 1 hour at room temperature, the membrane was washed three times with PBS-T. Proteins were detected with the Super Signal® West Pico Chemiluminescent Substrate (#34080, Thermo Scientific). 750 µl of both Solution A (Luminol Enhancer Solution) and Solution B (Stable Peroxide Solution) were mixed and immediately added to the membrane for a two min incubation. The membrane was developed by using the Chemidoc imaging system (Bio-Rad). All western blot protocols are listed in below.

Buffer	Composition
Transfer Buffer	25 mM Tris 250 mM Glycine 1 mM SDS 20% MeOH
Blocking milk	1 × PBS-T 5% (w/v) Non-Fat dry Milk Blocker

2. Materials and methods

Protocols for western blots:

Blocking solution	primary AB	secondary AB
1 × RotiBlock®	NE, rabbit monoclonal 1:1000, 4°C on	goat anti-rabbit, 1:20000
1 × RotiBlock®	PR3, goat serum 1:1000, 4°C on	mouse anti-goat, 1:40000
1 × RotiBlock®	CysC, rabbit monoclonal 1:10000, 4°C on	goat anti-rabbit, 1:20000
1 × RotiBlock®	AAT, rat monoclonal 1:1000, 4°C on	goat anti-rat, 1:40000
1 × RotiBlock®	cleaved Caspase3, rabbit monoclonal, 1:1000, 4°C on	goat anti-rabbit, 1:20000

2.7.2 Enzyme-linked immunosorbent assay (ELISA)

ELISAs were performed for the detection of inflammatory cytokines and neutrophil elastase in BALF, cell lysates and whole tissue lysates using the following specific commercial available kits.

Kit	Supplier
Mouse Inflammatory Cytokine Multi-Analyte ELISArray™ Kit	Qiagen, Hilden, Germany
Mouse Elastase/ELANE/ELA2 PicoKline™ ELISA Kit	BosterBio, Pleasanton, USA
Murine TNF- α Standard ABTS ELISA Development Kit	PeproTech, Hamburg, Germany

In principle the two kits work like a so called sandwich ELISA. The 96 well plates were already pre-coated with the specific target antibody to capture the desired protein from the sample. The detection antibody was either a biotinylated antibody or a horseradish peroxidase (HRP) coupled antibody against the specific protein of interest. For the development of the ELISA TMP substrate was added and the absorbance was read with a microplate reader at 450 nm.

2.7.3 Immunological staining of lung tissue

Immunofluorescence staining was performed with paraffin and frozen lung tissue sections of the transplanted left lung 4h after reperfusion.

2.7.3.1 Deparaffinization

Paraffin sections containing lung tissue slices were incubated for 20 minutes at 65 °C. Then they were sequentially transferred to 100% xylene, then 100%, 90%, 80% and 70% ethanol, followed by tap water for 5 min, and rinsed in distilled water. Antigen retrieval was performed in 0.01 M citric acid pH 6.0 in a cooker chamber for 30 minutes at 125°C. Tissue was rehydrated with PBS-Tween 20 (0,1%) for 10 min.

2.7.3.2 Immunohistochemical stainings

Hematoxylin and eosin staining

Sections were stained with Hematoxylin (Hematoxylin solution, GHS-232, Sigma Aldrich) for 6 min, rinsed in distilled water, and tap water for 15 min, followed by distilled water. Then they were stained with eosin for 10 min and washed in tap water for 5 min. Subsequently, sections were dehydrated with ethanol 100% and xylene, and mounted

with glue (Entellan, Merck). For visualization the slides were scanned with Myrax Desk.

Peroxidase staining

Endogenous peroxidases were quenched by incubation in 3% H₂O₂ (30%, H1009, Sigma Aldrich) in PBS for 10 min. After washing with PBS and PBS-Tween 20 (0,1%) avidin solution (Avidin/Biotin Blocking Kit, SP-2001; Vector Laboratories) was added and incubated for 15 min, followed by washing with PBS-T (1x PBS-Tween 20 0,1%); biotin solution was added for 15 min, washed with PBS-T; nonspecific antibody-binding sites were blocked with blocking solution, PBSA (BSA 3% in PBS) for 1 h, and sections were incubated for 1.5 h with the specific primary antibody diluted in blocking buffer. Sections were stained with monoclonal rat mouse-specific Ly-6G monoclonal antibody (working dilution 1:200, clone 1A8, Biolegend) for detection of neutrophils. After washing in PBS-T, visualization was performed via incubation with HRP-conjugated secondary antibody with goat rat-specific IgG (H+L), biotin conjugated (working dilution 1:250, Thermofisher) for 30 min at room temperature followed by addition of the corresponding peroxidase substrate (ImmPACT DAB Peroxidase (HRP) Substrate, SK-4105; Vector Laboratories). After counterstaining with hematoxylin, dehydration and mounting, the sections were scanned using the Axio Imager (Imager.M2, Zeiss). High resolution images, which were taken at the same magnification and areas were randomly chosen and microscopically analyzed for neutrophil counting. The mean number of at least ten images was used for quantification.

2.7.3.3 Immunofluorescence staining

Immunofluorescence staining is based on the fundamentality of antigen-antibody binding reaction. Antigens are visualized by fluorescence dyes conjugated with antibodies when activated by light of specific wavelength under the fluorescence microscope. Before staining, frozen tissue sections were fixed in 50% methanol/50% acetone for 20 min at -20°C. In order to exclude a signal due to unspecific binding of the secondary antibody, a negative control was performed for each staining where no primary antibodies were used. The lung sections were stained with either NE, Gal3, pro-SPC, Ly-6G (Research Unit Analytical Pathology, HMGU, München) or LAMP2. All staining protocols are listed in below.

Protocols for immunofluorescence staining

Blocking solution	primary AB	secondary AB
3% H ₂ O ₂ , 10 min 0.1% Triton, 1x TBS, 45 min	Ly-6G, rat 1:200, 4°C on	goat-anti-rabbit, 1:500 Alexa Fluor® 645 1:1000, 1h @RT
5% BSA, 0.3% Triton, 1x TBS , 1 h	NE, rabbit 1:400, 4°C on	Cy3-goat anti-rabbit, 1:100
5% BSA, 0.3% Triton, 1x TBS , 1 h	Gal3, mouse	goat-anti-mouse Alexa Fluor® 488, 1:500
5% BSA, 0.3% Triton, 1x TBS , 1 h	Pro-SPC, rabbit	goat-anti rabbit, 1:500 Alexa Fluor® 488

2.7.4 RNA analysis

2.7.4.1 RNA isolation

Total RNA from RAW264.7 cells was isolated using the peqGold total RNA kit (VWR) according to the manufacturer's protocol. RNA was stored at -80°C until further use.

Table 12: Real-time PCR program

Step	Temperatures	Periods	Cycles
1	94°C	2:00	
2	94°C	0:20	40x
3	60°C	0:10	
4	79°C	0:20	
5	95°C	1:00	
6	55°C	1:10	
7	55°C	0:06	80x

2.8 Microscopy

Immunological staining of left lung sections were analyzed with the Axio Imager Z1-microscope. Images were evaluated using the commercially available image analysis software Definiens Developer XD 2 (Definiens AG, Munich, Germany).

2.9 Statistics

All results are expressed as mean \pm SEM. Group comparisons were determined by One-way Anova, student's t-test or unpaired Mann-Whitney U-test using the commercially available statistical software GraphPad Prism version 5.0. Statistical significance was defined as $p \leq 0.05$.

.

3. Results

3.1 CysC-Alb in LTx - Results

3.1.1 Cloning of the fusion protein CysC-Alb

CysC is an endogenous small peptide inhibitor with a broad reactivity against cysteine proteases including CatS, CatL and CatB. To enhance the quality of CysC, it was fused directly to the N-terminus of Alb. The N-terminal end of CysC is critical for its tight enzyme-binding property and therefore important for effective inhibition of cysteine proteases (57). For monomer stabilization, we have introduced an additional third disulfide bond (CysC47-CysC69). DNA sequences can be found in the appendix.

3.1.2 Production of CysC-Alb and Alb in HEK 293E cells

CysC-Alb and Alb were successfully expressed in HEK 293E cells using the pTT5 expression vector. The cells were transfected with 1:1 CysC-Alb and harvested routinely after 4 days. High amount of protein was secreted into the supernatant. A Igk-signal peptide was used in the construct for secretion into the cell culture supernatant. Using a C-terminal His-tag, CysC-Alb was purified with Ni-NTA affinity chromatography (Figure 9A). After purification, the CysC-Alb elution fractions yielded only few other proteins, with a minor contaminant considered to be Alb (67 kDa), which may originate from dead cells. The highest yield of CysC-Alb was 10 mg and was obtained from 600 ml cell culture volume. Alb was purified via HiTrapTM Blue HP affinity chromatograph by using its interaction with the dye Cibacron Blue F3G-A (Figure 9B). 8 mg was the highest yield of Alb, which was obtained from 600 ml cell culture volume.

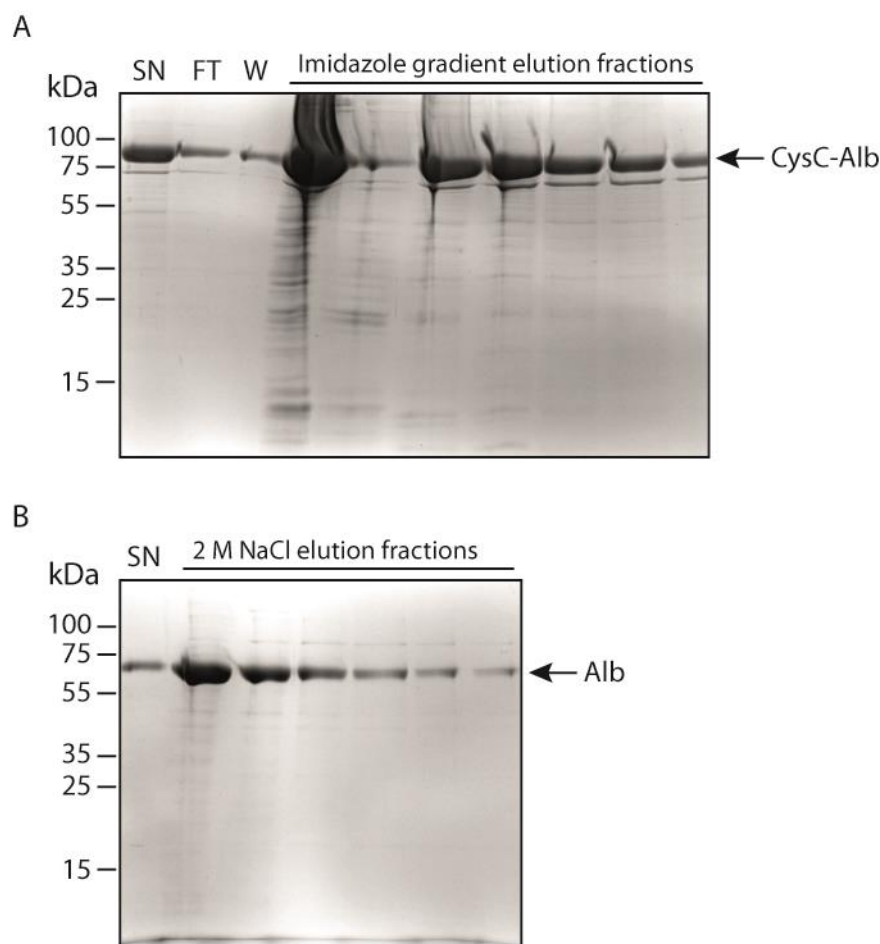


Figure 9: Production of CysC-Alb and Alb in HEK 293E cells. Coomassie staining of cell culture supernatants and purified elution fractions after transfection of HEK 293E cells with CysC-Alb or Alb. The CysC-Alb construct contains an Igk-signal peptide for secretion into the cell supernatant and a C-terminal his-tag for purification, whereas the Alb construct contains no his-tag. The sequences are listed in the appendix. (A) CysC-Alb was purified from 300 ml supernatant by Ni-NTA chromatography and eluted from the Ni-columns with an Imidazole gradient (40 mM, 60 mM, 75 mM, 150 mM, 300 mM, 500 mM, 1 M). (B) Alb was purified from 300 ml by HiTrapTM Blue HP affinity chromatography and eluted with 2 M NaCl. The volume of each elution fraction was 1.5 ml. 15 μ l of the supernatant, the wash (with 20 mM Na₂HPO₄, 300 mM NaCl pH 7.4), the flowthrough and the elution fractions were analyzed on a SDS-PAGE. (SN = supernatant, F = flowthrough, W = wash).

3.1.3 Production of further CysC variants

CysC-Alb and CysC were extended at their C-terminus with the fluorescence protein, ruby, to visualization studies *in vitro*. Ruby is a monomeric red fluorescence protein isolated from marine invertebrates and characterized as highly resistant to denaturation at extreme pH (58). As described above, both fusion proteins were expressed in HEK 293E cells by using an Igk-signal peptide for secretion and a C-terminal his-tag for Ni-affinity chromatography purification (Figure 10A). The fluorescence proteins, CysC-Alb-Ruby and CysC-Ruby were well expressed in HEK 293E cells and could be isolated from the supernatant relatively pure with only little contamination probably by degradation products (Figure 10B, C).

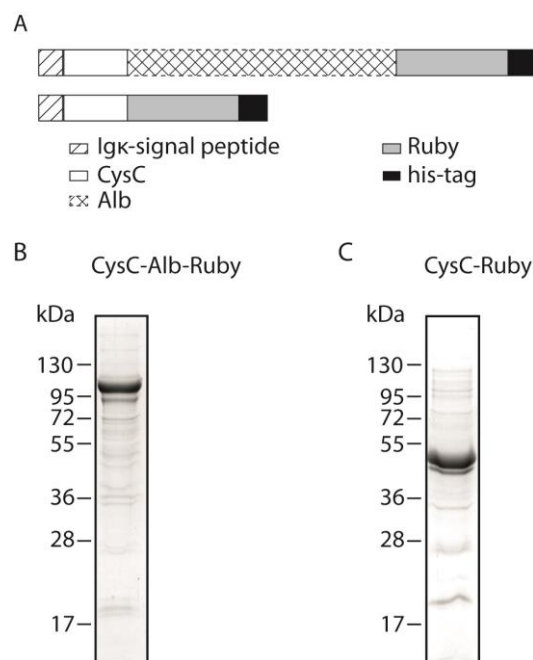


Figure 10: Production of further CysC variants. The pTT5/HEK293 expression system was used for recombinant production of CysC-Alb and CysC fused to the fluorescence protein, ruby. (A) The construct contains a C-terminal his-tag for purification and an Igk-signal peptide for secretion into the cell culture supernatant. In both constructs, the fluorescence protein ruby has been placed N-terminal to the his-tag. The sequences are listed in the appendix. (B, C) 2 µg of purified proteins were separated by SDS-PAGE (12% gel) and stained with Coomassie.

3.1.4 Functional analysis of CysC-Alb

3.1.4.1 Edman Sequencing

After Ni-chromatography purification, CysC-Alb was sent to Beate Jaschok-Kentner (Helmholtz Zentrum für Infektionskrankheiten, Braunschweig) for Edman sequencing in order to confirm a full length N-terminus of CysC in the CysC-Alb fusion protein. As already mentioned before, the two N-terminal amino acid residues are necessary for the tight binding of CysC to cysteine proteases and are therefore needed for successful inhibition. Figure 11A shows an interaction model of chicken CysC with papain, which is exemplary for the interaction of cysteine proteases with CysC. Expression of full length CysC-Alb was unsuccessful with the initial mouse CysC-Alb construct, as it was shortened by 5 amino acid residues at the N-terminus, most likely due to exopeptidase cleavage. Therefore, a second construct was designed in which the N-terminal amino residues of the mouse CysC construct were exchanged by the N-terminal amino acid residues of chicken CysC (Figure 11B), that are considered to be less prone to exopeptidase cleavage. As a result, we were able to express and purify clean CysC-Alb with a correct N-terminus verified by Edman sequencing (Figure 11C).

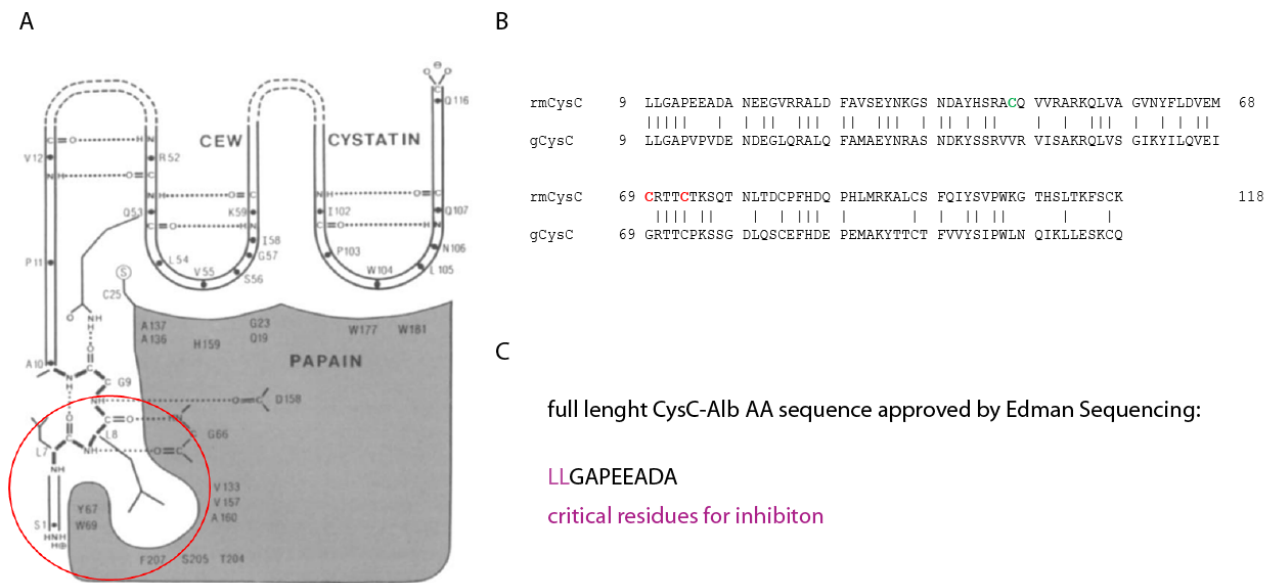


Figure 11. Full length CysC-Alb amino acid sequence was approved by Edman-sequencing. (A) Scheme of the “trunc model” for the interaction of chicken CysC with papain. The two lysines before the first glycine are crucial for the tight binding of cystatin C to papain. (B) Alignment of our recombinant mouse CysC (rmCysC) and chicken CysC (gCysC). rmCysC and gCysC share high sequence homologies. mCysC contains naturally two disulfide bonds (red), a third disulfide bond (green) was introduced for monomer stabilization. (B) For Edman Sequencing, 60 pmol CysC-Alb was run on a 12 % SDS gel and blotted on a PVDF membrane using natriumcarbonat transferbuffer without glycine. The membrane was stained with coomassie blue for 30 sec and CysC-Alb was analyzed for a full-length N-terminus by Edman sequencing.

3.1.4.2 Inhibitory activity of CysC-Alb

CysC is the endogenous inhibitor of the cysteine proteases CatB, CatL, Cat H, CatS (59). Since CatS and CatB were considered to be the most crucial cysteine proteases in the planned experiments, enzymatic activities of these two proteases were measured with CysC-Alb in a FRET-substrate based assay in order to ensure that CysC still contains its inhibitory activity after fusion to Alb. The inhibition of CatS and CatB was tested with different concentrations of CysC-Alb and compared to the inhibition of CatS and CatB by CysC (Figure 12A-D). Cys-Alb and CysC inhibited CatS and CatB partially at substoichiometric concentrations and fully with a slight molar excess of the inhibitor. The initial linear regression was used to calculate the concentration for CysC-Alb and CysC needed to inhibit 0.1 μ M CatS or 0.1 μ M CatB (Figure 12E).

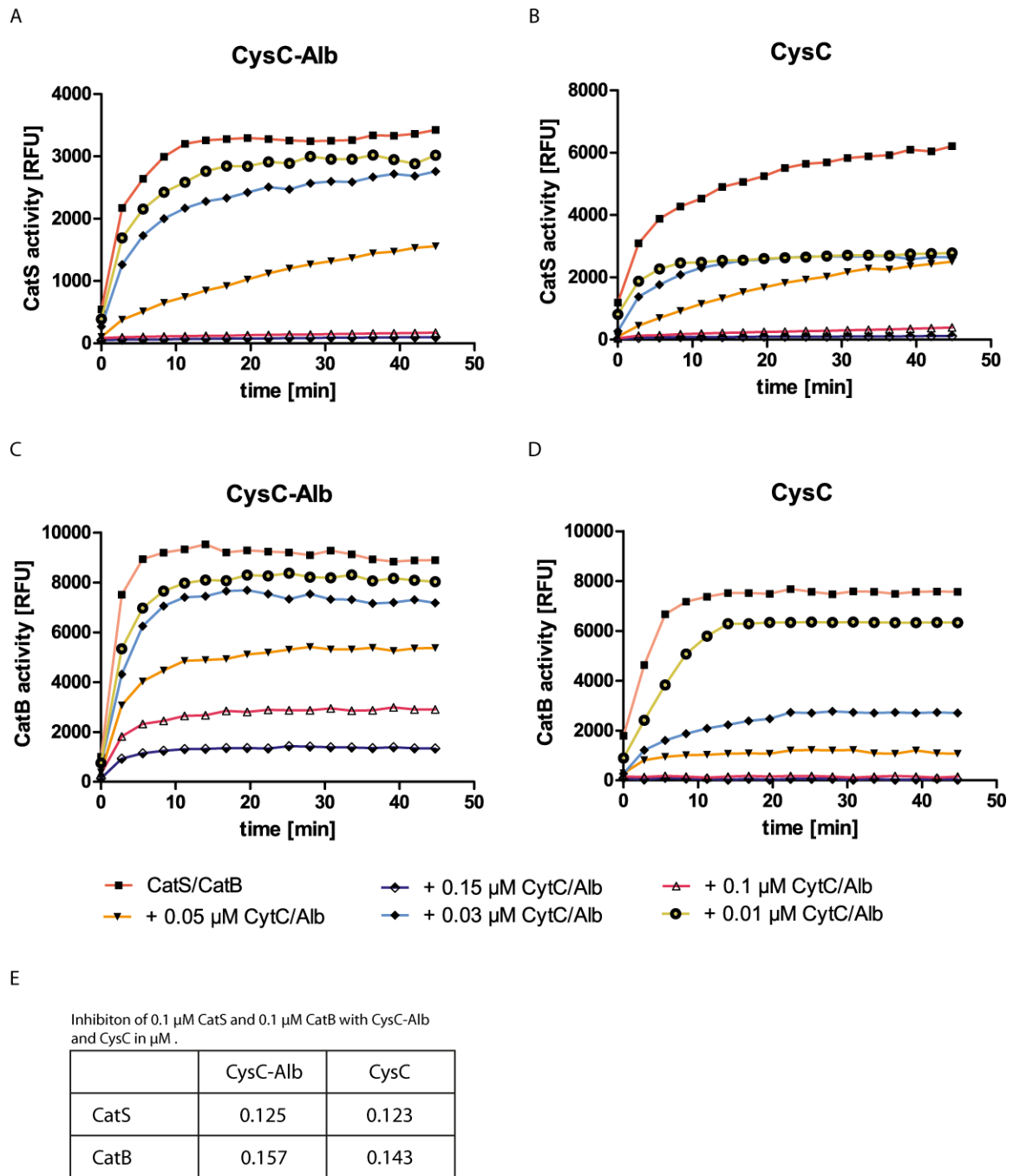


Figure 12: CysC-Alb and CysC inhibit CatS and CatB in a similar manner. To estimate the concentration of CysC-Alb or CysC needed to inhibit CatS or CatB, (A, B) 0.1 μ M recombinant CatS and (C, D) 0.1 μ M recombinant CatB were incubated with varying amounts of CysC-Alb or recombinant CysC. The residual activity was measured by adding 10 μ M of FRET-substrate (CatS: Z-Val-Val-Arg-AMC, CatB: Z-Arg-Arg-AMC) at extinction/emission = 360/440. Data was plotted as relative fluorescence units (RFU) versus time [min] for each sample and one representative example of three technical repeats is shown. (E) The linear regression of the initial time points during which the reaction is linear was used to obtain the concentration of CysC-Alb and CysC needed to inhibit 0.1 μ M CatS or 0.1 μ M CatB.

3.1.4.3 Macrophages internalize CysC-Alb-Ruby

CysC-Alb-Ruby and CysC-Ruby were especially developed and produced for imaging studies of the inhibitor CysC-Alb. Hence, to investigate whether macrophages internalize CysC-Alb, the fluorescent protein CysC-Alb-Ruby was used. RAW264.7 cells were incubated with 40 $\mu\text{g}/\text{ml}$ CysC-Alb-Ruby at 37°C for 2 h. Immediately thereafter, live cell imaging was performed by bright field and fluorescence microscopy. Indeed, macrophages internalized CysC-Alb-Ruby after 2 h incubation (Figure 13).

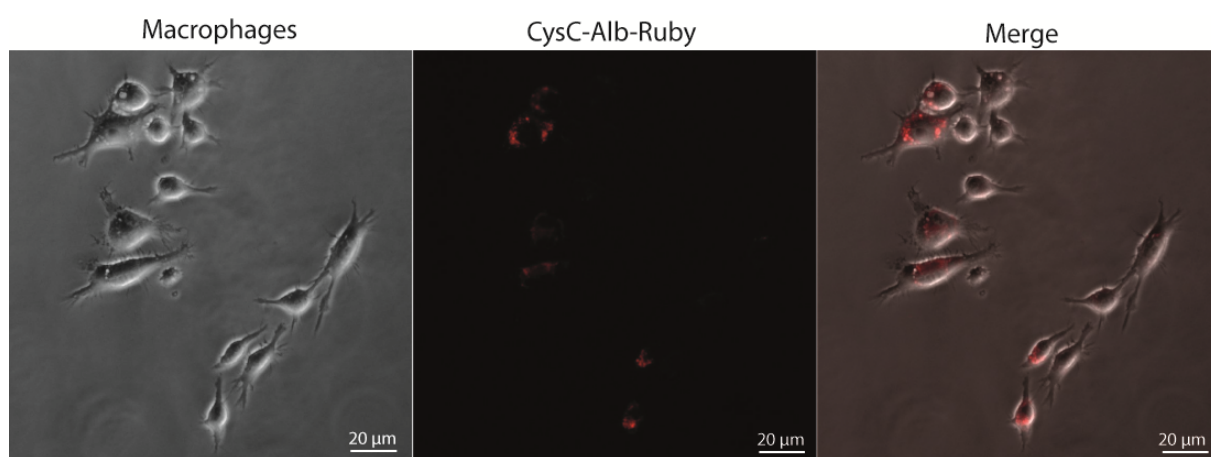


Figure 13: Macrophages internalize CysC-Alb-Ruby. Macrophages were treated with 40 $\mu\text{g}/\text{ml}$ CysC-Alb-Ruby in culture medium for 2h at 37°C. Macrophages were visualized by bright field imaging and CysC-Alb-Ruby by fluorescence imaging (Excitation/Emission=558/605), and images were merged. Magnification is indicated as 62x, *scale bars* = 20 μm

3.1.4.4 CysC-Alb is protected from lysosomal degradation in macrophages

To analyze the advantage of the CysC-Alb fusion protein over CysC, macrophages were incubated with a lysotracker and localization of CysC-Alb-Ruby was compared with CysC-Ruby. Live cell imaging of macrophages using a confocal microscope clarified that CysC-Alb-Ruby is protected from lysosomal degradation by the FcRn-mediated recycling mechanism in macrophages. CysC-Alb-Ruby (red) was not collocated with the signal of the lysotracker (green). In comparison CysC-Ruby was clearly located in lysosomes as indicated as a bright yellow signal due to the double fluorescence signal of CysC-Ruby and the lysotracker (Figure 14).

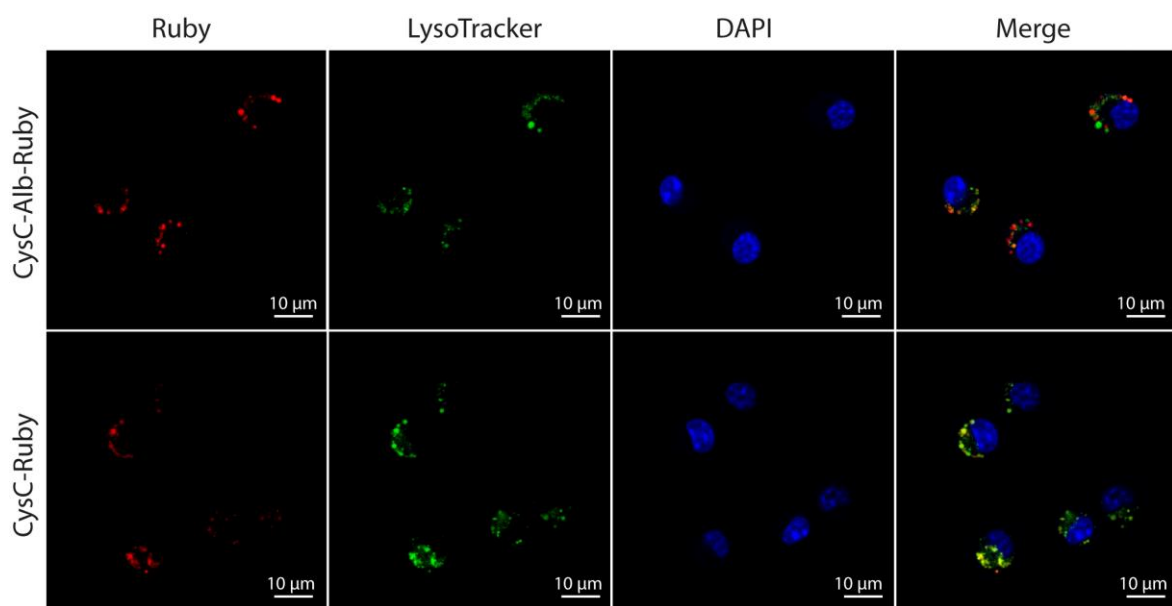


Figure 14: CysC-Alb is protected from lysosomal degradation. Simultaneous visualization of lysosomes (green) by fluorescent labeling and use of CysC-Alb-Ruby or CysC-Ruby (red) in macrophages. Macrophages were seeded onto imaging dishes and incubated with lysotracker (1:1000) and CysC-Alb-Ruby or CysC-Ruby (40 $\mu\text{g}/\text{ml}$) in serum free culturing medium for 2 h. Cell nuclei were stained with Hoechst (blue, 1:10000). Shown are representative fields of live cell imaging by confocal microscopy. Magnification is indicated as 63x, *scale bars* = 10 μm .

3.1.5 CysC-Alb graft preservation in a murine model of LTx

In order to investigate if lung storage in Perfadex containing CysC-Alb protects the graft from cysteine protease mediated graft damage during cold storage and reperfusion, an orthotopic LTx model was used. As EVLP is experimentally used in clinical research to reassess and regenerate donor lungs before LTx, we additionally combined this method with our experimental approach (Figure 15). The orthotopic LTx was performed by Natalia Smirnova (iLBD, Helmholtz Zentrum München).

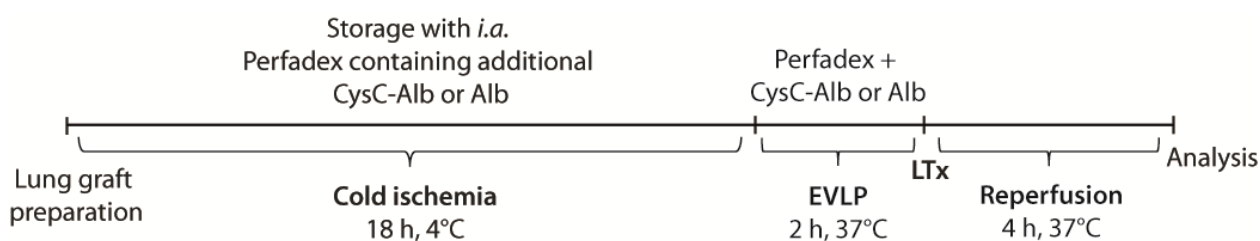


Figure 15: Lung graft preservation, EVLP and lung transplantation procedure. Experimental outline for storage in Perfadex containing 40 µg/ml CysC-Alb or Alb during cold ischemia (18h, 4°C) and *ex vivo* lung perfusion (EVLP, 2h, 37°C), followed by lung transplantation (LTx) and reperfusion (4h, 37°C).

3.1.5.1 CysC-Alb is detectable in lung tissue 4 h after reperfusion

To inhibit lysosomal cathepsins in the extracellular space, CysC-Alb needs to diffuse in the perivascular and interstitial space during CS and EVLP. Hence, whole lung tissue lysates from the transplanted lung were analyzed 4 h after reperfusion for the presence of CysC. The lung has been stored under cold ischemia condition and perfusion with either CysC-Alb or Alb *ex vivo*. Briefly, upon perfusion with PBS to remove blood from the vessels, specimens of the transplanted lung lobe were collected and whole lung tissue lysates were run on a 12% SDS gel. Using a monoclonal CysC antibody, immunoblot analysis revealed the presence of CysC in lung tissue of all CysC-Alb treated lungs. No levels of

CysC were detected in the Alb control group. β -actin was used as an internal loading control (Figure 16).

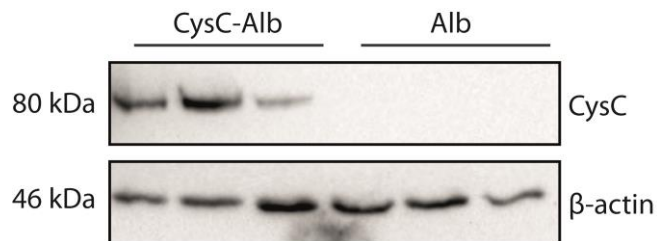


Figure 16: CysC-Alb is present in lung tissue after LTx. Tissue samples of the transplanted left lung were collected 4 h after reperfusion and subsequently lysed for total protein analyses. 15 μ g of whole protein were loaded on a 12% SDS gel followed by immunoblot analysis of CysC. CysC was detected in lung tissue lysates of CysC-Alb treated animals 4 h after reperfusion using a rabbit anti-CysC mAb (1:10000). Detection of β -actin served as loading control.

3.1.5.2 Storage of lung transplants in CysC-Alb improves lung function

After stopping the air flow of the right lung by clamping the right bronchus, the partial oxygen pressure (pO₂) in the left ventricle was measured to examine the potential beneficial effect of CysC-Alb addition to Perfadex during storage and perfusion of the lung transplant in the cold. CysC-Alb and Alb were directly compared at the same concentration (0.04 µg/ml) in our murine LTx model. As envisaged, we found a highly protective effect on graft preservation on the functional level. Addition of CysC-Alb to Perfadex resulted in an almost 30% higher blood oxygenation (Figure 17A) in the left ventricle. Even in the periphery increased pO₂ levels compared to the control were observed (Figure 17B). Nevertheless, morphological studies revealed pulmonary hemorrhage and edema formation in both groups (Figure 17C). This was confirmed by assessing the wet/dry lung weight ratio after CS and EVLP, which is an index for edema formation (Figure 17D). The supplementation of CysC-Alb to the preservation solution did not suppress edema formation.

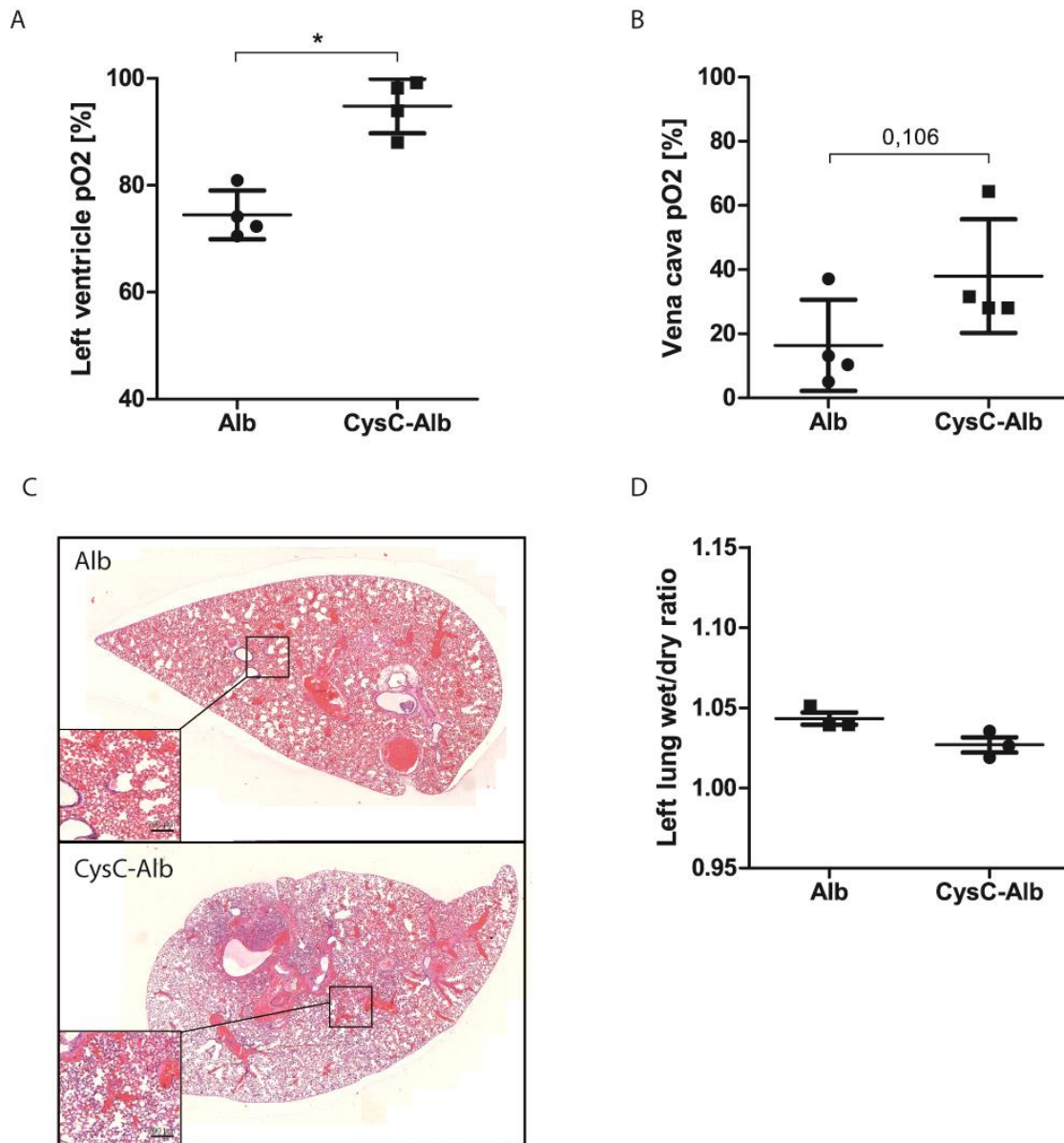


Figure 17: Primary graft dysfunction is reduced by CysC-Alb. Left donor lungs of C57BL/6J mice were stored and perfused in Perfadex supplemented with either Alb or CysC-Alb at 4°C for 18 h (cold storage) and 37°C for 2 h (EVLP). Recipient mice were sacrificed 4 h after reperfusion and the pO₂ (partial oxygen pressure) was measured in the blood from (B) the left ventricle and (A) the vena cava after clamping the right bronchus for 5 min. (C) Haematoxylin and Eosin (HE) staining illustrated the morphology of left lung tissue after LTx (scale bars: 200 µm). (D) Lung wet/dry weight ratio of the left lung was measured after CS and EVLP. Data are presented as means ± SEM of 3-4 mice per group and compared with a Mann-Whitney test (* $p \leq 0.05$)

3.1.5.3 CysC-Alb treatment selectively blocks TNF- α increase in the perfusate

As we expected that CysC-Alb has an anti-inflammatory effect, perfusate samples were collected after 2 h EVLP and subsequently analyzed for inflammatory mediators using a multianalyte cytokine Elisa kit. Pro-inflammatory TNF- α was increased in the Alb control group after EVLP, while CysC-Alb Perfadex supplementation blocked the increase of TNF- α in EVLP perfusate (Figure 18A). Increased Interleukin 6 (IL-6) levels were observed in both groups with no significant reduction after CysC-Alb treatment (Figure 18B). The levels of IL-1 α , IL-1 β , IL-4, IL-10, IL-12, IL-17A, INF- γ , G-CSF, GM-CSF were undetectable in perfusate after EVLP.

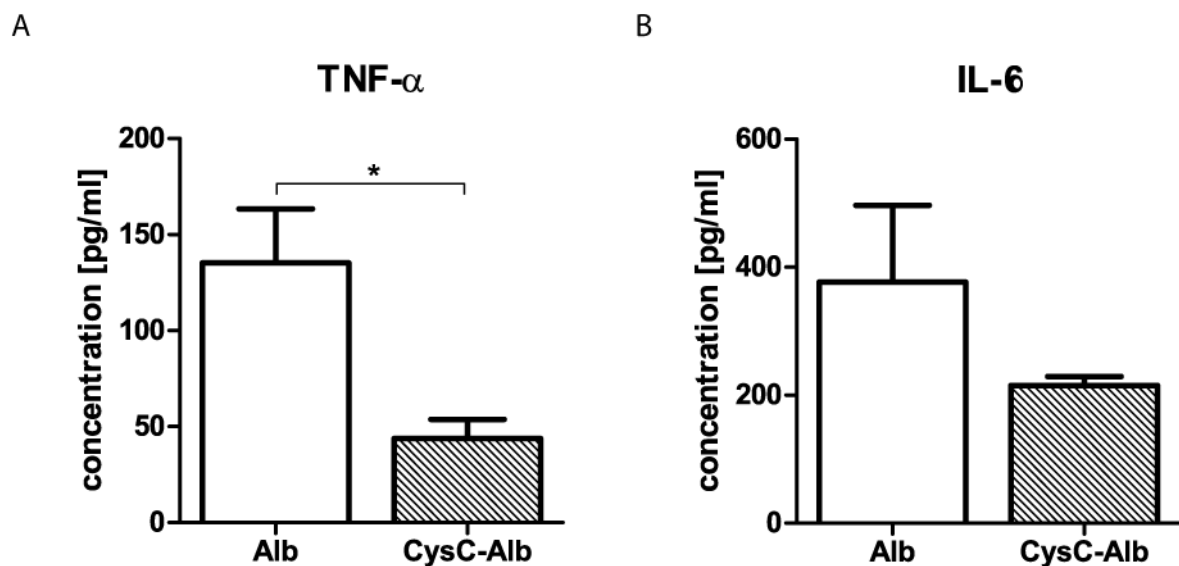


Figure 18: Effect of CysC-Alb on inflammatory mediators in perfusates. (A) TNF- α and (B) IL-6 were measured in the EVLP perfusate after 2 h using a multianalyte ELISA kit. Data expressed as mean \pm SEM of 4 mice per group and compared with a Mann-Whitney test (* $p \leq 0.05$)

3.1.5.5 CysC-Alb protects from apoptotic cell death

To further investigate the protective effect of CysC-Alb preservation supplementation, apoptotic cell death in lung tissue was evaluated 4 h after reperfusion. The total number of apoptotic cells (TUNEL) was significantly lower in lung tissue, which was preserved in Perfadex containing CysC-Alb during cold storage and EVLP compared to the Alb control group (Figure 19A/B). In order to identify the specific cell type protected from apoptotic cell death in the lung, double fluorescence staining of apoptotic cells (TUNEL) and alveolar type 2 cells (AT2, pro-SPC), as well as apoptotic cells (TUNEL) and macrophages (Gal3) was performed. Double immunofluorescent staining demonstrated a high number of AT2 cells that are affected by apoptosis (Figure 19C). Lung macrophages are similarly compromised as evidenced by the colocalization of TUNEL and Gal3 positive cells (Figure 19E). Quantification of double-positive signals revealed that supplementation of Perfadex with CysC-Alb diminished apoptotic cell death of AT2 and macrophages (Figure 19D/F). Quantitative analysis was performed by counting all TUNEL positive and double positive cells for TUNEL/pro-SPC and TUNEL/Gal3 per field of vision in lung sections of the two groups.

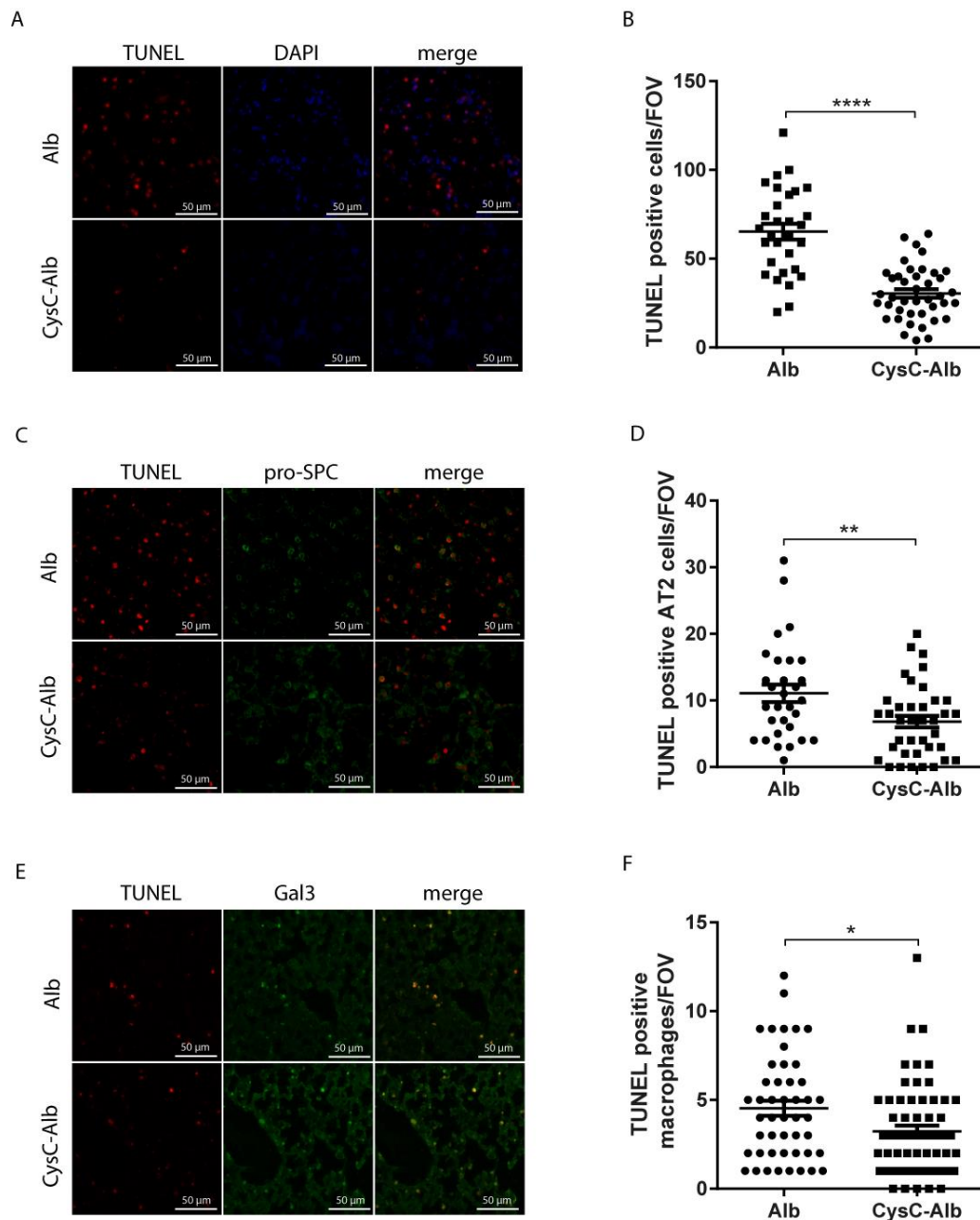


Figure 19: Analysis of apoptotic cell death in lung tissue by TUNEL assay. TUNEL staining of lung paraffin sections was performed to quantitate the protective effect of CysC-Alb compared to Alb added to the lung preservation solution. (A) Apoptotic cells are marked in red, the nuclei of the cells are stained in blue (DAPI). (B) Number of TUNEL-positive cells of all fields of vision in CysC-Alb and Alb treated lungs. (C) Double fluorescent staining of TUNEL and pro-SPC (marker for alveolar type II cells (ATII), green), and (D) total cell count of TUNEL/pro-SPC positive cells in all fields of vision (FOV). (E) Double fluorescent staining of TUNEL and Gal3 (marker for macrophages, green), and (F) total cell count of TUNEL/Gal3 positive cells in all fields of vision (FOV). Values are represented as means \pm SEM of 3-4 mice per group and compared with a Mann-Whitney test (* $p \leq 0.05$, ** $p \leq 0.01$, **** $p \leq 0.0001$). Magnification is indicated as 20x, scale bars = 50 μ m.

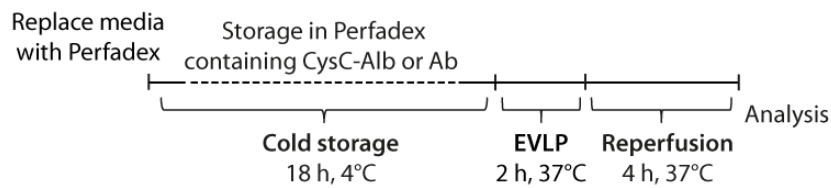
3.1.6 In vitro model of CS and simulated EVLP/Reperfusion

To further investigate events occurring during storage and transplantation an *in vitro* model of non-hypoxic cold storage and EVLP/Reperfusion (R) simulation at 37°C was used, which was adapted from Casiraghi et al. (40). CS and EVLP were simulated in RAW264.7 macrophages by replacing culture medium with Perfadex containing either Alb or CysC-Alb. Following 18 h incubation at 4°C (CS), cell culture plates were rewarmed to 37°C for 6 h to simulate temperatures during 2 h of EVLP and the 4 h period of reperfusion (R) (Figure 20A).

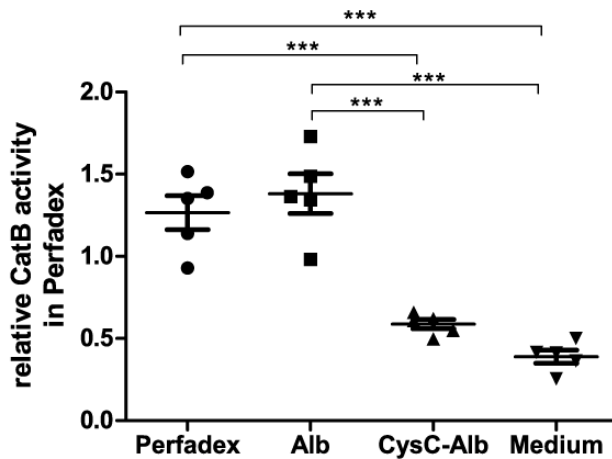
3.1.6.1 CysC-Alb inhibits CatB activity after CS and simulated EVLP/R

Perfadex samples were analyzed for CatB activity following CS and simulated EVLP/R. CS followed by simulated EVLP/R was associated with CatB activity in Alb complemented Perfadex samples and non-treated Perfadex samples. CatB activity was significantly lower in Perfadex samples containing CysC-Alb, which correlated with the activity of CatB in the medium of macrophages cultured at 37°C for 24 h (corresponding to 18 h CS and 6 h EVLP/R) (Figure 20B). The comparison of CatB activity in Perfadex samples of macrophages after CS and CS followed by simulated EVLP/R revealed a significant higher activity of CatB after CS followed by EVLP/R (Figure 20C).

A



B



C

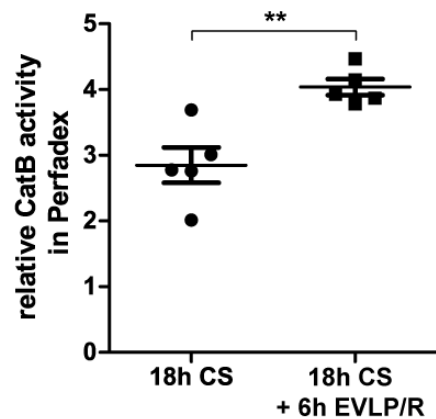


Figure 20: CysC-Alb reduces CatB activity after CS and stimulated EVLP/R. A) Time course of the *in vitro* modeling of CS and simulated EVLP/R. Warm medium was replaced by cold Perfadex (4°C) containing 80 µg/ml CysC-Alb or Alb and incubated for 18 h at 4°C. Following cold storage (CS), cell plates are placed in the incubator at 37°C for 6 h to mimic temperatures during EVLP (2 h) and reperfusion (R, 4 h). B,C) CatB activity in 50 µl Perfadex after 18 h CS, or 18 h CS + 6 h EVLP/R was determined by a FRET-based activity assay. CatB activity was measured in Perfadex containing CysC-Alb or Alb with the FRET-substrate Z-RR- AMC (10 µM) over time. Measurement of CatB activity in Perfadex without supplementation and medium served as controls. The initial reaction velocity (V_0) was obtained in RFU/min by determining the slope of the linear portion of the data plot. Data shown are mean \pm SEM of 5 replicates per group, and a two-tailed Mann-Whitney test was used for statistical analysis. ** $p \leq 0.01$, *** $p \leq 0.005$

3.1.6.2 CysC-Alb does not influence cell death *in vitro*

Since CysC-Alb protected lung cells from apoptotic cell death during CS and EVLP/R *in vivo*, cell viability was assessed by MTT assay in our *in vitro* model of CS and simulated EVLP/R. Even though viability of macrophages treated with Alb and CysC-Alb containing perfadex was drastically decreased in comparison to macrophages cultured in medium, no differences in cell viability was found between macrophages treated with Alb and macrophages treated with CysC-Alb. *In vitro* CS and simulated EVLP/R resulted in a decreased viability of 27% in the Alb group and 29% in the CysC-Alb group compared to the medium control group (Figure 21A). When viability of the different treatment groups (Alb and CysC-Alb) were compared between 18 h CS alone, and 18 h CS following 6 h simulated EVLP/R it became apparent that the viability of macrophages is significantly diminished after the warm up phase of EVLP and R in both treatment groups compared to the viability after CS alone (Figure 21B). To verify if apoptosis is a possible mechanism of programmed cell death, macrophages were examined for cleaved caspase 3 protein by WB. WB analysis showed clearly that there were no differences in cleaved caspase 3 levels in macrophage lysates treated with Alb or CysC-Alb during 18h CS and 6h EVLP/R (Figure 21C, D). We thereby exclude that CysC-Alb has a protective effect in primary cell death events in macrophages in our *in vitro* model of CS and simulated EVLP/R.

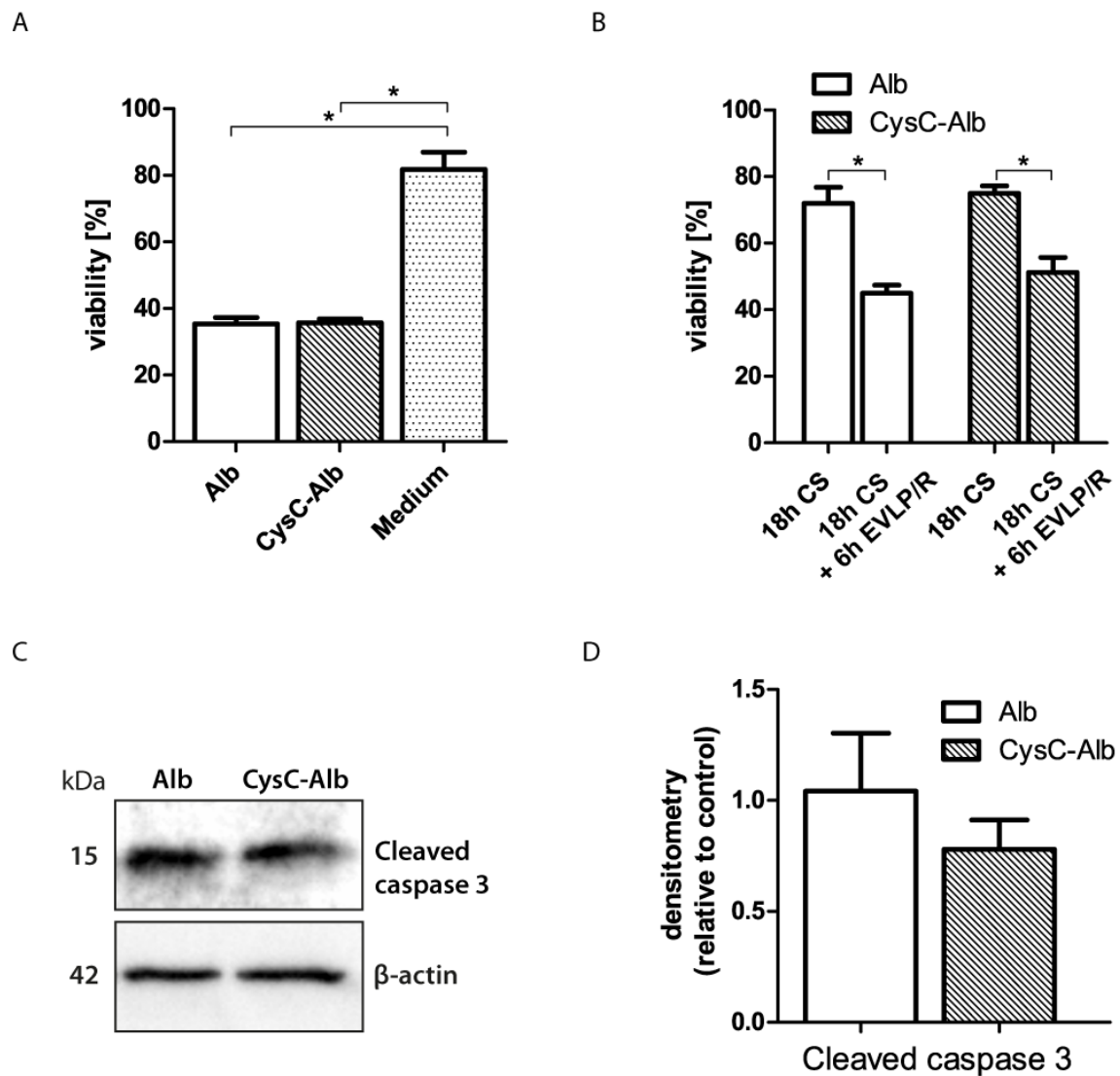


Figure 21: CysC-Alb has no effect on cell death *in vitro*. Macrophages were treated with 40 μ g/ml Alb or CysC-Alb in Perfadex during 18 h CS, or 18 h CS + 6 h simulated EVLP/R at 37°C. Cell viability was detected by MTT assay. (A) Cell viability of CysC-Alb and Alb treated macrophages was directly compared to macrophages cultured in medium after 18 h CS + 6 h simulated EVLP/R. (B) Comparison of cell viability between 18 h CS and 18 h CS followed by 6 h simulated EVLP/R of the different treatment groups (Alb and CysC-Alb). (C) Representative western blot image and (D) densitometry analysis of cleaved caspase 3 in whole macrophage lysates after 18 h CS following 6 h simulated EVLP/R. β -actin served as loading control. Data are shown as means \pm SEM of 5 replicates per group and a two-tailed Mann-Whitney test was used for statistical analysis. * $p \leq 0.05$

3.1.6.3 CatB inhibition results in the reduction of TNF- α release after CS and simulated EVLP/R

To determine the levels of TNF- α released in Perfadex medium, macrophages were treated with Alb or CysC-Alb during *in vitro* CS alone and CS followed by simulated EVLP/R. As expected, CysC-Alb significantly reduced levels of TNF- α in Perfadex compared to the Alb treatment group after CS and simulated EVLP/R (Figure 22A). To clarify whether the reduction of TNF- α in Perfadex is a direct effect of CysC or due to CatB inhibition, we included a CatB inhibitor, CA-074, as treatment group during CS and simulated EVLP/R. In a similar manner like CysC-Alb, CA-074 treatment significantly lowered TNF- α in Perfadex compared to Alb after CS and simulated EVLP/R (Figure 20A). Furthermore, it is noteworthy that the TNF- α level in Perfadex after CS alone were significant lower in the Alb treatment group compared to TNF- α level after CS and simulated EVLP/R (Figure 22B), indicating that the release of TNF- α is induced during the rewarming phase of the macrophages.

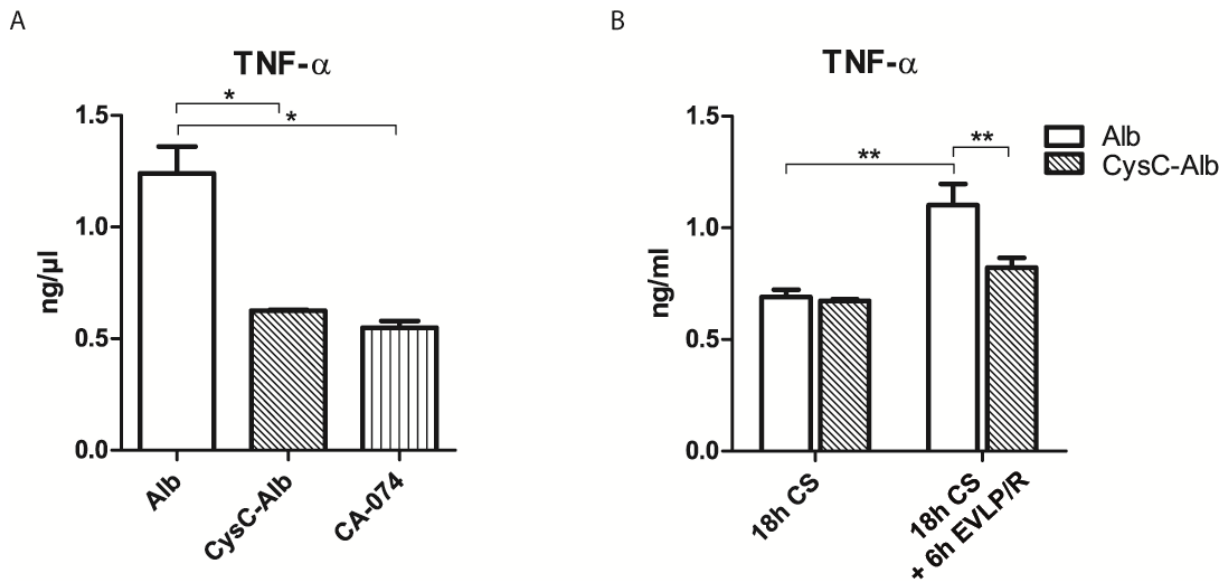


Figure 22: CysC-Alb and CA-074 reduces TNF- α in an *in vitro* model of CS and simulated EVLP/R. Macrophages were treated with Alb, CysC-Alb or CA-074 (CatB inhibitor) in Perfadex during 18 h CS, or 18 h CS + 6 h simulated EVLP/R, followed by the measurement of TNF- α in the Perfadex samples by ELISA. (A) Detection of TNF- α in Perfadex samples containing Alb, CysC-Alb or CA-074. (B) Comparison of TNF-alpha levels in Perfadex containing CysC-Alb or Alb after 18 h CS alone and 18 h CS following 6 h simulated EVLP/R. Data are shown as means \pm SEM of 5 replicates per group and a two-tailed Mann-Whitney test was used for statistical analysis. * $p \leq 0.05$, ** $p \leq 0.01$

3.1.6.4 CysC-Alb has no effect on TNF- α expression

To examine the modulatory effect of CysC-Alb on cytokine expression during CS and EVLP/R, CS and EVLP/R at 37°C was simulated in macrophages. As illustrated in Figure 23, the gene expression of TNF- α (Figure 23B), IL-1 α (Figure 23C), and IL-1 β (Figure 23D) were not altered in the CysC-Alb group compared to the Alb control group. CysC-Alb significantly up-regulated the mRNA expression of anti-inflammatory IL-10 relative to the control (Figure 23A). However, it is noteworthy that the relative expression of IL-10 is very low in both treatment groups and thus should not be taken into consideration.

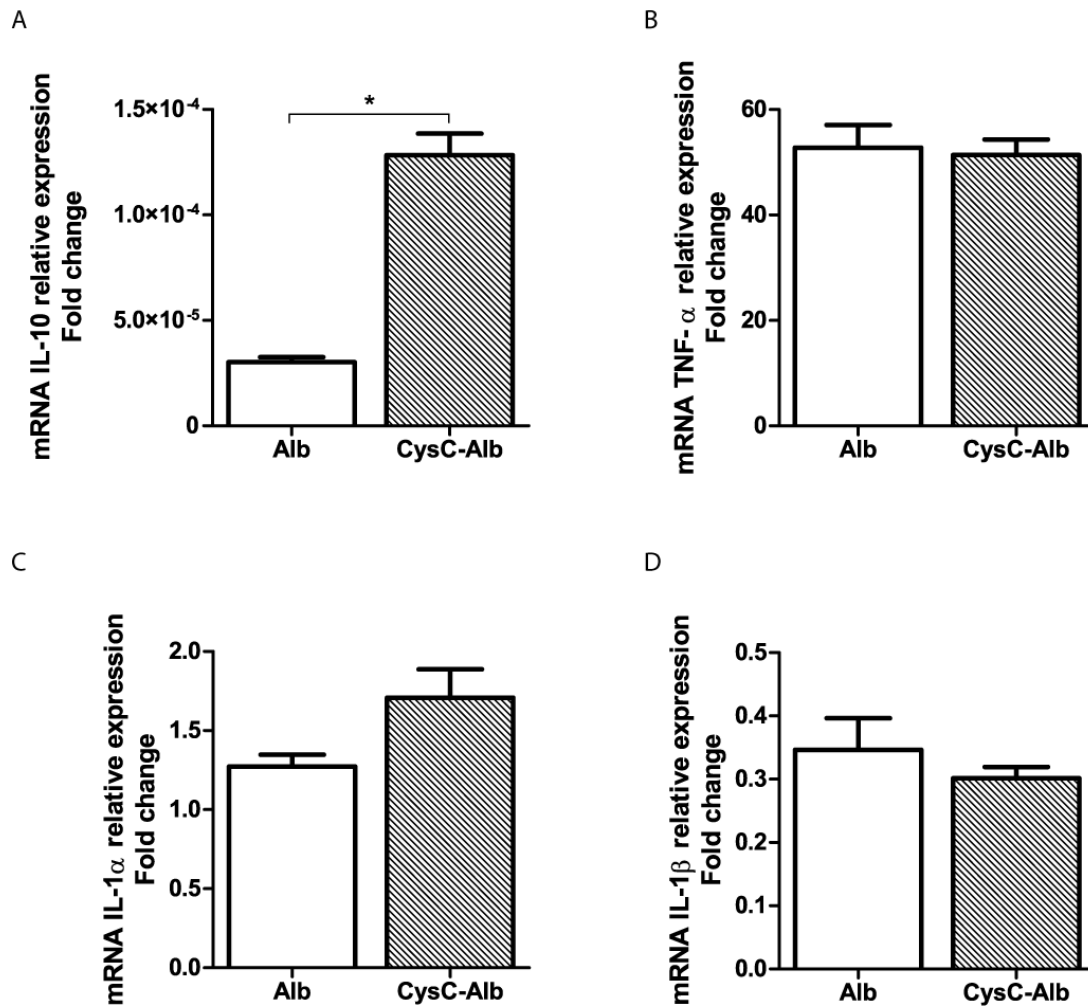


Figure 23: CysC-Alb does not affect TNF- α gene expression. Macrophages were treated with Perfadex containing Alb or CysC-Alb during 18 h of CS and 6 h simulated EVLP/R. mRNA expression levels of IL-10, TNF- α , IL-1 α and IL-1 β were measured by quantitative real time PCR. Hypoxanthine-guanine-phosphoribosyltransferase (HPRT) was used as reference gene for normalization. Data are shown as mean \pm SEM of 4 replicates and a two-tailed Mann-Whitney test was used for statistical analysis. * $p \leq 0.05$

3.1.6.5 CysC-Alb inhibits CatB-induced activation of TACE

TNF- α release is mainly mediated by shedding of the membrane-bound TNF- α by TNF- α converting enzyme (TACE). As we demonstrated that the addition of CysC-Alb to Perfadex diminished TNF- α release as a response of CatB inhibition in our *in vitro* model of CS and simulated EVLP/R, we analyzed if CatB is involved in the regulation of TACE

activity in whole macrophage lysates. Consistent with the reduction in TNF- α , CysC-Alb significantly inhibited TACE activity compared to Alb (Figure 24A), implicating that active CatB regulates TACE activity and thereby induces TNF- α shedding. Moreover TACE activity of CysC-Alb treated macrophages correlated with the activity of TACE in macrophages treated with specific TACE/ADAM10 inhibitors (TACE/ADAM10 inhibitor: **GW280264**, Figure 22A). GW treatment during CS and simulated EVLP/R also significantly blocked TNF- α release from macrophages in Perfadex (Figure 24B).

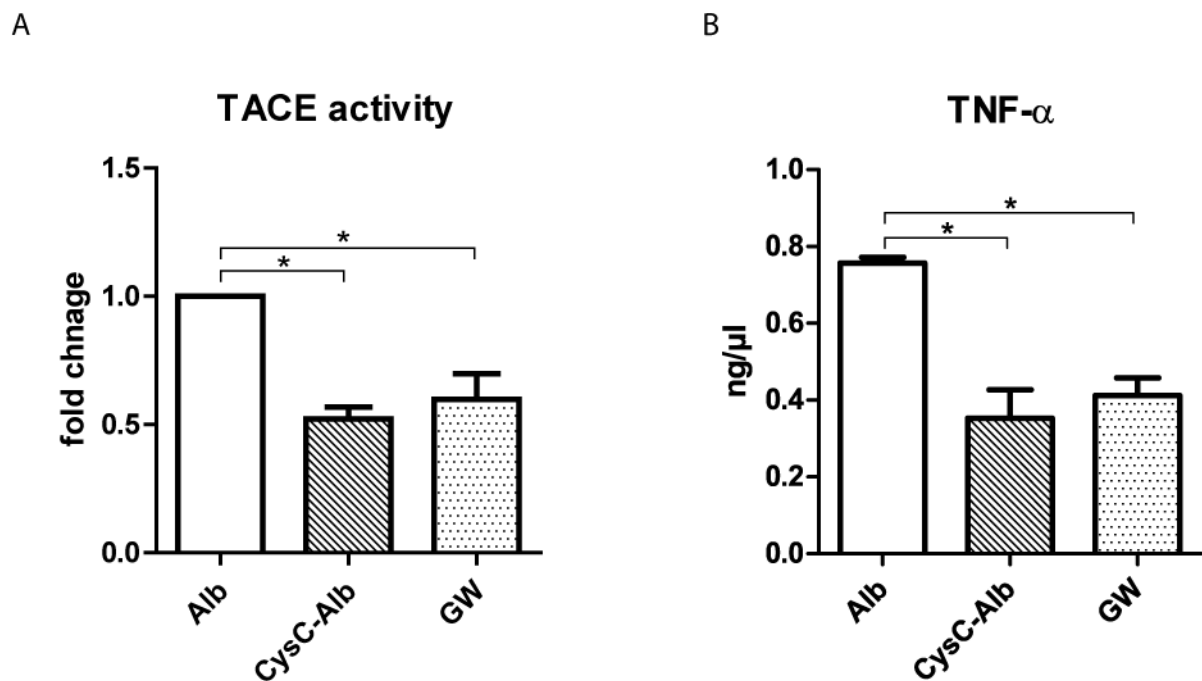


Figure 24: CatB is involved in the regulation of TACE. Macrophages were treated with Perfadex containing Alb, CysC-Alb or the TACE/ADAM10 inhibitor **GW280264** during 18 h of CS and 6 h simulated EVLP/R. (A) TACE activity was detected in whole macrophage lysates using SensoLyte® 520 TACE (α -Secretase) Activity Assay Kit. (B) Perfadex samples were collected for detection of TNF- α by ELISA assay. Data are shown as mean \pm SEM of 4 replicates and a two-tailed Mann-Whitney test was used for statistical analysis. * $p \leq 0.05$

3.2 CatC inhibition in LTx - Results

In order to evaluate the potential beneficial effect of ICatC pretreatment in mice recipients we have chosen a murine experimental model of orthotopic LTx illustrated in Figure 25. From a previous study with rats we knew that 10 days of ICatC treatment would be sufficient to effectively reduce NSP activities in circulating neutrophils and two doses per day are needed because of the short circulation half-life of ICatC. The outcome of ICatC pretreatment of the two treatment groups (ICatC and vehicle) were compared by analyzing different parameters 4 h after reperfusion of the transplanted left lung lobe. The orthotopic LTx was performed by Natalia Smirnova (iLBD, Helmholtz Zentrum München) and the EVLP by Carmela Morrone (iLBD, Helmholtz Zentrum München).

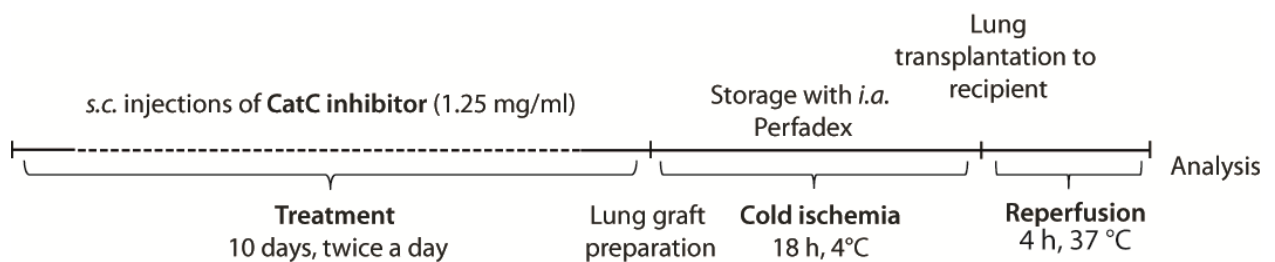


Figure 25: ICatC premedication and lung transplantation procedure. Experimental outline of subcutaneously injections of 100 μ l ICatC (1.25 mg/ml) in C57BL/6J recipient mice, donor lung graft storage in Perfadex during cold ischemia (18 h, 4°C) followed by graft transplantation and reperfusion (4 h, 37°C). Specimen were collected 4 h after reperfusion and analyzed.

3.2.1 CatC inhibition leads to reduced NSP activity in the bone marrow

To investigate, if preventive ICatC treatment of recipient mice eliminated the conversion of serine-protease zymogens to their active forms during biosynthesis, we measured the relative PR3 and NE activities in lysates of purified BM-derived neutrophils using optimized FRET substrates for murine serine proteases. Cleavage of the murine PR3

substrate, TAMRA-GVRRVVQYQD-dap-(CF) and the substrate ABZ-GAVVASELR-Y-(NO₂)-D for both, murine NE and PR3 was determined in PMN lysates of ICatC and Veh treated mice. PMN lysates of ICatC mice revealed significantly less enzymatic activity of (Figure 26A) PR3 and (Figure 26B) NE compared to vehicle (Veh) treated mice. As negative control, PMN lysates of PR3/NE double knockout (PR3/NE -/-) mice were used. The obtained fluorescence signal in these cells reflects the unspecific substrate cleavage by the lysates. Consequently, the remaining PR3 activities in ICatC treated mice are due to unspecific cleavage of the substrate. Our results indicate that PR3 and NE activities are almost completely eliminated in BM-derived neutrophils.

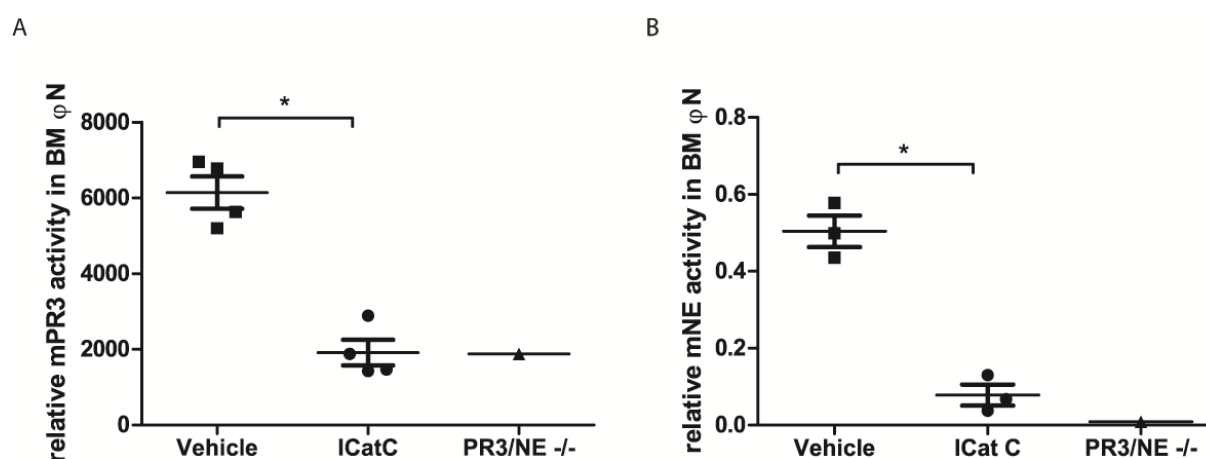


Figure 26: ICatC treatment reduces NSP activity in the bone marrow. Neutrophils were isolated from the BM 4 h after reperfusion. To determine NSP activity after 10 days ICatC treatment neutrophil lysates were tested by a FRET-based activity assay. (A) PR3 activity was measured with the FRET-substrate TAMRA-GVRRVVQYQD-Dap-(CF) and (B) NE activity with the FRET-substrate Abz-GAVVASELR-Y-(NO₂)-D. Neutrophil lysate from PR3/NE -/- mice were used as negative control. The initial reaction velocity (V_0) was obtained by determining the slope of the linear portion of the data plot. Values are represented as means \pm SEM of 3-4 mice per group and compared with a Mann-Whitney test (* $p \leq 0.05$). The y-axis shows the fluorescence in relative fluorescence units (RFU).

Next, we performed WB analysis with PMN protein lysates to examine whether the reduced enzymatic activities after ICatC treatment correlate with the protein content of

PR3 and NE. Densitometry and statistical evaluation revealed no differences of PR3 and NE immunoreactive proteins in PMN lysates of ICatC and vehicle treated mice (Figure 27A,B).

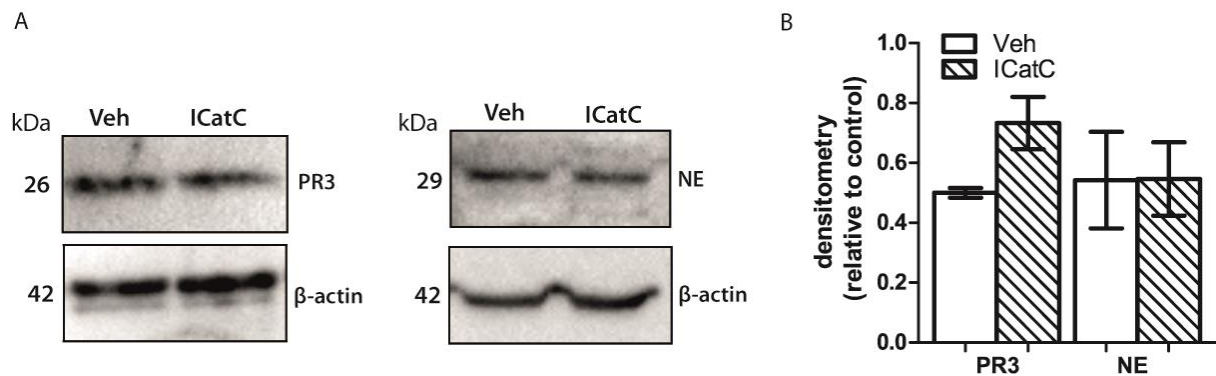


Figure 27: Western blot analysis for PR3 and NE in PMN lysates. 15 µg of PMN lysates of ICatC and Veh treated mice were loaded onto a 12% SDS gel, followed by immunoblot analysis of PR3 and NE. (A) Representative Western blot images and (B) densitometry analysis of PMN lysates for PR3 and NE using specific polyclonal PR3 (1:1000) and monoclonal NE (1:1000) antibodies. Immunodetection of β-actin served as loading control. Values are represented as means ±SEM of 4 mice per group.

3.2.2 ICatC pretreatment improves PGD and reduces the inflammatory response

4 h after reperfusion mice were euthanized and the air and blood flow of the non-transplanted right lung was stopped by clamping the right bronchus to measure the partial oxygen pressure (pO_2) in the left heart ventricle. Decreased pO_2 values indicate graft dysfunctions after prolonged cold ischemic storage. Pretreatment with ICatC resulted in an almost 20% higher blood oxygenation (Figure 28) in the transplanted left lung.

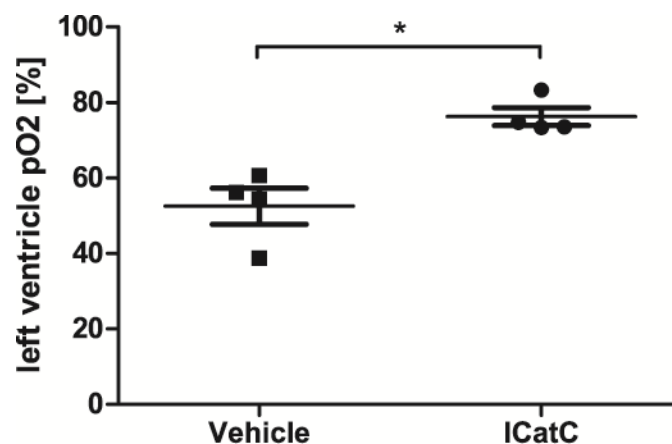


Figure 28: ICatC pretreatment improves primary graft function. Recipient C57BL/6J mice were euthanized 4 h after reperfusion and the partial oxygen pressure (pO₂) of the oxygenated blood in the left heart ventricle was measured after clamping the right bronchus for 5 min. Data is presented as group means \pm SEM of 4 and compared with a Mann-Whitney test (* $p \leq 0.05$).

After the pO₂ measurements, different specimen were collected to analyse the impact of ICatC treatment on graft protection. As envisioned, we found a highly protective effect of ICatC against the inflammatory response after LTx. Immunohistochemical staining of lung graft tissue by the neutrophil-specific antibody Ly-6G were performed to compare neutrophil infiltration in the lung tissue after reperfusion (Figure 29A). Analytical evaluation of images revealed no differences in the number of lung infiltrating neutrophils in both groups (Figure 29B). BAL neutrophil counts for the two different treatment groups showed a clearly decreased amount of neutrophils in ICatC treated mice compared to Veh treated mice (Figure 29C), indicating the preservation of the capillary barrier after ICatC treatment. Furthermore, we looked into changes in the proinflammatory cytokine levels of IL-1 β , IL-6, IL-8, IL-12, IL-17, TNF α and INF γ , and found a significant reduction in IL-6 after ICatC treatment (Figure 29D).

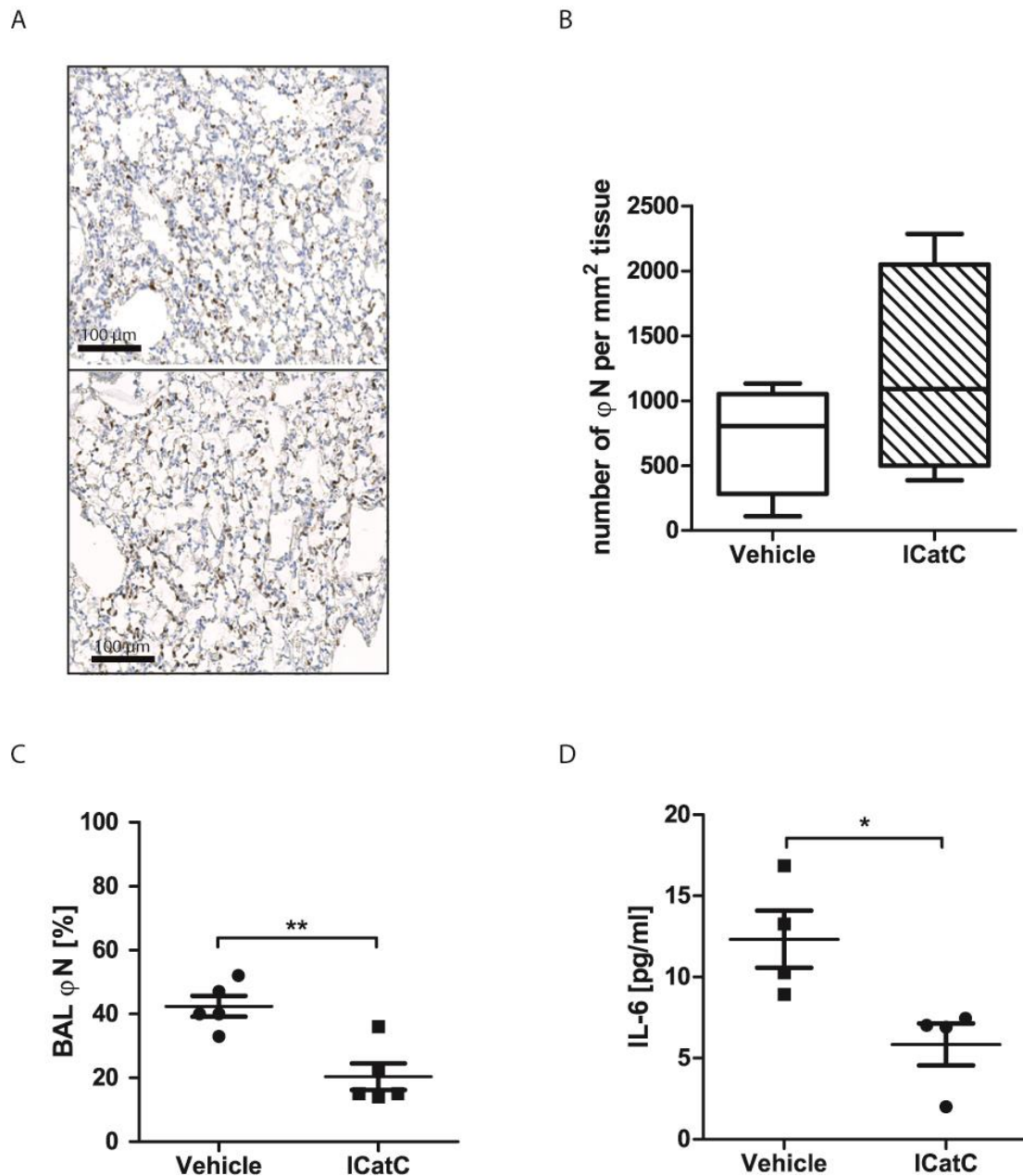


Figure 29: ICatC pretreatment improved lung graft quality and reduced inflammatory response. The outcomes of ICatC and vehicle treatment were compared after sacrificing the mice 4 h after LTx. (A) Immunohistochemical staining and (B) quantification of neutrophils in the transplanted left lung from 10 randomly chosen visual fields. (C) Bronchoalveolar lavage neutrophil counts for ICatC and vehicle treated animals. (D) BAL fluid was obtained and analyzed for proinflammatory IL-6 for the two different treatment groups. Scale bar = 100 μm . Magnification is indicated as 20x. Data is presented as group means \pm SEM. $n = 4\text{-}5$ mice per group. $*p \leq 0.05$ (Mann-Whitney test), $**p \leq 0.01$ (independent t-test)

3.2.3 Presence of NSP positive neutrophils in the lung

As Papillon-Lefevre patients, which are characterized by a loss of function mutation in the CatC gene (CTST), do not only show a defect in zymogen processing, but also eliminate NSP zymogens completely, we hypothesized that this is also the fate in mice. To test the hypothesis in our experimental model after pharmacological CatC inhibition, we stained paraffin lung sections with Ly-6G and NE antibodies for co-localization detection of neutrophils and NE. All neutrophils were positive for NE revealing the presence of the NE protein in the lung (Figure 30).

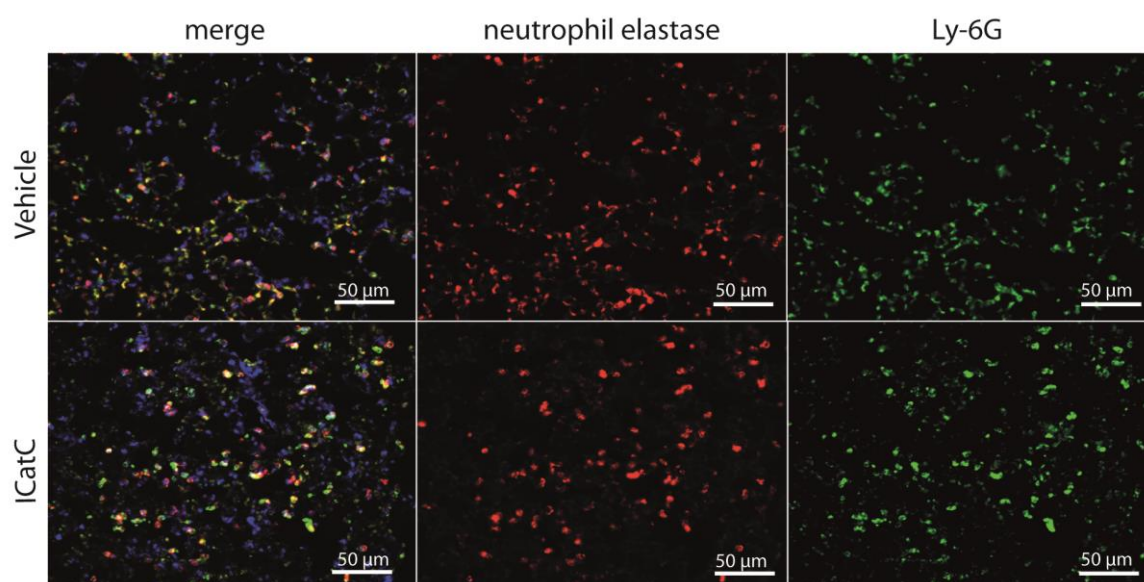


Figure 30: Appearance of NE positive neutrophils in lung tissue after ICatC treatment and LTx. Paraffin-embedded tissue sections of the transplanted left lung of ICatC and vehicle treated mice were fluorescently stained with both a monoclonal Ly-6G - (clone 1A8, 1:400) and a polyclonal NE specific (1:1000) antibody for colocalization analysis of neutrophils and NE. Sections shown are representative images of 4 mice per group. Magnification is indicated as 20x, *scale bars* = 50 µm.

Additionally, we found no differences in PR3 and NE protein levels after ICatC treatment when whole lung tissue was analyzed by semi-quantitative WB and densitometry (Figure 31A/B). These findings were supported by quantitative ELISA measurements of NE, which did not show a significant difference between ICatC and Veh treated mice (Figure 31C).

Moreover, the graph reveals the differences in NE protein in whole lung tissue and PMN lysate (Figure 31C). Whole lung tissue and PMN lysate from PR3/NE $-/-$ mice was used as negative control. Since the NE antibody used for immunohistochemistry and WB analysis is not able to distinguish between active and inactive (zymogen) NE we wanted to clarify whether the detected PR3 protein in whole lung lysates was enzymatically active. Alpha-1-antitrypsin (AAT) antibody was used to detect the formation of an irreversible complex with active PR3/NE, which is expected to appear as a 77 kDa band after SDS PAGE and Western blotting. Alpha-1-antitrypsin (AAT) is only able to form a complex with mature PR3/NE, not with the inactive pro-PR3/NE. The results reveal that PR3/NE is not proteolytically active after ICatC treatment as indicated by the lack of 77kDa complex formation in comparison to vehicle treatment (Figure 31D).

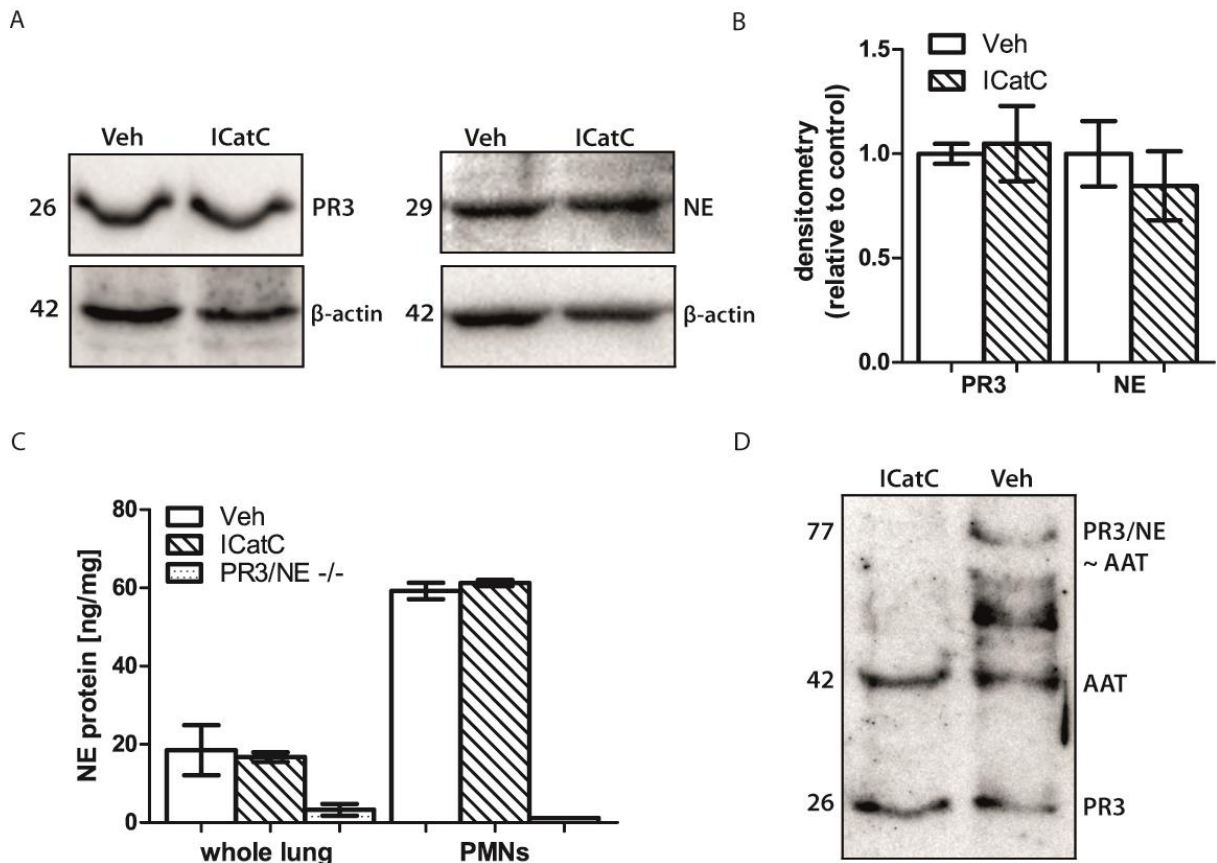


Figure 31: PR3 and NE zymogens are present in lung tissue after ICatC pretreatment. Whole lung tissue lysate of the transplanted left lung lobe of both groups were analyzed by Western blot and ELISA. (A) Representative Western blots and (B) densitometry determination of whole lung lysate PR3 and NE in ICatC treated mice compared to vehicle treated mice. (C) Quantitative determination of NE protein in whole lung tissue and in PMN lysates from vehicle-, ICatC-treated and PR3/NE-/- mice. (D) In order to determine if the detectable PR3 and NE are enzymatically active, PR3, AAT and PR3/AAT complexes were simultaneously detected by immunoblotting. Immunodetection of β -actin served as loading control.

4. Discussion

4.1 CysC-Alb in LTx – Discussion

Donor lungs transported and stored for more than 6 h are not accepted for transplantation because of a high risk of postsurgical complications and transplant dysfunction. The short storage period limits the availability of lung grafts for transplantation. Extended storage times increase the extent of metabolic and structural changes in the transplant and as a consequence the severity of the early inflammatory response in the transplant after reperfusion.

In this study, we investigated the role of CatB released from lysosomes during extended CS of 18 h and 2 h EVLP, and its impact on early graft dysfunction after 4 h LTx. To this end, we developed different variants of the endogenous cysteine protease inhibitor, CysC, and as a result were able to show that it is protected from lysosomal degradation and can be utilized for imaging applications *in vitro*. We explored its clinical potential in organ preservation during CS and EVLP in graft protection from I/R injury after LTx using a clinically relevant mouse model and an *in vitro* model of CS and simulated EVLP/R. Our results demonstrate that CysC-Alb protects lung cells from apoptosis and improves early graft function immediately after reperfusion of the transplanted lung. Moreover, our findings indicate that TNF- α release during simulated CS and EVLP/R is a consequence of CatB induced TACE activation.

4.1.1 Development of a highly potent cysteine protease inhibitor

Biopharmaceuticals generally face the problem of rapid clearance. In order to create a more efficient inhibitor for therapeutic applications, the endogenous cysteine protease inhibitor, CysC was covalently attached to the N-terminus of Alb by gene fusion. Due to

the unique recycling mechanism of Alb via the FcRn, we developed a novel inhibitor with anticipated prolonged circulatory half-life and a high inhibitory activity against CatS and CatB. The fusion of small therapeutic molecules, such as α and β interferon (60, 61), insulin (62) and granulocyte stimulating factor (52), to Alb has already been intensively explored and all reports documented improved pharmacokinetics compared to the non-fused analogues. The first Alb fusion therapeutic was approved for the treatment of diabetes mellitus type II in 2014 (63).

Initially, the authentic sequence of mouse CysC was used for the production of the Alb fusion inhibitor. However, N-terminal protein sequencing revealed three different protein variants, with only one having a full length N-terminus. The most crucial part for the interaction of CysC with cysteine proteases are the three N-terminal amino residues before the first glycine, which are highly conserved (64). Since CysC-Alb is able to enter endosomal compartments due to its binding affinity to FcRn, we suggest that CysC-Alb was posttranslational processed by endosomal endo-peptidases and -proteases. Hence, we have chosen to exchange the mouse N-terminal sequence by the N-terminal sequence of chicken CysC which is not prone to posttranslational processing. CysC is a monomeric protein with two conserved disulfide bridges (Cys73-Cys83 and Cys97-Cys117), but when crystallized it forms domain-swapped homo-dimers. Once formed, CysC dimers completely lose their inhibitory activity against cysteine proteases. In order to avoid dimer formation, a monomeric stable mouse CysC was designed by introducing an engineered third disulfide bond (Cys47-Cys69). According to Kolodziejczyk et al. this variant of human CysC is significantly less susceptible to dimerization and its inhibition of papain is unaltered (65).

In the present pre-clinical LTx study, CysC alone would be rapidly cleared metabolically.

Hence, we used the newly invented efficient inhibitor with enhanced tissue and cell penetration and were able to detect high levels of CysC in lung tissue perfused with CysC-Alb during CS and EVLP. Other specific small molecule inhibitors of lysosomal cysteine proteases would possibly have a similar effect; however, low toxicity and site specific actions of therapeutics are crucial for their safety. The organ preservation procedure presented in this study would be technically feasible in a clinical trial with no intolerance risk for the patients due to the fact that CysC and Alb are endogenous proteins and are tolerated as self-antigens.

4.1.2 Effect of CysC-Alb on lung graft quality

The results of our preclinical study strongly support our hypothesis that inhibition of extracellular lysosomal cysteine proteases by CysC-Alb during CS and EVLP is suited to protect lung cells from apoptosis inducing signals and could improve early lung transplant function in patients. We assume that CysC-Alb of the preservation solution diffused into the perivascular and interstitial space of the lung graft during CS and EVLP and was therefore optimally positioned to protect the graft against extracellular cysteine proteases released from lysosomes. EVLP complies with existent ethical standards in clinical research and was therefore included in our setting.

The inhibitory effect of CysC-Alb on cysteine protease activity appears to represent a major mechanism of lung transplant protection in this pre-clinical model. Our results indicate that the inhibitory activity of CysC-Alb attenuated apoptotic cell death of AT2 cells and macrophages in the lung transplant which usually occurs during CS, EVLP and R. Apoptosis has been described to contribute to I/R injury in various models of human and mouse I/R injury, including lung models. Ischemic storage is associated with necrosis,

whereas apoptosis dominates during early reperfusion. In a human LTx study lungs had about 30% of their cells undergoing apoptosis 2 h after reperfusion (66). Similar results were obtained experimentally after 6 and 12 h ischemic storage, however longer storage periods were associated with predominantly necrotic cells in lung tissue of rats (67). Whether apoptotic cell death is harmful for organ function remains controversial. Fischer et al. have demonstrated a correlation between necrosis and transplanted lung function, but apoptosis did not correlate with lung function (67). In contrast, other authors stated that injections of anti-apoptotic agents before reperfusion reduced I/R injury of the kidney and heart in mouse models after warm ischemia (68, 69). We have observed improved lung function of transplants preserved in CysC-Alb 4 h after reperfusion and could show the reduction of AT2 apoptosis, suggesting a link between AT2 survival and lung function after transplantation. AT2 cells are mostly found at the alveolar-capillary barrier, where they play important roles for the normal pulmonary function: Production of pulmonary surfactant, transepithelial movement of water, and regeneration of the alveolar epithelium following lung injury (40).

Ischemic CS initiates the activation of resident macrophages, which release proinflammatory cytokines and mediate I/R injury during reperfusion. TNF- α is one of them and is a key player in the induction of the extrinsic apoptotic pathway. Moreover, TNF- α has been described to activate nuclear factor κ B (NF κ B), which is known to be involved in the apoptosis signaling pathway (70). As the supplementation of CysC-Alb to Perfadex during CS and EVLP reduced both, TNF- α and apoptotic cells 4 h after LTx, it seems likely that TNF- α functions as a mediator of the apoptotic cascade in our setting. Additionally, there is evidence that TNF- α is implicated in the early phase of organ

reperfusion during which it was shown to induce organ damage (71-73). TNF- α blockade had a protective effect against organ injury after intestinal I/R injury (74).

With the development of CysC-Alb we intended to target extracellular cysteine proteases either actively released from lysosomes or leaked from permeable lysosomes. Due to the fusion to Alb, CysC might also act intracellularly while it is bound to FcRn in early endosomes. Apart from its extracellular function, CysC has been shown to inhibit human coronavirus replication (75) and CatB and legumain activity in cancer cells (76, 77), indicating that CysC functions intracellularly too. Using CysC-Alb-Ruby, we showed for the first time by immunofluorescence imaging that CysC-Alb is internalized by macrophages via FcRn binding. Despite these possibilities our results let us assume that the effect of CysC-Alb on TNF- α release and apoptosis is primarily mediated via an extracellular mechanism.

4.1.3 CysC-Alb protects lung cells from CatB mediated damage

To clarify the therapeutic mechanism of CysC-Alb in immediate lung graft protection, we tested the anti-apoptotic and anti-inflammatory effects of CysC-Alb in a cell culture model that simulates features of lung preservation and reperfusion at body temperatures. 18 h of CS and 6 h EVLP/R simulation at 37°C resulted in reduced cell viability, a result similar to what was observed in another cell model of simulated I/R injury (78), as well as in rat lung transplant studies in which significant cell death was found after 18 h of ischemic storage (67, 78). CysC-Alb was not able to reduce cell death in our *in vitro* model of CS and EVLP/R simulation, as shown by analyzing cleaved caspase 3. These findings indicate that primary cell death caused by the harsh physical conditions, such as CS and the incubation solution, cannot be prevented by CysC-Alb. Nevertheless

CysC-Alb significantly inhibited CatB activity in Perfadex samples, which were released from lysosomes of dying or stored cells. Consequently, we assume that CysC-Alb has an effect on the secondary damage of lung cells caused by extracellular CatB, which cannot be demonstrated in our *in vitro* model of CS and simulated EVLP/R.

The greatest lung tissue damage is thought to be caused by the return of blood components at body temperature after transplantation (79). This is supported by our findings that cell viability and CatB release is significant increased after CS followed by simulated EVLP/R at 37°C compared to CS preservation alone.

4.1.4 CatB is involved in the regulation of TACE

The metalloprotease TACE performs ectodomain shedding of various transmembrane proteins, most of which are regulators involved in inflammatory processes, including TNF- α , both its receptors (TNFR1, TNFR2), IL-6R and ligands of the epithelial growth factor receptor (EGFR) (80-82). Hence, TACE activity is a key player in controlling inflammatory signaling pathways (81, 83). TACE activates TNF- α signaling by proteolytic cleavage of membrane-bound pro-TNF- α thereby releasing active TNF- α from the cell surface (80).

In this study, we were able to reduce TNF- α release *in vivo* during EVLP as well as in our *in vitro* model of I/R injury by CysC-Alb treatment. CysC has been shown to reduce TNF- α mRNA expression and subsequently release of TNF- α in LPS activated monocytes by downregulating phosphorylation of the ERK1/2 pathway (84). By contrast, in our study gene expression levels of TNF- α were not affected pointing to an ERK1/2 signaling pathway independent mechanism of TNF- α release. Therefore, we examined whether CatB inhibition might have a direct effect on TACE activity. We analyzed the activity of TACE on the surface of macrophages after CS and EVLP/R simulation at 37°C. TACE

activity was found to be lower on the cell membrane after CysC-Alb treatment. The possibility of a direct effect of CysC-Alb on TACE activity was excluded by confirming the results with a specific CatB inhibitor.

To date, the regulatory mechanisms leading to TACE maturation and subsequent activation are not fully elucidated. Catalytic active TACE is synthesized as inactive proenzyme, in which the N-terminal pro-domain acts as autoinhibitor preventing the enzyme from inappropriate premature processing of substrates (85). One of the most important posttranslational modifications is the removal of the pro-domain in the Golgi that occurs at two different sites before active TACE is trafficked to the cell surface. One site, namely the downstream site, is located between the pro-domain and the catalytic domain and contains a proprotein convertase (PC) consensus cleavage site (86). The secondary cleavage site to this prerequisite cleavage is embedded within the N-terminal pro-domain (referred to as upstream site) (87). Furin like proteases, members of the PC family, have been demonstrated to be involved in the activation of metalloproteases in several studies. For instance, mutations in the furin cleavage site of the downstream site of metalloproteases ADAM10, ADAM12 and ADAM19 prevented the removal of the pro-domain and as a consequence kept the enzyme inactive (88, 89). According to Wong and colleagues only furin like proteases are implicated in the processing of the upstream site of TACE, whereas the downstream site cleavage can be processed by other proteases or could be autocatalytically nicked (87). By contrast, myeloid cells were shown to have TACE shedding activity despite blocking of all PCs (90). This indicates that the role of furin in processing of TACE is complex and still not understood in detail. Another posttranscriptional modification, which has been argued to be hallmark of TACE activity, is the phosphorylation of the cytoplasmic domain of TACE by mitogen-activated protein

kinases (MAPK) and polo-like kinase2 (PLK2) (91, 92). Furthermore it is speculated that phosphatidylserine is required to be exposed on the cell surface to bring TACE into position for shedding its targets (93). Activation of TACE seems to depend on the availability of co-factors influencing TACE biology and might be cell type specific. Recently, iRhom has been described as one of these cofactors promoting the trafficking from the ER to the Golgi and after the release of the pro-domain the trafficking to the plasma membrane (94). We suggest that CatB is involved in the activation of TACE as a cofactor under pathological conditions such as I/R injury. A possible scenario would be the processing of an adjacent cleavage site to the downstream PC site of the prodomain. Whether the CatB dependent TACE regulation occurs during TACE maturation, export or on the cell surface and by which mechanism remains to be elucidated in the future.

4.1.5 Limitations

Several limitations to the EVLP and the LTx procedure performed here needs to be addressed. The EVLP circuit design in this study is “open” rather than “closed” as usually used in EVLP protocols in clinics. We envisaged a favorable effect by replacing the perfusate solution during EVLP, and hereby removing proinflammatory cytokines and neutrophils that could concentrate in the lung in a closed circuit. The potential benefit of this approach has been stated before in a murine and a human EVLP study (95, 96). Parameters that are evaluated as standard in human EVLP protocols, such as pulmonary vascular resistance and airway pressures could not be monitored, as it is technically not feasible in our murine EVLP system. In comparison to human allogenic lung grafts, the transplanted lungs were taken from young, healthy isogenic donors. The unavoidable blood loss in the recipient mice during the microsurgical procedure was not

compensated by blood transfusions. Hence, the hemodynamic and circulatory status of the transplanted mice during the post-surgical phase was not ideal. Despite these challenges, which affected all experimental groups, we believe that our results are a promising basis for future studies. Another important point that should be mentioned is that we only examined the impact of CatB inhibition by CysC-Alb in our experimental setting. However, CysC-Alb also inhibits lysosomal CatS and CatL; hence there is a possibility that our results are the consequence of multiple cysteine protease inhibition, and not only CatB inhibition alone.

In summary, by analyzing the protective effect of CysC-Alb during lung transplant preservation, we have demonstrated that CysC-Alb improves lung function and diminishes apoptotic cell death after LTx. We propose that CatB released from lysosomes of macrophages during CS and EVLP/R mediates TACE activation on the cell surface, which induces TNF- α secretion. TNF- α binds to death receptors on other lung cells and induces the extrinsic apoptotic signaling cascade leading to apoptosis (Figure 23). CysC-Alb inhibited extracellular CatB in our experimental set-up and thereby prevented shedding of membrane bound TNF- α , and the subsequent induction of AT2 and macrophage apoptosis. By using CysC-Alb containing perfadex we were able to prevent the secondary damage of lung cells caused by lysosomal CatB.

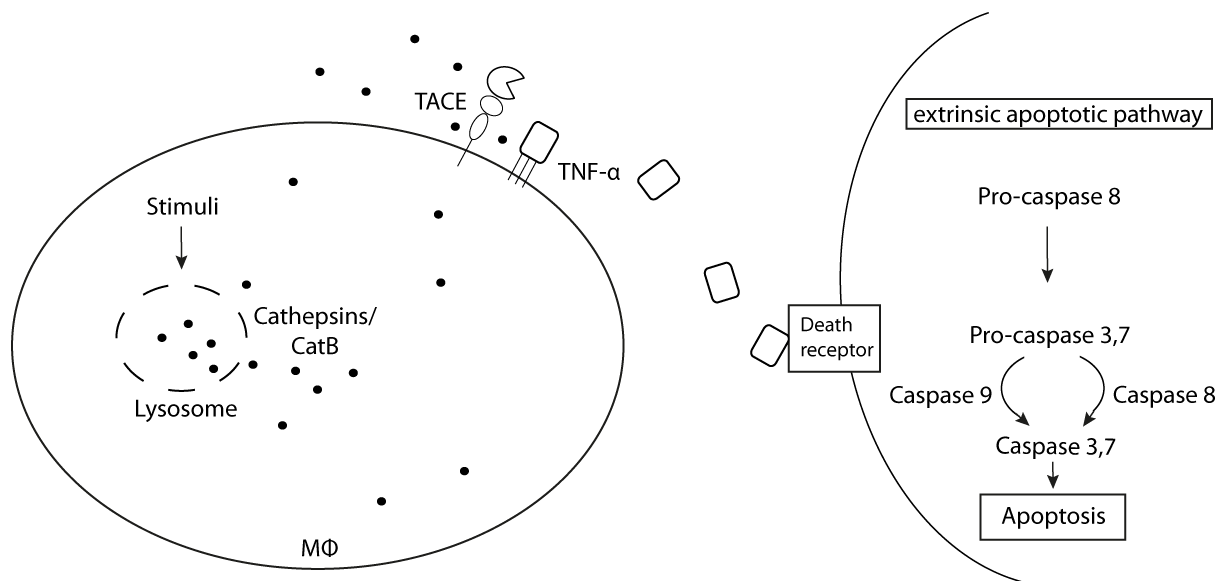


Figure 32: Proposed mechanism of apoptosis induction during CS and EVLP/R. In the course of CS and EVLP/R, cathepsins including CatB are released from lysosomes of dying or reversibly stressed cells. Extracellular CatB activates TACE on these and other cells. As a consequence, TNF- α is shedded from the cell membrane and binds to death receptors on other cells, inducing the intrinsic apoptotic pathway by cleavage of pro-caspase 8 and pro-caspase 3, 7.

4.2 CatC inhibition in LTx - Discussion

Neutrophils are usually the first leukocytes to infiltrate transplanted organs during reperfusion and are well recognized to be critical mediators for I/R injury (135). Therefore, they are a great risk factor for the development of PGD and chronic allograft rejection. Most work on neutrophils during I/R has focused on their destructive properties, that causes tissue damage by the release of oxidative effectors and NSPs (116, 117, 136). In this preclinical study, we demonstrate that NSP mediated inflammation and dysfunction of the lung transplant can be mitigated by the prevention of their biosynthesis in the BM by CatC inhibition several days before LTx. We revealed that the pharmacological inhibition of CatC did not only reduce NSP maturation in the bone marrow of mice recipients, but also had a protective effect on post-operative lung function and reduced the inflammatory response after reperfusion.

4.2.1 Effects of eliminated NSP activity on LTx outcome

NE and PR3 are both destructive enzymes with a wide range of substrates including various components of the extracellular matrix. In addition to matrix degradation, NE influences cell signaling by cleavage of receptors, cytokines and adhesion molecules (102). The exact role of NE and PR3 in I/R injury still remains poorly defined at the molecular biochemical level *in vivo* and *vitro*. Nevertheless, clear evidence for the involvement of NSPs in I/R injury and PGD development following organ transplantation has been provided in previous pre-clinical studies. Silvestat, a synthetic NE inhibitor, was successfully used to suppress neutrophil activation and secretion of proinflammatory mediators after I/R injury in rodents and in an *ex vivo* perfusion model in pigs. In

addition, Silvestat increased the survival rate after I/R injury caused by supravisceral aortic clamping in rats (116, 117, 137). We could confirm the beneficial effect of reduced NSP activity by showing decreased alveolar permeability, improved lung function and reduced inflammatory mediators as a result of CatC inhibition.

Furthermore, in the present study we demonstrated significant decreased IL-6 levels in BALF after ICatC treatment of the recipient shortly after reperfusion of the transplanted lung. IL-6 is an important mediator of the acute phase response, but also stimulates inflammatory and auto-immune processes in many diseases by multiple pathways. As such, IL-6 has been implicated in the pathophysiology of PGD. In a large cohort of 336 patients, early post-transplant BALF IL-6 was associated with an increased prevalence of PGD (138). Indeed, it was revealed in another small patients cohort that BALF IL-6 levels were increased in patients with PGD compared to those without PGD development (139). Furthermore, gene set enrichment and gene expression analyses already identified IL-6 as a key mediator in the inflammatory pathway of PGD development in patients and a rat I/R injury model (140, 141). Similarly to our study, Iskender et al. used AAT, a proteinase inhibitor with anti-inflammatory properties in a pig LTx study to reduce the inflammatory response related to IR injury. All observed cytokines were lower in the AAT treatment group with IL-6 being significantly reduced (142). Beyond its proteolytic function, NE further enhances inflammatory responses probably via an induction of IL-6 and IL-8 release.

4.2.2 CatC inhibition severely reduces NSP activity in the BM and lung

Activation of NSP zymogens requires the cleavage after a glutamic acid residue at their N-terminus by CatC (143). In the absence of CatC activity, zymogens are synthesized in

neutrophil precursors in the BM, but are differently eliminated during neutrophil maturation in mice and men. As reported for mice deficient in the CatC gene, CatG was undetectable in BM-derived PMN lysates, while NE bands were still present as shown by WB. NE activity in PMN lysates, however, were severely reduced and equivalent with the background activity in NE knockout mice (107). These previous findings from mice with genetic CatC deficiency are in line with our data in ICatC treated mice, revealing immunoreactive PR3 and NE in lysates from BM-derived PMNs. After LTx, PR3 and NE were detected by immunofluorescence in transplant infiltrating neutrophils in ICatC and Veh treated recipient mice. Moreover, their protein levels were verified by WB in whole lung tissue of both groups. Adding an excess of AAT, a protease activity dependent NSP inhibitor, we investigated whether or not the immunoreactive NSPs in whole lung tissue are zymogens. We found inactive zymogens of PR3 in ICatC treated recipients, but active PR3 in Veh treated recipients. Covalent complexes between NSPs and AAT are susceptible to degradation by other proteases, which most likely explains the additional bands of smaller size in the lung lysates of Veh treated mice. Our observations indicate that sorting of NE/PR3 to azurophil granules occurs normally in the presence of the prodiptide in mice. The fact that CatG levels were found to be reduced in a previous study, suggest that NSPs may not be sorted in an identical manner. In the absence of CatC, CatG zymogens can be missorted into a different class of granules (144), which potentially targets them for degradation.

Biallelic missense mutations with loss of CatC and its activity in PLS patients are associated with a concomitant reduction in the amounts and activities of NSPs in circulating mature neutrophils in PLS patients. Zymogens, however, are normally synthesized and sorted in PLS promyelocytes and disappear during subsequent stages of

neutrophil differentiation probably because of intracellular degradation (145). These findings were in agreement with observations in macaques after prolonged pharmacological inhibition of CatC. In contrast, our data show the presence of zymogens in mature neutrophils in murine lung tissue. The difference between primates and rodents could be attributed to differences in the number of neutrophils and their serine protease zymogen levels or by an increased susceptibility of zymogens to intracellular degradation in humans.

4.2.3 Clinical potential of our translational approach

Despite conservative clinical approaches of the lung graft, about 25% of lung transplant recipients still develop PGD. Hence, ameliorating treatment options for LTx recipients is crucial to improve LTx outcome. In two phase 1 studies of healthy volunteers, Cat C inhibition was well tolerated with only minor skin desquamation as side effects, but these were not considered to prevent further clinical studies (127, 128). Long-term administration of a CatC inhibitor developed by AstraZeneca is currently assessed in bronchiectasis patients over a 24 week treatment period (ClinicalTrials.gov Identifier: NCT03218917). Solid evidence for a safe and ethically acceptable application of CatC inhibitors have been given; hence they may also be considered as a treatment option for patients on the LTx waiting list. As patients on the LTx waiting list usually suffer from end-stage pulmonary diseases and are therefore closely or stationarily monitored with intensive medical care, it would be feasible to treat them long term during their waiting time for a lung transplant. With the pre-operative ICatC treatment of the recipient it would be possible to suppress the inflammatory response mediated by recruited and activated neutrophils, and the subsequent local NSP release. Our results indicate that 10 days of CatC inhibition are sufficient to reduce NSP activities completely in mice. Looking

100

at neutrophil maturation kinetics in humans, treatment with a CatC inhibitor will require 21 days of administration to be efficacious in humans (146, 147). This is not a limiting factor as transplantation patients usually face more than 15 days on the LTx waiting list. Furthermore, according to this study and a previous one in primates, CatC inhibition does not compromise neutrophil recruitment to the site of inflammation, indicating that the diverse and highly redundant neutrophil defense mechanisms are not impaired by CatC inhibition in general.

4.2.4 Limitations

As the investigational novel drug INS1007 was not available to us for transplantation studies in mice, a functionally similar CatC inhibitor, XPZ-01, was assessed by *subcutaneous* administration of two daily doses in this pilot study. Due to the highly challenging transplantation procedure in mice, we studied only the outcome of PGD 4 h after LTx and evaluated the effect of only one dose of ICatC. Many data which are routinely monitored in the clinics cannot be recorded in a small animal transplantation model. Therefore, we have not measured blood pH, carbon dioxide in the left pulmonary artery or right ventricle and graft compliance 4 hours LTx. However, our positive results encourage for future studies assessing beneficial effects after longer treatment periods, different doses and longer observation post LTx.

In conclusion, nearly complete inhibition of NE and PR3 activities was demonstrated with a reversible CatC inhibitor in an experimental murine LTx model. With this anti-proteolytic shield early LTx outcome of transplanted mice has been improved. We anticipate that preoperative treatment with CatC inhibitors in humans is a safe and adjustable treatment option for LTx candidates. In view of the promising phase I trials,

CatC inhibitors can be rapidly translated into clinics. CatC inhibitors alone or in combination with improved organ preservation procedures represent a novel drug class for the prevention of early post-operative complications and the development of PDG post LTx.

5. Reference list

1. Travis WD, Costabel U, Hansell DM, King TE, Jr., Lynch DA, Nicholson AG, et al. An official American Thoracic Society/European Respiratory Society statement: Update of the international multidisciplinary classification of the idiopathic interstitial pneumonias. *Am J Respir Crit Care Med*. 2013;188(6):733-48.
2. Yusen RD, Christie JD, Edwards LB, Kucheryavaya AY, Benden C, Dipchand AI, et al. The Registry of the International Society for Heart and Lung Transplantation: Thirtieth Adult Lung and Heart-Lung Transplant Report--2013; focus theme: age. *J Heart Lung Transplant*. 2013;32(10):965-78.
3. Christie JD, Kotloff RM, Ahya VN, Tino G, Pochettino A, Gaughan C, et al. The effect of primary graft dysfunction on survival after lung transplantation. *Am J Respir Crit Care Med*. 2005;171(11):1312-6.
4. Christie JD, Sager JS, Kimmel SE, Ahya VN, Gaughan C, Blumenthal NP, et al. Impact of primary graft failure on outcomes following lung transplantation. *Chest*. 2005;127(1):161-5.
5. King RC, Binns OAR, Rodriguez F, Kanithanon RC, Daniel TM, Spotnitz WD, et al. Reperfusion injury significantly impacts clinical outcome after pulmonary transplantation. *Ann Thorac Surg*. 2000;69(6):1681-5.
6. de Perrot M, Liu M, Waddell TK, Keshavjee S. Ischemia-reperfusion-induced lung injury. *Am J Respir Crit Care Med*. 2003;167(4):490-511.
7. Eltzschig HK, Eckle T. Ischemia and reperfusion--from mechanism to translation. *Nat Med*. 2011;17(11):1391-401.
8. Carden DL, Granger DN. Pathophysiology of ischaemia-reperfusion injury. *J Pathol*. 2000;190(3):255-66.

9. Ogawa S, Gerlach H, Esposito C, Pasagian-Macaulay A, Brett J, Stern D. Hypoxia modulates the barrier and coagulant function of cultured bovine endothelium. Increased monolayer permeability and induction of procoagulant properties. *J Clin Invest.* 1990;85(4):1090-8.
10. Carroll MC, Holers VM. Innate autoimmunity. *Adv Immunol.* 2005;86:137-57.
11. Todd JL, Palmer SM. Bronchiolitis Obliterans Syndrome The Final Frontier for Lung Transplantation. *Chest.* 2011;140(2):502-8.
12. Hicks M, Hing A, Gao L, Ryan J, Macdonald PS. Organ preservation. *Methods Mol Biol.* 2006;333:331-74.
13. Southard JH, Belzer FO. Organ preservation. *Annu Rev Med.* 1995;46:235-47.
14. McCord JM. Oxygen-derived free radicals in postischemic tissue injury. *N Engl J Med.* 1985;312(3):159-63.
15. Zimmerman BJ, Granger DN. Mechanisms of reperfusion injury. *Am J Med Sci.* 1994;307(4):284-92.
16. Mura M, Andrade CF, Han B, Seth R, Zhang Y, Bai XH, et al. Intestinal ischemia-reperfusion-induced acute lung injury and oncotic cell death in multiple organs. *Shock.* 2007;28(2):227-38.
17. Jennings RB, Sommers HM, Smyth GA, Flack HA, Linn H. Myocardial necrosis induced by temporary occlusion of a coronary artery in the dog. *Arch Pathol.* 1960;70:68-78.
18. Tecchio C, Cassatella MA. Neutrophil-derived chemokines on the road to immunity. *Semin Immunol.* 2016;28(2):119-28.
19. Tecchio C, Micheletti A, Cassatella MA. Neutrophil-derived cytokines: facts beyond expression. *Front Immunol.* 2014;5:508.
20. Winterbourn CC, Kettle AJ, Hampton MB. Reactive Oxygen Species and Neutrophil Function. *Annu Rev Biochem.* 2016;85:765-92.

21. Klausner JM, Paterson IS, Goldman G, Kobzik L, Rodzen C, Lawrence R, et al. Postischemic renal injury is mediated by neutrophils and leukotrienes. *Am J Physiol.* 1989;256(5 Pt 2):F794-802.
22. Albadawi H, Oklu R, Raacke Malley RE, O'Keefe RM, Uong TP, Cormier NR, et al. Effect of DNase I treatment and neutrophil depletion on acute limb ischemia-reperfusion injury in mice. *J Vasc Surg.* 2016;64(2):484-93.
23. Sawa Y, Matsuda H. Myocardial protection with leukocyte depletion in cardiac surgery. *Semin Thorac Cardiovasc Surg.* 2001;13(1):73-81.
24. Zheng Z, Chiu S, Akbarpour M, Sun H, Reyfman PA, Anekalla KR, et al. Donor pulmonary intravascular nonclassical monocytes recruit recipient neutrophils and mediate primary lung allograft dysfunction. *Sci Transl Med.* 2017;9(394).
25. Van Raemdonck D, Neyrinck A, Verleden GM, Dupont L, Coosemans W, Decaluwe H, et al. Lung donor selection and management. *Proc Am Thorac Soc.* 2009;6(1):28-38.
26. Wierup P, Haraldsson A, Nilsson F, Pierre L, Schersten H, Silverborn M, et al. Ex vivo evaluation of nonacceptable donor lungs. *Ann Thorac Surg.* 2006;81(2):460-6.
27. Cypel M, Yeung JC, Liu M, Anraku M, Chen F, Karolak W, et al. Normothermic ex vivo lung perfusion in clinical lung transplantation. *N Engl J Med.* 2011;364(15):1431-40.
28. Otto HH, Schirmeister T. Cysteine proteases and their inhibitors. *Chemical Reviews.* 1997;97(1):133-71.
29. Berti PJ, Storer AC. Alignment/phylogeny of the papain superfamily of cysteine proteases. *J Mol Biol.* 1995;246(2):273-83.
30. Bromme D. Papain-like cysteine proteases. *Curr Protoc Protein Sci.* 2001;Chapter 21:Unit 21.2.

31. Turk V, Stoka V, Vasiljeva O, Renko M, Sun T, Turk B, et al. Cysteine cathepsins: from structure, function and regulation to new frontiers. *Biochim Biophys Acta*. 2012;1824(1):68-88.
32. Sloane BF, Moin K, Krepela E, Rozhin J. Cathepsin B and its endogenous inhibitors: the role in tumor malignancy. *Cancer Metastasis Rev*. 1990;9(4):333-52.
33. Huet G, Flipo RM, Richet C, Thiebaut C, Demeyer D, Balduyck M, et al. Measurement of elastase and cysteine proteinases in synovial fluid of patients with rheumatoid arthritis, sero-negative spondylarthropathies, and osteoarthritis. *Clin Chem*. 1992;38(9):1694-7.
34. Lecaille F, Kaleta J, Bromme D. Human and parasitic papain-like cysteine proteases: their role in physiology and pathology and recent developments in inhibitor design. *Chem Rev*. 2002;102(12):4459-88.
35. Schechter I, Berger A. On the size of the active site in proteases. I. Papain. 1967. *Biochem Biophys Res Commun*. 2012;425(3):497-502.
36. Barrett AJ. The cystatins: small protein inhibitors of cysteine proteinases. *Prog Clin Biol Res*. 1985;180:105-16.
37. Turk V, Bode W. The cystatins: protein inhibitors of cysteine proteinases. *FEBS Lett*. 1991;285(2):213-9.
38. Pfister H, Ollert M, Frohlich LF, Quintanilla-Martinez L, Colby TV, Specks U, et al. Antineutrophil cytoplasmic autoantibodies against the murine homolog of proteinase 3 (Wegener autoantigen) are pathogenic in vivo. *Blood*. 2004;104(5):1411-8.
39. Krupnick AS, Lin X, Li W, Okazaki M, Lai J, Sugimoto S, et al. Orthotopic mouse lung transplantation as experimental methodology to study transplant and tumor biology. *Nat Protoc*. 2009;4(1):86-93.
40. Casiraghi M, Tatreau JR, Abano JB, Blackwell JW, Watson L, Burridge K, et al. In vitro modeling of nonhypoxic cold ischemia-reperfusion simulating lung transplantation. *J Thorac Cardiovasc Surg*. 2009;138(3):760-7.

41. Kratz F, Elsadek B. Clinical impact of serum proteins on drug delivery. *J Control Release*. 2012;161(2):429-45.
42. Quinlan GJ, Martin GS, Evans TW. Albumin: biochemical properties and therapeutic potential. *Hepatology*. 2005;41(6):1211-9.
43. Peters T. All About Albumin: Biochemistry, Genetics and Medical Applications. San Diego, CA: Academic Press Limited; 1966.
44. Chaudhury C, Brooks CL, Carter DC, Robinson JM, Anderson CL. Albumin binding to FcRn: distinct from the FcRn-IgG interaction. *Biochemistry*. 2006;45(15):4983-90.
45. Simister NE, Mostov KE. An Fc receptor structurally related to MHC class I antigens. *Nature*. 1989;337(6203):184-7.
46. Andersen JT, Dee Qian J, Sandlie I. The conserved histidine 166 residue of the human neonatal Fc receptor heavy chain is critical for the pH-dependent binding to albumin. *Eur J Immunol*. 2006;36(11):3044-51.
47. Chaudhury C, Mehnaz S, Robinson JM, Hayton WL, Pearl DK, Roopenian DC, et al. The major histocompatibility complex-related Fc receptor for IgG (FcRn) binds albumin and prolongs its lifespan. *J Exp Med*. 2003;197(3):315-22.
48. Anderson CL, Chaudhury C, Kim J, Bronson CL, Wani MA, Mohanty S. Perspective-- FcRn transports albumin: relevance to immunology and medicine. *Trends Immunol*. 2006;27(7):343-8.
49. Home P, Kurtzhals P. Insulin detemir: from concept to clinical experience. *Expert Opin Pharmacother*. 2006;7(3):325-43.
50. Elsadek B, Kratz F. Impact of albumin on drug delivery--new applications on the horizon. *J Control Release*. 2012;157(1):4-28.

51. Tijink BM, Laeremans T, Budde M, Stigter-van Walsum M, Dreier T, de Haard HJ, et al. Improved tumor targeting of anti-epidermal growth factor receptor Nanobodies through albumin binding: taking advantage of modular Nanobody technology. *Mol Cancer Ther.* 2008;7(8):2288-97.
52. Halpern W, Riccobene TA, Agostini H, Baker K, Stelow D, Gu ML, et al. Albugranin, a recombinant human granulocyte colony stimulating factor (G-CSF) genetically fused to recombinant human albumin induces prolonged myelopoietic effects in mice and monkeys. *Pharm Res.* 2002;19(11):1720-9.
53. Kratz F. Albumin as a drug carrier: Design of prodrugs, drug conjugates and nanoparticles. *J Control Release.* 2008;132(3):171-83.
54. Rawlings ND, Barrett AJ. Evolution of proteins of the cystatin superfamily. *J Mol Evol.* 1990;30(1):60-71.
55. Tenstad O, Roald AB, Grubb A, Aukland K. Renal handling of radiolabelled human cystatin C in the rat. *Scand J Clin Lab Invest.* 1996;56(5):409-14.
56. Bode W, Engh R, Musil D, Thiele U, Huber R, Karshikov A, et al. The 2.0 Å X-ray crystal structure of chicken egg white cystatin and its possible mode of interaction with cysteine proteinases. *EMBO J.* 1988;7(8):2593-9.
57. Machleidt W, Thiele U, Laber B, Assfalg-Machleidt I, Esterl A, Wiegand G, et al. Mechanism of inhibition of papain by chicken egg white cystatin. Inhibition constants of N-terminally truncated forms and cyanogen bromide fragments of the inhibitor. *FEBS Lett.* 1989;243(2):234-8.
58. Kredel S, Oswald F, Nienhaus K, Deuschle K, Rocker C, Wolff M, et al. mRuby, a bright monomeric red fluorescent protein for labeling of subcellular structures. *PLoS One.* 2009;4(2):e4391.
59. Abrahamson M, Alvarez-Fernandez M, Nathanson CM. Cystatins. *Biochem Soc Symp.* 2003(70):179-99.

60. Bain VG, Kaita KD, Yoshida EM, Swain MG, Heathcote EJ, Neumann AU, et al. A phase 2 study to evaluate the antiviral activity, safety, and pharmacokinetics of recombinant human albumin-interferon alfa fusion protein in genotype 1 chronic hepatitis C patients. *J Hepatol.* 2006;44(4):671-8.
61. Subramanian GM, Fiscella M, Lamouse-Smith A, Zeuzem S, McHutchison JG. Albinterferon alpha-2b: a genetic fusion protein for the treatment of chronic hepatitis C. *Nat Biotechnol.* 2007;25(12):1411-9.
62. Duttaroy A, Kanakaraj P, Osborn BL, Schneider H, Pickeral OK, Chen C, et al. Development of a long-acting insulin analog using albumin fusion technology. *Diabetes.* 2005;54(1):251-8.
63. Poole RM, Nowlan ML. Albiglutide: first global approval. *Drugs.* 2014;74(8):929-38.
64. Carrette O, Burkhard PR, Hughes S, Hochstrasser DF, Sanchez JC. Truncated cystatin C in cerebrospinal fluid: Technical [corrected] artefact or biological process? *Proteomics.* 2005;5(12):3060-5.
65. Kolodziejczyk R, Michalska K, Hernandez-Santoyo A, Wahlbom M, Grubb A, Jaskolski M. Crystal structure of human cystatin C stabilized against amyloid formation. *FEBS J.* 2010;277(7):1726-37.
66. Fischer S, Cassivi SD, Xavier AM, Cardella JA, Cutz E, Edwards V, et al. Cell death in human lung transplantation: apoptosis induction in human lungs during ischemia and after transplantation. *Ann Surg.* 2000;231(3):424-31.
67. Fischer S, Maclean AA, Liu M, Cardella JA, Slutsky AS, Suga M, et al. Dynamic changes in apoptotic and necrotic cell death correlate with severity of ischemia-reperfusion injury in lung transplantation. *Am J Respir Crit Care Med.* 2000;162(5):1932-9.
68. Daemen MA, van 't Veer C, Denecker G, Heemskerk VH, Wolfs TG, Clauss M, et al. Inhibition of apoptosis induced by ischemia-reperfusion prevents inflammation. *J Clin Invest.* 1999;104(5):541-9.

69. Yaoita H, Ogawa K, Maehara K, Maruyama Y. Attenuation of ischemia/reperfusion injury in rats by a caspase inhibitor. *Circulation*. 1998;97(3):276-81.
70. Van Antwerp DJ, Martin SJ, Kafri T, Green DR, Verma IM. Suppression of TNF- α -induced apoptosis by NF- κ B. *Science*. 1996;274(5288):787-9.
71. Eppinger MJ, Deeb GM, Bolling SF, Ward PA. Mediators of ischemia-reperfusion injury of rat lung. *Am J Pathol*. 1997;150(5):1773-84.
72. Colletti LM, Burtch GD, Remick DG, Kunkel SL, Strieter RM, Guice KS, et al. The production of tumor necrosis factor α and the development of a pulmonary capillary injury following hepatic ischemia/reperfusion. *Transplantation*. 1990;49(2):268-72.
73. Colletti LM, Remick DG, Burtch GD, Kunkel SL, Strieter RM, Campbell DA, Jr. Role of tumor necrosis factor- α in the pathophysiologic alterations after hepatic ischemia/reperfusion injury in the rat. *J Clin Invest*. 1990;85(6):1936-43.
74. Caty MG, Guice KS, Oldham KT, Remick DG, Kunkel SL. Evidence for tumor necrosis factor-induced pulmonary microvascular injury after intestinal ischemia-reperfusion injury. *Ann Surg*. 1990;212(6):694-700.
75. Collins AR, Grubb A. Inhibitory effects of recombinant human cystatin C on human coronaviruses. *Antimicrob Agents Chemother*. 1991;35(11):2444-6.
76. Wallin H, Abrahamson M, Ekstrom U. Cystatin C properties crucial for uptake and inhibition of intracellular target enzymes. *J Biol Chem*. 2013;288(23):17019-29.
77. Ekstrom U, Wallin H, Lorenzo J, Holmqvist B, Abrahamson M, Aviles FX. Internalization of cystatin C in human cell lines. *FEBS J*. 2008;275(18):4571-82.
78. Gao WX, Zhao JB, Kim H, Xu SY, Chen MY, Bai XH, et al. α 1-Antitrypsin inhibits ischemia reperfusion-induced Lung injury by reducing inflammatory response and cell death. *J Heart Lung Transpl*. 2014;33(3):309-15.

79. Chen F, Date H. Update on ischemia-reperfusion injury in lung transplantation. *Curr Opin Organ Transplant*. 2015;20(5):515-20.
80. Black RA, Rauch CT, Kozlosky CJ, Peschon JJ, Slack JL, Wolfson MF, et al. A metalloproteinase disintegrin that releases tumour-necrosis factor-alpha from cells. *Nature*. 1997;385(6618):729-33.
81. Yan I, Schwarz J, Lucke K, Schumacher N, Schumacher V, Schmidt S, et al. ADAM17 controls IL-6 signaling by cleavage of the murine IL-6R alpha from the cell surface of leukocytes during inflammatory responses. *J Leukocyte Biol*. 2016;99(5):749-60.
82. Lee DC, Sunnarborg SW, Hinkle CL, Myers TJ, Stevenson M, Russell WE, et al. TACE/ADAM17 processing of EGFR ligands indicates a role as a physiological convertase. *Ann Ny Acad Sci*. 2003;995:22-38.
83. Chalaris A, Adam N, Sina C, Rosenstiel P, Lehmann-Koch J, Schirmacher P, et al. Critical role of the disintegrin metalloprotease ADAM17 for intestinal inflammation and regeneration in mice. *J Exp Med*. 2010;207(8):1617-24.
84. Gren ST, Janciauskiene S, Sandeep S, Jonigk D, Kvist PH, Gerwien JG, et al. The protease inhibitor cystatin C down-regulates the release of IL-beta and TNF-alpha in lipopolysaccharide activated monocytes. *J Leukoc Biol*. 2016;100(4):811-22.
85. Peiretti F, Canault M, Deprez-Beauclair P, Berthet V, Bonardo B, Juhan-Vague I, et al. Intracellular maturation and transport of tumor necrosis factor alpha converting enzyme. *Exp Cell Res*. 2003;285(2):278-85.
86. Molloy SS, Bresnahan PA, Leppla SH, Klimpel KR, Thomas G. Human furin is a calcium-dependent serine endoprotease that recognizes the sequence Arg-X-X-Arg and efficiently cleaves anthrax toxin protective antigen. *J Biol Chem*. 1992;267(23):16396-402.

87. Wong E, Maretzky T, Peleg Y, Blobel CP, Sagi I. The Functional Maturation of A Disintegrin and Metalloproteinase (ADAM) 9, 10, and 17 Requires Processing at a Newly Identified Proprotein Convertase (PC) Cleavage Site. *J Biol Chem*. 2015;290(19):12135-46.
88. Anders A, Gilbert S, Garten W, Postina R, Fahrenholz F. Regulation of the alpha-secretase ADAM10 by its prodomain and proprotein convertases. *FASEB J*. 2001;15(10):1837-9.
89. Kang TB, Zhao YG, Pei DQ, Sucic JF, Sang QXA. Intracellular activation of human adamalysin 19/disintegrin and metalloproteinase 19 by furin occurs via one of the two consecutive recognition sites. *Journal of Biological Chemistry*. 2002;277(28):25583-91.
90. Le Gall SM, Maretzky T, Issuree PDA, Niu XD, Reiss K, Saftig P, et al. ADAM17 is regulated by a rapid and reversible mechanism that controls access to its catalytic site. *J Cell Sci*. 2010;123(22):3913-22.
91. Xu P, Derynck R. Direct activation of TACE-mediated ectodomain shedding by p38 MAP kinase regulates EGF receptor-dependent cell proliferation. *Mol Cell*. 2010;37(4):551-66.
92. Schwarz J, Schmidt S, Will O, Koudelka T, Kohler K, Boss M, et al. Polo-like kinase 2, a novel ADAM17 signaling component, regulates tumor necrosis factor alpha ectodomain shedding. *J Biol Chem*. 2014;289(5):3080-93.
93. Sommer A, Kordowski F, Buch J, Maretzky T, Evers A, Andra J, et al. Phosphatidylserine exposure is required for ADAM17 sheddase function. *Nat Commun*. 2016;7.
94. Dulloo I, Muliyl S, Freeman M. The molecular, cellular and pathophysiological roles of iRhom pseudoproteases. *Open Biol*. 2019;9(3):190003.
95. Stone ML, Sharma AK, Mas VR, Gehrau RC, Mulloy DP, Zhao Y, et al. Ex Vivo Perfusion With Adenosine A2A Receptor Agonist Enhances Rehabilitation of Murine Donor Lungs After Circulatory Death. *Transplantation*. 2015;99(12):2494-503.
96. Cypel M, Yeung JC, Hirayama S, Rubacha M, Fischer S, Anraku M, et al. Technique for prolonged normothermic ex vivo lung perfusion. *J Heart Lung Transplant*. 2008;27(12):1319-25.

97. Ley K, Laudanna C, Cybulsky MI, Nourshargh S. Getting to the site of inflammation: the leukocyte adhesion cascade updated. *Nat Rev Immunol*. 2007;7(9):678-89.
98. Borregaard N. Neutrophils, from marrow to microbes. *Immunity*. 2010;33(5):657-70.
99. Dale DC, Boxer L, Liles WC. The phagocytes: neutrophils and monocytes. *Blood*. 2008;112(4):935-45.
100. Brinkmann V, Reichard U, Goosmann C, Fauler B, Uhlemann Y, Weiss DS, et al. Neutrophil extracellular traps kill bacteria. *Science*. 2004;303(5663):1532-5.
101. Perera NC, Schilling O, Kittel H, Back W, Kremmer E, Jenne DE. NSP4, an elastase-related protease in human neutrophils with arginine specificity. *Proc Natl Acad Sci U S A*. 2012;109(16):6229-34.
102. Pham CT. Neutrophil serine proteases: specific regulators of inflammation. *Nat Rev Immunol*. 2006;6(7):541-50.
103. Zimmer M, Medcalf RL, Fink TM, Mattmann C, Lichter P, Jenne DE. Three human elastase-like genes coordinately expressed in the myelomonocyte lineage are organized as a single genetic locus on 19pter. *Proc Natl Acad Sci U S A*. 1992;89(17):8215-9.
104. Hedstrom L. Serine protease mechanism and specificity. *Chem Rev*. 2002;102(12):4501-24.
105. Kessenbrock K, Frohlich L, Sixt M, Lammermann T, Pfister H, Bateman A, et al. Proteinase 3 and neutrophil elastase enhance inflammation in mice by inactivating antiinflammatory progranulin. *J Clin Invest*. 2008;118(7):2438-47.
106. Korkmaz B, Caughey GH, Chapple I, Gauthier F, Hirschfeld J, Jenne DE, et al. Therapeutic targeting of cathepsin C: from pathophysiology to treatment. *Pharmacol Ther*. 2018;190:202-36.

107. Adkison AM, Raptis SZ, Kelley DG, Pham CT. Dipeptidyl peptidase I activates neutrophil-derived serine proteases and regulates the development of acute experimental arthritis. *J Clin Invest.* 2002;109(3):363-71.
108. McGuire MJ, Lipsky PE, Thiele DL. Generation of active myeloid and lymphoid granule serine proteases requires processing by the granule thiol protease dipeptidyl peptidase I. *J Biol Chem.* 1993;268(4):2458-67.
109. Doyle K, Lonn H, Kack H, Van de Poel A, Swallow S, Gardiner P, et al. Discovery of Second Generation Reversible Covalent DPP1 Inhibitors Leading to an Oxazepane Amidoacetonitrile Based Clinical Candidate (AZD7986). *J Med Chem.* 2016;59(20):9457-72.
110. Korkmaz B, Horwitz MS, Jenne DE, Gauthier F. Neutrophil Elastase, Proteinase 3, and Cathepsin G as Therapeutic Targets in Human Diseases. *Pharmacol Rev.* 2010;62(4):726-59.
111. Roghanian A, Sallenave JM. Neutrophil elastase (NE) and NE inhibitors: canonical and noncanonical functions in lung chronic inflammatory diseases (cystic fibrosis and chronic obstructive pulmonary disease). *J Aerosol Med Pulm Drug Deliv.* 2008;21(1):125-44.
112. Korkmaz B, Moreau T, Gauthier F. Neutrophil elastase, proteinase 3 and cathepsin G: physicochemical properties, activity and physiopathological functions. *Biochimie.* 2008;90(2):227-42.
113. De Perrot M, Sekine Y, Fischer S, Waddell TK, McRae K, Liu M, et al. Interleukin-8 release during ischemia-reperfusion correlates with early graft function in human lung transplantation. *J Heart Lung Transplant.* 2001;20(2):175-6.
114. Belperio JA, Keane MP, Burdick MD, Gomperts BN, Xue YY, Hong K, et al. CXCR2/CXCR2 ligand biology during lung transplant ischemia-reperfusion injury. *J Immunol.* 2005;175(10):6931-9.
115. Nomura N, Asano M, Saito T, Nakayama T, Mishima A. Sivelestat attenuates lung injury in surgery for congenital heart disease with pulmonary hypertension. *Ann Thorac Surg.* 2013;96(6):2184-91.

116. Uchida Y, Freitas MC, Zhao D, Busuttil RW, Kupiec-Weglinski JW. The protective function of neutrophil elastase inhibitor in liver ischemia/reperfusion injury. *Transplantation*. 2010;89(9):1050-6.
117. Fujimura N, Obara H, Suda K, Takeuchi H, Miyasho T, Kawasaki K, et al. Neutrophil elastase inhibitor improves survival rate after ischemia reperfusion injury caused by supravisceral aortic clamping in rats. *J Surg Res*. 2013;180(1):e31-6.
118. Inoue Y, Tanaka H, Ogura H, Ukai I, Fujita K, Hosotsubo H, et al. A neutrophil elastase inhibitor, sivelestat, improves leukocyte deformability in patients with acute lung injury. *J Trauma*. 2006;60(5):936-43; discussion 43.
119. Ginzberg HH, Cherapanov V, Dong Q, Cantin A, McCulloch CA, Shannon PT, et al. Neutrophil-mediated epithelial injury during transmigration: role of elastase. *Am J Physiol Gastrointest Liver Physiol*. 2001;281(3):G705-17.
120. Carden D, Xiao F, Moak C, Willis BH, Robinson-Jackson S, Alexander S. Neutrophil elastase promotes lung microvascular injury and proteolysis of endothelial cadherins. *Am J Physiol*. 1998;275(2 Pt 2):H385-92.
121. Soehnlein O. An elegant defense: how neutrophils shape the immune response. *Trends Immunol*. 2009;30(11):511-2.
122. Chen HC, Lin HC, Liu CY, Wang CH, Hwang T, Huang TT, et al. Neutrophil elastase induces IL-8 synthesis by lung epithelial cells via the mitogen-activated protein kinase pathway. *J Biomed Sci*. 2004;11(1):49-58.
123. Suzuki T, Yamashita C, Zemans RL, Briones N, Van Linden A, Downey GP. Leukocyte elastase induces lung epithelial apoptosis via a PAR-1-, NF-kappaB-, and p53-dependent pathway. *Am J Respir Cell Mol Biol*. 2009;41(6):742-55.

124. Pham CT, Ivanovich JL, Raptis SZ, Zehnbauser B, Ley TJ. Papillon-Lefevre syndrome: correlating the molecular, cellular, and clinical consequences of cathepsin C/dipeptidyl peptidase I deficiency in humans. *J Immunol*. 2004;173(12):7277-81.
125. Lefevre C, Blanchet-Bardon C, Jobard F, Bouadjar B, Stalder JF, Cure S, et al. Novel point mutations, deletions, and polymorphisms in the cathepsin C gene in nine families from Europe and North Africa with Papillon-Lefevre syndrome. *J Invest Dermatol*. 2001;117(6):1657-61.
126. Guarino C, Hamon Y, Croix C, Lamort AS, Dallet-Choisy S, Marchand-Adam S, et al. Prolonged pharmacological inhibition of cathepsin C results in elimination of neutrophil serine proteases. *Biochem Pharmacol*. 2017;131:52-67.
127. Miller BE, Mayer RJ, Goyal N, Bal J, Dallow N, Boyce M, et al. Epithelial desquamation observed in a phase I study of an oral cathepsin C inhibitor (GSK2793660). *Br J Clin Pharmacol*. 2017;83(12):2813-20.
128. Palmer R, Maenpaa J, Jauhiainen A, Larsson B, Mo J, Russell M, et al. Dipeptidyl Peptidase 1 Inhibitor AZD7986 Induces a Sustained, Exposure-Dependent Reduction in Neutrophil Elastase Activity in Healthy Subjects. *Clin Pharmacol Ther*. 2018.
129. Kam CM, Gotz MG, Koot G, McGuire M, Thiele D, Hudig D, et al. Design and evaluation of inhibitors for dipeptidyl peptidase I (Cathepsin C). *Arch Biochem Biophys*. 2004;427(2):123-34.
130. Bondebjerg J, Fuglsang H, Valeur KR, Kaznelson DW, Hansen JA, Pedersen RO, et al. Novel semicarbazide-derived inhibitors of human dipeptidyl peptidase I (hDPPI). *Bioorg Med Chem*. 2005;13(14):4408-24.
131. Hamon Y, Legowska M, Herve V, Dallet-Choisy S, Marchand-Adam S, Vanderlynden L, et al. Neutrophilic Cathepsin C Is Matured by a Multistep Proteolytic Process and Secreted by Activated Cells during Inflammatory Lung Diseases. *Journal of Biological Chemistry*. 2016;291(16):8486-99.

-
132. Methot N, Rubin J, Guay D, Beaulieu C, Ethier D, Reddy TJ, et al. Inhibition of the activation of multiple serine proteases with a cathepsin C inhibitor requires sustained exposure to prevent pro-enzyme processing. *J Biol Chem*. 2007;282(29):20836-46.
 133. Frizler M, Stirnberg M, Sisay MT, Gutschow M. Development of nitrile-based peptidic inhibitors of cysteine cathepsins. *Curr Top Med Chem*. 2010;10(3):294-322.
 134. Korkmaz B, Lesner A, Wysocka M, Gieldon A, Hakansson M, Gauthier F, et al. Structure-based design and in vivo anti-arthritic activity evaluation of a potent dipeptidyl cyclopropyl nitrile inhibitor of cathepsin C. *Biochem Pharmacol*. 2019;164:349-67.
 135. Schofield ZV, Woodruff TM, Halai R, Wu MC, Cooper MA. Neutrophils--a key component of i
ischemia-reperfusion injury. *Shock*. 2013;40(6):463-70.
 136. Granger DN, Kvietys PR. Reperfusion injury and reactive oxygen species: The evolution of a concept. *Redox Biol*. 2015;6:524-51.
 137. Harada M, Oto T, Otani S, Miyoshi K, Okada M, Iga N, et al. A neutrophil elastase inhibitor improves lung function during ex vivo lung perfusion. *Gen Thorac Cardiovasc Surg*. 2015;63(12):645-51.
 138. Verleden SE, Martens A, Ordies S, Neyrinck AP, Van Raemdonck DE, Verleden GM, et al. Immediate post-operative broncho-alveolar lavage IL-6 and IL-8 are associated with early outcomes after lung transplantation. *Clin Transplant*. 2018;32(4):e13219.
 139. Moreno I, Vicente R, Ramos F, Vicente JL, Barbera M. Determination of interleukin-6 in lung transplantation: association with primary graft dysfunction. *Transplant Proc*. 2007;39(7):2425-6.
 140. Cantu E, Lederer DJ, Meyer K, Milewski K, Suzuki Y, Shah RJ, et al. Gene set enrichment analysis identifies key innate immune pathways in primary graft dysfunction after lung transplantation. *Am J Transplant*. 2013;13(7):1898-904.

141. Yamane M, Liu M, Kaneda H, Uhlig S, Waddell TK, Keshavjee S. Reperfusion-induced gene expression profiles in rat lung transplantation. *Am J Transplant*. 2005;5(9):2160-9.
142. Iskender I, Sakamoto J, Nakajima D, Lin H, Chen M, Kim H, et al. Human alpha1-antitrypsin improves early post-transplant lung function: Pre-clinical studies in a pig lung transplant model. *J Heart Lung Transplant*. 2016;35(7):913-21.
143. Salvesen G, Enghild JJ. Zymogen activation specificity and genomic structures of human neutrophil elastase and cathepsin G reveal a new branch of the chymotrypsinogen superfamily of serine proteinases. *Biomed Biochim Acta*. 1991;50(4-6):665-71.
144. Garwicz D, Lindmark A, Persson AM, Gullberg U. On the role of the proform-conformation for processing and intracellular sorting of human cathepsin G. *Blood*. 1998;92(4):1415-22.
145. Sorensen OE, Clemmensen SN, Dahl SL, Ostergaard O, Heegaard NH, Glenthoj A, et al. Papillon-Lefevre syndrome patient reveals species-dependent requirements for neutrophil defenses. *J Clin Invest*. 2014;124(10):4539-48.
146. Gotzfried J, Smirnova NF, Morrone C, Korkmaz B, Yildirim AO, Eickelberg O, et al. Preservation with alpha1-antitrypsin improves primary graft function of murine lung transplants. *J Heart Lung Transplant*. 2018.
147. Summers C, Rankin SM, Condliffe AM, Singh N, Peters AM, Chilvers ER. Neutrophil kinetics in health and disease. *Trends Immunol*. 2010;31(8):318-24.

6. Abbreviations

μl	Microliter
aa	Amino acid
AAT	α-1-antitrypsin proteinase inhibitor
Alb	Albumin
APS	Ammonium persulfate
Asp	Aspartic acid
BAL	Bronchoalveolar lavage
BALF	Bronchoalveolar lavage fluid
BM	Bone marrow
BOS	Bronchiolitis obliterans syndrome
bp	Base pair
Cat. No.	Catalog number
CatB	Cathepsin B
CatC	Cathepsin C
CatG	Cathepsin G
CatH	Cathepsin H
CatL	Cathepsin L
CatS	Cathepsin S
COPD	Chronic obstructive pulmonary disease
CS	Cold storage
CysC	Cystatin C
CytC	Cytochrome C
Da	Dalton
ddH ₂ O	Double distilled water
DNA	Deoxyribonucleic acid

DPPI	Dipeptidylpeptidase I
EGFR	Epithelial growth factor receptor
ELISA	Enzyme-linked immunosorbent assay
Endo H	Endo- β -N-acetylglucosaminidase H
EVLP	Ex vivo lung perfusion
FcRn	neonatal Fc receptor
FRET	Förster/Fluorescence resonance energy transfer
gCysC	chicken Cystatin C
HDL	High density lipoprotein
HE	Hematoxylin Eosin
HEK	Human embryonic kidney cell line
hFcRn	Human neonatal Fc receptor
His	Histidine
HRP	Horseradish peroxidase
IL-6	Interleukin 6
i. p.	Intra peritoneal
IPF	Idiopathic pulmonary fibrosis
I/R	Ischemia reperfusion
LDL	Low density lipoprotein
LPS	Lipopolysaccharide
LTx	Lung transplantation
mAb	Monoclonal antibody
MHC-I	Major histocompatibility class I
mCysC	Chicken Cystatin C
mFcRn	Mouse neonatal Fc receptor
min	Minutes

mRNA	Messenger ribonucleic acid
NE	Neutrophil elastase
NEB	New England Biolabs
NFκB	nuclear factor κB
NSPs	Neutrophil serine protease
NSP4	Neutrophil serine protease 4
OD	Optic density
on	over night
PBMC	Peripheral blood mononuclear cell
PBS	Phosphate buffered saline
PC	Proprotein convertase
PEI	Polyethyleneimine
PGD	Primary graft dysfunction
pI	Isoelectric point
PIPES	Piperazine-N,N'-bis(2-ethanesulfonic acid)
PMN	Polymorphonuclear cells
PNGase F	Peptide -N-Glycosidase F
PR3	Proteinase 3
PVDF	Polyvinylidene difluoride
RCL	Reactive center loop
RIPA	Radioimmunoprecipitation assay buffer
ROS	Reactive oxygen species
rpm	Rounds per minute
s.c.	Subcutaneous
sec	Seconds
Ser	Serine

6. Abbreviations

Serpin	Serine protease inhibitor
TACE	Tumor-necrosis-factor- α -converting enzyme
TCEP	Tris(2-carboxyethyl) phosphine
TEMED	Tetramethylethylenediamine
TNF α	Tumor necrosis factor α
TNFR	Tumor necrosis factor receptor

7. Appendix

7.1 Vector map

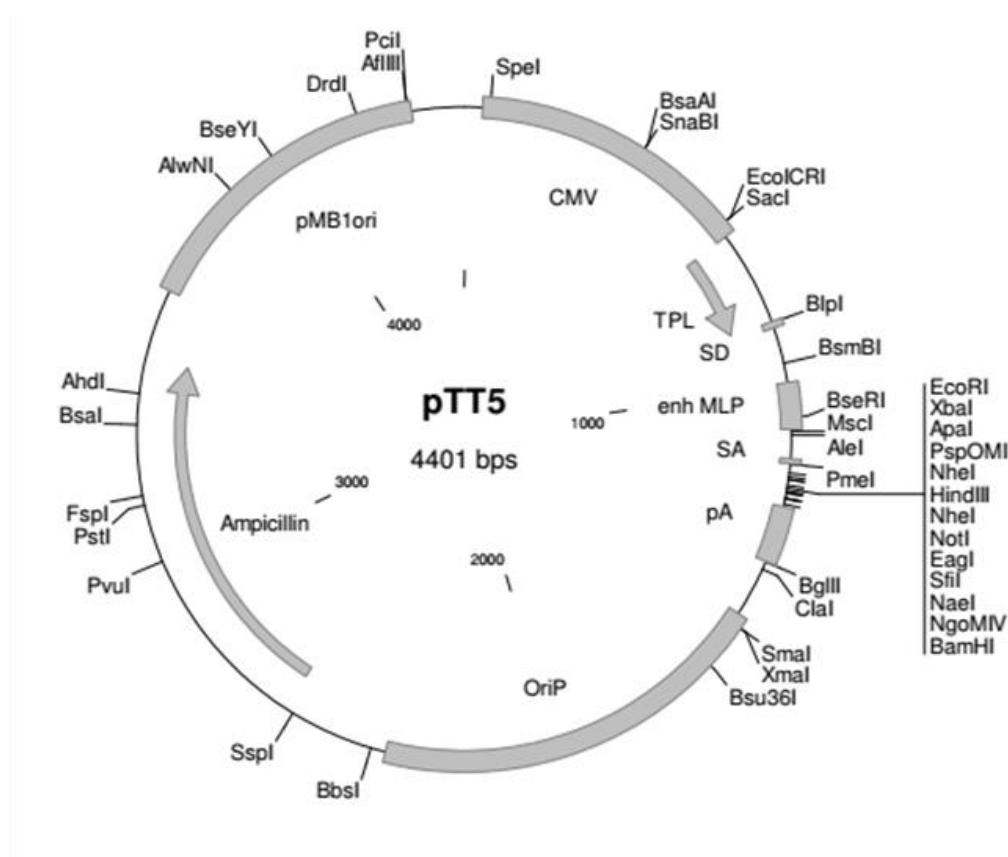


Figure 4 Vector map of the pTT5 plasmid. This vector was used to express CysC fusion proteins in HEK 293 cells. The important features of this vector are an *E. coli* (pMB1ori) and EBV (OriP) specific origin of replication, a promoter of the cytomegalovirus (CMV), an adenovirus tripartite leader (TPL), a major late promoter (MLP), a rabbit bet-globin polyadenylation signal (pA) and an ampicillin resistance gene.

7.2 Sequences of expressed proteins

The amino acid sequence is shown in a single letter code. The sequence begins with the Igk signal peptide in grey. The C-terminal His-tag is marked in *italics* and the stop codon is represented by a star (*).

7.2.1 pTT5-Alb

```

1 M E T D T L L L W V L L L W V
1 ATGGAGACAGACACACTCCTGCTATGGGTACTGCTGCTCTGGGTA
16 P G S T G E A H K S E I A H R
46 CCAGGTTCCACTGGTGAAGCACACAAGAGTGAGATCGCCCATCGG
31 Y N D L G E Q H F K G L V L I
91 TATAATGATTTGGGAGAACAACATTTCAAAGGCCTAGTCCTGATT
46 A F S Q Y L Q K C S Y D E H A
136 GCCTTTTCCCAGTATCTCCAGAAATGCTCATAACGATGAGCATGCC
61 K L V Q E V T D F A K T C V A
181 AAATTAGTGCAGGAAGTAACAGACTTTGCAAAGACGTGTGTTGCC
76 D E S A A N C D K S L H T L F
226 GATGAGTCTGCCGCCAACTGTGACAAATCCCTTCACACTCTTTTT
91 G D K L C A I P N L R E N Y G
271 GGAGATAAGTTGTGTGCCATTCCAAACCTCCGTGAAAACCTATGGT
106 E L A D C C T K Q E P E R N E
316 GAACTGGCTGACTGCTGTACAAAACAAGAGCCCGAAAGAAACGAA
121 C F L Q H K D D N P S L P P F
361 TGTTTCCTGCAACACAAAGATGACAACCCCAGCCTGCCACCATTT
136 E R P E A E A M C T S F K E N
406 GAAAGGCCAGAGGCTGAGGCCATGTGCACCTCCTTTAAGGAAAAC
151 P T T F M G H Y L H E V A R R
451 CCAACCACCTTTATGGGACACTATTTGCATGAAGTTGCCAGAAGA
166 H P Y F Y A P E L L Y Y A E Q
496 CATCCTTATTTCTATGCCCCAGAACTTCTTTACTATGCTGAGCAG
181 Y N E I L T Q C C A E A D K E
541 TACAATGAGATTCTGACCCAGTGTTGTGCAGAGGCTGACAAGGAA
196 S C L T P K L D G V K E K A L
586 AGCTGCCTGACCCCGAAGCTTGATGGTGTGAAGGAGAAAGCATTG
211 V S S V R Q R M K C S S M Q K
631 GTCTCATCTGTCCGTCAGAGAAATGAAGTGCTCCAGTATGCAGAAG
226 F G E R A F K A W A V A R L S
676 TTTGGAGAGAGAGCTTTTAAAGCATGGGCAGTAGCTCGTCTGAGC
241 Q T F P N A D F A E I T K L A

```

721 CAGACATTCCCAATGCTGACTTTGCAGAAATCACCAAATTGGCA
256 T D L T K V N K E C C H G D L
766 ACAGACCTGACCAAAGTCAACAAGGAGTGCTGCCATGGTGACCTG
271 L E C A D D R A E L A K Y M C
811 CTGGAATGCGCAGATGACAGGGCGGAACTTGCCAAGTACATGTGT
286 E N Q A T I S S K L Q T C C D
856 GAAAACCAGGCGACTATCTCCAGCAAAGTGCAGACTTGCTGCGAT
301 K P L L K K A H C L S E V E H
901 AAACCACTGTTGAAGAAAGCCCACTGTCTTAGTGAGGTGGAGCAT
316 D T M P A D L P A I A A D F V
946 GACACCATGCCTGCTGATCTGCCTGCCATTGCTGCTGATTTTGT
331 E D Q E V C K N Y A E A K D V
991 GAGGACCAGGAAGTGTGCAAGAACTATGCTGAGGCCAAGGATGTC
346 F L G T F L Y E Y S R R H P D
1036 TTCCTGGGCACGTTCTTGTATGAATATTCAAGAAGACACCCTGAT
361 Y S V S L L L R L A K K Y E A
1081 TACTCTGTATCCCTGTTGCTGAGACTTGCTAAGAAATATGAAGCC
376 T L E K C C A E A N P P A C Y
1126 ACTCTGGAAAAGTGCTGCGCTGAAGCCAATCCTCCCGCATGCTAC
391 G T V L A E F Q P L V E E P K
1171 GGCACAGTGCTTGCTGAATTTTCAGCCTCTTGTAGAAGAGCCTAAG
406 N L V K T N C D L Y E K L G E
1216 AACTTGGTCAAAACCAACTGTGATCTTTACGAGAAGCTTGGAGAA
421 Y G F Q N A I L V R Y T Q K A
1261 TATGGATTCCAAAATGCCATTCTAGTTTCGCTACACCCAGAAAGCA
436 P Q V S T P T L V E A A R N L
1306 CCTCAGGTGTCAACCCCAACTCTCGTGGAGGCTGCAAGAAACCTA
451 G R V G T K C C T L P E D Q R
1351 GGAAGAGTGGGCACCAAGTGTGTACACTTCCTGAAGATCAGAGA
466 L P C V E D Y L S A I L N R V
1396 CTGCCTTGTGTGGAAGACTATCTGTCTGCAATCCTGAACCGTGTG
481 C L L H E K T P V S E H V T K
1441 TGTCTGCTGCATGAGAAGACCCAGTGAGTGAGCATGTTACCAAG
496 C C S G S L V E R R P C F S A
1486 TGCTGTAGTGGATCCCTGGTGGAAAGGCGGCCATGCTTCTCTGCT
511 L T V D E T Y V P K E F K A E
1531 CTGACAGTTGATGAAACATATGTCCCCAAAGAGTTTAAAGCTGAG
526 T F T F H S D I C T L P E K E
1576 ACCTTCACCTTCCACTCTGATATCTGCACACTTCCAGAGAAGGAG
541 K Q I K K Q T A L A E L V K H
1621 AAGCAGATTAAGAAACAAACGGCTCTTGCTGAGCTGGTGAAGCAC
556 K P K A T A E Q L K T V M D D
1666 AAGCCCAAGGCTACAGCGGAGCAACTGAAGACTGTCATGGATGAC
571 F A Q F L D T C C K A A D K D

```

1711 TTTGCACAGTTCCTGGATACATGTTGCAAGGCTGCTGACAAGGAC
586 T C F S T E G P N L V T R C K
1756 ACCTGCTTCTCGACTGAGGGTCCAAACCTTGCTACTAGATGCAAA
601 D A L A *
1801 GAcGCgTTAGCCTGA

```

7.2.2 pTT5-CysC-Alb

```

1 M E T D T L L L W V L L L W V
1 ATGGAGACAGACACACTCCTGCTATGGGTACTGCTGCTCTGGGTA
16 P G S T G P R L L G A P E E A
46 CCTGGCTCAACCGGACCTAGGCTGCTGGGGGCTCCCGAGGAAGCG
31 D A N E E G V R R A L D F A V
91 GATGCTAACGAGGAAGGCGTCAGAAGGGCCTTGGATTTTCGCTGTC
46 S E Y N K G S N D A Y H S R A
136 TCAGAGTATAATAAGGGTTCCAACGACGCGTATCATAGCAGGGCA
61 C Q V V R A R K Q L V A G V N
181 TGTCAGGTTGTACGCGCACGGAAACAACCTCGTCGCAGGCGTTAAC
76 Y F L D V E M C R T T C T K S
226 TACTTCTTGGATGTGGAATGTGCCGGACCACGTGCACCAAGAGT
91 Q T N L T D C P F H D Q P H L
271 CAGACCAATCTTACCGACTGCCCATTTTCATGACCAACCCACCTT
106 M R K A L C S F Q I Y S V P W
316 ATGAGAAAGGCCTTGTGCAGTTTCCAGATATATAGCGTACCCTGG
121 K G T H S L T K F S C K N A G
361 AAGGGAACTCATAGCCTGACGAAGTTTtagCTGTAAAAACGCTGGT
136 G G G T G E A H K S E I A H R
406 GGAGGCGGCAccGGTGAAGCACACAAGAGTGAGATCGCCCATCGG
151 Y N D L G E Q H F K G L V L I
451 TATAATGATTTGGGAGAACAACATTTCAAAGGCCTAGTCCTGATT
166 A F S Q Y L Q K S S Y D E H A
496 GCCTTTTCCCAGTATCTCCAGAAAaGCTCATACGATGAGCATGCC
181 K L V Q E V T D F A K T C V A
541 AAATTAGTGCAGGAAGTAACAGACTTTGCAAAGACGTGTGTTGCC
196 D E S A A N C D K S L H T L F
586 GATGAGTCTGCCGCCAACTGTGACAAATCCCTTCACACTCTTTTT
211 G D K L C A I P N L R E N Y G
631 GGAGATAAGTTGTGTGCCATTCCAAACCTCCGTGAAAACCTATGGT
226 E L A D C C T K Q E P E R N E
676 GAACTGGCTGACTGCTGTACAAAACAAGAGCCCGAAAGAAACGAA
241 C F L Q H K D D N P S L P P F
721 TGTTTCCTGCAACACAAAGATGACAACCCCAGCCTGCCACCATTT

```


256 E R P E A E A M C T S F K E N
766 GAAAGGCCAGAGGCTGAGGCCATGTGCACCTCCTTTAAGGAAAAC
271 P T T F M G H Y L H E V A R R
811 CCAACCACCTTTATGGGACACTATTTGCATGAAGTTGCCAGAAGA
286 H P Y F Y A P E L L Y Y A E Q
856 CATCCTTATTTCTATGCCCCAGAACTTCTTTACTATGCTGAGCAG
301 Y N E I L T Q C C A E A D K E
901 TACAATGAGATTCTGACCCAGTGTTGTGCAGAGGCTGACAAGGAA
316 S C L T P K L D G V K E K A L
946 AGCTGCCTGACCCCGAAGCTTGATGGTGTGAAGGAGAAAGCATTG
331 V S S V R Q R M K C S S M Q K
991 GTCTCATCgGTCCGTCAGAGAATGAAGTGCTCCAGTATGCAGAAG
346 F G E R A F K A W A V A R L S
1036 TTTGGAGAGAGAGCCTTTTAAAGCATGGGCAGTAGCTCGTCTGAGC
361 Q T F P N A D F A E I T K L A
1081 CAGACATTCCCAATGCTGACTTTGCAGAAATCACCAAATTGGCA
376 T D L T K V N K E C C H G D L
1126 ACAGACCTGACCAAAGTCAACAAGGAGTGCTGCCATGGTGACCTG
391 L E C A D D R A E L A K Y M C
1171 CTGGAATGCGCAGATGACAGGGCGGAAGTGGCAAGTACATGTGT
406 E N Q A T I S S K L Q T C C D
1216 GAAAACCAGGCGACTATCTCCAGCAAAGTGCAGACTTGCTGCGAT
421 K P L L K K A H C L S E V E H
1261 AAACCACTGTTGAAGAAAGCCCACTGTCTTAGTGAGGTGGAGCAT
436 D T M P A D L P A I A A D F V
1306 GACACCATGCCTGCTGATCTGCCTGCCATTGCTGCTGATTTTGT
451 E D Q E V C K N Y A E A K D V
1351 GAGGACCAGGAAGTGTGCAAGAACTATGCTGAGGCCAAGGATGTC
466 F L G T F L Y E Y S R R H P D
1396 TTCCTGGGCACGTTCTTGTATGAATATTCAAGAAGACACCCTGAT
481 Y S V S L L L R L A K K Y E A
1441 TACTCTGTATCCCTGTTGCTGAGACTTGCTAAGAAATATGAAGCC
496 T L E K C C A E A N P P A C Y
1486 ACTCTGGAAAAGTGCTGCGCTGAAGCCAATCCTCCCGCATGCTAC
511 G T V L A E F Q P L V E E P K
1531 GGCACAGTGCTTGCTGAATTTGAGCCTCTTGTAGAAGAGCCTAAG
526 N L V K T N C D L Y E K L G E
1576 AACTTGGTCAAAACCAACTGTGATCTTTACGAGAAGCTTGGAGAA
541 Y G F Q N A I L V R Y T Q K A
1621 TATGGATTCCAAAATGCCATTCTAGTTCGCTACACCCAGAAAGCA
556 P Q V S T P T L V E A A R N L
1666 CCTCAGGTGTCAACCCCAACTCTCGTGGAGGCTGCAAGAAACCTA
571 G R V G T K C C T L P E D Q R
1711 GGAAGAGTGGGCACCAAGTGTGTACACTTCCTGAAGATCAGAGA

586 L P C V E D Y L S A I L N R V
1756 CTGCCCTTGTGTGGAAGACTATCTGTCTGCAATCCTGAACCGTGTG
601 C L L H E K T P V S E H V T K
1801 TGTCTGCTGCATGAGAAGACCCAGTGAGTGAGCATGTTACCAAG
616 C C S G S L V E R R P C F S A
1846 TGCTGTAGTGGATCCCTGGTGGAAAGGCGGCCATGCTTCTCTGCT
631 L T V D E T Y V P K E F K A E
1891 CTGACAGTTGATGAAACATAcGTaCCCAAAGAGTTTAAAGCTGAG
646 T F T F H S D I C T L P E K E
1936 ACCTTCACCTTCCACTCTGATATCTGCACACTTCCAGAGAAGGAG
661 K Q I K K Q T A L A E L V K H
1981 AAGCAGATTAAGAAACAAACGGCTCTTGCTGAGCTGGTGAAGCAC
676 K P K A T A E Q L K T V M D D
2026 AAGCCCAAGGCTACAGCGGAGCAACTGAAGACTGTCATGGATGAC
691 F A Q F L D T C C K A A D K D
2071 TTTGCACAGTTCCTGGATACATGTTGCAAGGCTGCTGACAAGGAC
706 T C F S T E G P N L V T R C K
2116 ACCTGCTTCTCGACTGAGGGTCCAAACCTTGTCAGTAGATGCAAA
721 D A L A T G H H H H H H *
2161 GAcGCgTTagccaccggtCATCATCACCATCACCATTGA

7.2.3 pTT5-CysC-Alb-Ruby

1 M E T D T L L L W V L L L W V
1 ATGGAGACAGACACACTCCTGCTATGGGTACTGCTGCTCTGGGTA
16 P G S T G L L G A P E E A D A
46 CCTGGCTCAACCGGACTGCTGGGGGCTCCCGAGGAAGCGGATGCT
31 N E E G V R R A L D F A V S E
91 AACGAGGAAGGCGTCAGAAGGGCCTTGGATTTGCTGTCTCAGAG
46 Y N K G S N D A Y H S R A C Q
136 TATAATAAGGGTTCCAACGACGCGTATCATAGCAGGGCATGTCAG
61 V V R A R K Q L V A G V N Y F
181 GTTGTACGCGCACGGAAACAACCTCGTCGCAGGCGTTAACTACTTC
76 L D V E M C R T T C T K S Q T
226 TTGGATGTGGAAATGTGCCGGACCACGTGCACCAAGAGTCAGACC
91 N L T D C P F H D Q P H L M R
271 AATCTTACCGACTGCCCATTTCATGACCAACCCACCTTATGAGA
106 K A L C S F Q I Y S V P W K G
316 AAGGCCTTGTGCAGTTTCCAGATATATAGCGTACCCTGGAAGGGA
121 T H S L T K F S C K N A G G G
361 ACTCATAGCCTGACGAAGTTTAGCTGTAAAAACGCTGGTGGAGGC
136 G T G E A H K S E I A H R Y N
406 GGCAccGGTGAAGCACACAAGAGTGAGATCGCCCATCGGTATAAT

151 D L G E Q H F K G L V L I A F
451 GATTTGGGAGAACAACATTTCAAAGGCCTAGTCCTGATTGCCTTT
166 S Q Y L Q K S S Y D E H A K L
496 TCCCAGTATCTCCAGAAAaGCTCATACGATGAGCATGCCAAATTA
181 V Q E V T D F A K T C V A D E
541 GTGCAGGAAGTAACAGACTTTGCAAAGACGTGTGTTGCCGATGAG
196 S A A N C D K S L H T L F G D
586 TCTGCCGCCAACTGTGACAAATCCCTTCACACTCTTTTTTGGAGAT
211 K L C A I P N L R E N Y G E L
631 AAGTTGTGTGCCATTCCAAACCTCCGTGAAAACCTATGGTGAACCTG
226 A D C C T K Q E P E R N E C F
676 GCTGACTGCTGTACAAAACAAGAGCCCGAAAGAAACGAATGTTTC
241 L Q H K D D N P S L P P F E R
721 CTGCAACACAAAGATGACAACCCCAGCCTGCCACCATTTGAAAGG
256 P E A E A M C T S F K E N P T
766 CCAGAGGCTGAGGCCATGTGCACCTCCTTTAAGGAAAACCCAACC
271 T F M G H Y L H E V A R R H P
811 ACCTTTATGGGACACTATTTGCATGAAGTTGCCAGAAGACATCCT
286 Y F Y A P E L L Y Y A E Q Y N
856 TATTTCTATGCCCCAGAACTTCTTTACTATGCTGAGCAGTACAAT
301 E I L T Q C C A E A D K E S C
901 GAGATTCTGACCCAGTGTTGTGCAGAGGCTGACAAGGAAAGCTGC
316 L T P K L D G V K E K A L V S
946 CTGACCCCGAAGCTTGATGGTGTGAAGGAGAAAGCATTGGTCTCA
331 S V R Q R M K C S S M Q K F G
991 TCTGTCCGTCAGAGAATGAAGTGCTCCAGTATGCAGAAGTTTGGA
346 E R A F K A W A V A R L S Q T
1036 GAGAGAGCTTTTAAAGCATGGGCAGTAGCTCGTCTGAGCCAGACA
361 F P N A D F A E I T K L A T D
1081 TTCCCCAATGCTGACTTTGCAGAAATCACCAAATTGGCAACAGAC
376 L T K V N K E C C H G D L L E
1126 CTGACCAAAGTCAACAAGGAGTGCTGCCATGGTGACCTGCTGGAA
391 C A D D R A E L A K Y M C E N
1171 TGCGCAGATGACAGGGCGGAACCTGCCAAGTACATGTGTGAAAAC
406 Q A T I S S K L Q T C C D K P
1216 CAGGCGACTATCTCCAGCAAACCTGCAGACTTGCTGCGATAAACCA
421 L L K K A H C L S E V E H D T
1261 CTGTTGAAGAAAGCCCACTGTCTTAGTGAGGTGGAGCATGACACC
436 M P A D L P A I A A D F V E D
1306 ATGCCTGCTGATCTGCCTGCCATTGCTGCTGATTTTGTGAGGAC
451 Q E V C K N Y A E A K D V F L
1351 CAGGAAGTGTCGAAGAACTATGCTGAGGCCAAGGATGTCTTCCTG
466 G T F L Y E Y S R R H P D Y S
1396 GGCACGTTCTTGTATGAATATTCAAGAAGACACCCTGATTACTCT

481 V S L L L R L A K K Y E A T L
1441 GTATCCCTGTTGCTGAGACTTGCTAAGAAATATGAAGCCACTCTG
496 E K C C A E A N P P A C Y G T
1486 GAAAAGTGCTGCGCTGAAGCCAATCCTCCCGCATGCTACGGCACA
511 V L A E F Q P L V E E P K N L
1531 GTGCTTGCTGAATTTTCAGCCTCTTGTTAGAAGAGCCTAAGAACTTG
526 V K T N C D L Y E K L G E Y G
1576 GTCAAAACCAACTGTGATCTTTACGAGAAGCTTGGAGAATATGGA
541 F Q N A I L V R Y T Q K A P Q
1621 TTCCAAAATGCCATTCTAGTTCGCTACACCCAGAAAGCACCTCAG
556 V S T P T L V E A A R N L G R
1666 GTGTCAACCCCAACTCTCGTGGAGGCTGCAAGAAACCTAGGAAGA
571 V G T K C C T L P E D Q R L P
1711 GTGGGCACCAAGTGTTGTACACTTCCTGAAGATCAGAGACTGCCT
586 C V E D Y L S A I L N R V C L
1756 TGTGTGGAAGACTATCTGTCTGCAATCCTGAACCGTGTGTGTCTG
601 L H E K T P V S E H V T K C C
1801 CTGCATGAGAAGACCCAGTGAGTGAGCATGTTACCAAGTGCTGT
616 S G S L V E R R P C F S A L T
1846 AGTGGATCCCTGGTGGAAGGCGGCCATGCTTCTCTGCTCTGACA
631 V D E T Y V P K E F K A E T F
1891 GTTGATGAAACATATGTCCCCAAAGAGTTTAAAGCTGAGACCTTC
646 T F H S D I C T L P E K E K Q
1936 ACCTTCCACTCTGATATCTGCACACTTCCAGAGAAGGAGAAGCAG
661 I K K Q T A L A E L V K H K P
1981 ATTAAGAAACAAACGGCTCTTGCTGAGCTGGTGAAGCACAAGCCC
676 K A T A E Q L K T V M D D F A
2026 AAGGCTACAGCGGAGCAACTGAAGACTGTCATGGATGACTTTGCA
691 Q F L D T C C K A A D K D T C
2071 CAGTTCCTGGATACATGTTGCAAGGCTGCTGACAAGGACACCTGC
706 F S T E G P N L V T R C K D A
2116 TTCTCGACTGAGGGTCCAAACCTTGTCACTAGATGCAAAGAcGCg
721 L A T G S G G G E D N S L I K
2161 TTAGCCACCGGTTCTGGTGGCGGTGAGGATAACAGCCTGATCAAA
736 E N M R M K V V L E G S V N G
2206 GAAACATGCGGATGAAGGTGGTGTCTGGAAGGCAGCGTGAACGGC
751 H Q F K C T G E G E G N P Y M
2251 CACCAGTTCAAGTGCACCGGCGAGGGCGAGGGCAACCCCTACATG
766 G T Q T M R I K V I E G G P L
2296 GGCACCCAGACCATGCGGATCAAAGTGATCGAGGGCGGACCTCTG
781 P F A F D I L A T S F M Y G S
2341 CCCTTCGCCTTCGACATCCTGGCCACATCCTTCATGTACGGCAGC
796 R T F I K Y P K G I P D F F K
2386 CGGACCTTCATCAAGTACCCCAAGGGCATCCCCGATTCTTCAAG

811 Q S F P E G F T W E R V T R Y
 2431 CAGAGCTTCCCCGAGGGCTTCACCTGGGAGAGAGTGACCAGATAC
 826 E D G G V I T V M Q D T S L E
 2476 GAGGACGGCGGCGTGATCACCGTGATGCAGGACACCAGCCTGGAA
 841 D G C L V Y H A Q V R G V N F
 2521 GATGGCTGCCTGGTGTACCATGCCCAGGTCAGGGGCGTGAATTTT
 856 P S N G A V M Q K K T K G W E
 2566 CCCAGCAACGGCGCCGTGATGCAGAAGAAAACCAAGGGCTGGGAG
 871 P N T E M M Y P A D G G L R G
 2611 CCCAACACCGAGATGATGTACCCCGCTGACGGCGGACTGAGAGGC
 886 Y T H M A L K V D G G G H L S
 2656 TACACCCACATGGCCCTGAAGGTGGACGGCGGAGGGCACCTGAGC
 901 C S F V T T Y R S K K T V G N
 2701 TGCAGCTTCGTGACCACCTACCGATCCAAGAAAACCGTGGGCAAC
 916 I K M P G I H A V D H R L E R
 2746 ATCAAGATGCCCCGGCATCCACGCCGTGGACCACCGGCTGGAAAGG
 931 L E E S D N E M F V V Q R E H
 2791 CTGGAAGAGTCCGACAACGAGATGTTCGTGGTGCAGCGGGAGCAC
 946 A V A K F A G L P G G H H H H
 2836 GCCGTGGCCAAGTTCGCCGGCCTGCCTGGAGGGCACCATCACCAT
 961 H H *
 2881 CACCATTGA

7.2.4 pTT5-CysC-Ruby

1 M E T D T L L L W V L L L W V
 1 ATGGAGACAGACACACTCCTGCTATGGGTACTGCTGCTCTGGGTA
 16 P G S T G A T P K Q G P R M L
 46 CCTGGCTCAACCGGAGCTACGCCAAAACAAGGTCCTaGgATGCTG
 31 G A P E E A D A N E E G V R R
 91 GGGGCTCCCGAGGAAGCGGATGCTAACGAGGAAGGCGTCAGAAGG
 46 A L D F A V S E Y N K G S N D
 136 GCCTTGGAATTCGCTGTCTCAGAGTATAATAAGGGTTCCAACGAC
 61 A Y H S R A I Q V V R A R K Q
 181 GCGTATCATAGCAGGGCAATACAGGTTGTACGCGCACGGAAACAA
 76 L V A G V N Y F L D V E M G R
 226 CTCGTGCGCAGGCGTTAACTACTTCTTGGATGTGGAAATGGGACGG
 91 T T C T K S Q T N L T D C P F
 271 ACCaCgTGACCAAGAGTCAGACCAATCTTACCGACTGCCCATTT
 106 H D Q P H L M R K A L C S F Q
 316 CATGACCAACCCACCTTATGAGAAAgGCcTTGTGCAGTTTCCAG
 121 I Y S V P W K G T H S L T K F
 361 ATATATAGCGTACCCTGGAAGGGAACATAGCCTGACGAAGTTT
 136 S C K N A G G G G T G S G G G

406 AGCTGTAAAAACGCTGGTGGAGGCGGCACCGGTTCTGGTGGCGGT
151 E D N S L I K E N M R M K V V
451 GAGGATAACAGCCTGATCAAAGAAAACATGCGGATGAAGGTGGTG
166 L E G S V N G H Q F K C T G E
496 CTGGAAGGCAGCGTGAACGGCCACCAGTTCAAGTGCACCGGCGAG
181 G E G N P Y M G T Q T M R I K
541 GGCGAGGGCAACCCCTACATGGGCACCCAGACCATGCGGATCAAA
196 V I E G G P L P F A F D I L A
586 GTGATCGAGGGCGGACCTCTGCCCTTCGCCTTCGACATCCTGGCC
211 T S F M Y G S R T F I K Y P K
631 ACATCCTTCATGTACGGCAGCCGGACCTTCATCAAGTACCCCAAG
226 G I P D F F K Q S F P E G F T
676 GGCATCCCCGATTTCTTCAAGCAGAGCTTCCCCGAGGGCTTCACC
241 W E R V T R Y E D G G V I T V
721 TGGGAGAGAGTGACCAGATACGAGGACGGCGGCGTGATCACCGTG
256 M Q D T S L E D G C L V Y H A
766 ATGCAGGACACCAGCCTGGAAGATGGCTGCCTGGTGTACCATGCC
271 Q V R G V N F P S N G A V M Q
811 CAGGTCAGGGGCGTGAATTTTCCCAGCAACGGCGCCGTGATGCAG
286 K K T K G W E P N T E M M Y P
856 AAGAAAACCAAGGGCTGGGAGCCCAACACCGAGATGATGTACCCC
301 A D G G L R G Y T H M A L K V
901 GCTGACGGCGGACTGAGAGGCTACACCCACATGGCCCTGAAGGTG
316 D G G G H L S C S F V T T Y R
946 GACGGCGGAGGGCACCTGAGCTGCAGCTTCGTGACCACCTACCGA
331 S K K T V G N I K M P G I H A
991 TCCAAGAAAACCGTGGGCAACATCAAGATGCCCGGCATCCACGCC
346 V D H R L E R L E E S D N E M
1036 GTGGACCACCGGCTGGAAGGCTGGAAGAGTCCGACAACGAGATG
361 F V V Q R E H A V A K F A G L
1081 TTCGTGGTGCAGCGGGAGCACCCGTGGCCAAGTTCGCCGGCCTG
376 P G G H H H H H H *
1126 cctggagggCACCATCACCATCACCATTGA

8. Publications and international meetings

8.1 Publications

Parts of this thesis are published by Scientific Reports - Nature:

Salome Rehm, Natalia Smirnova, Carmela Morrone, Jessica Götzfried, Annette Feuchtinger, John Pedersen, Brice Korkmaz, Ali Önder Yildirim, Dieter E. Jenne.

„Premedication with a cathepsin C inhibitor alleviates early primary graft dysfunction in mouse recipients after lung transplantation’

Parts of this thesis are in preparation for publication:

Salome Rehm, Carmela Morrone, Ali Önder Yildirim , Dieter E. Jenne.

„CatB inhibition has a tissue protective effect during cold ischemic storage and ex vivo lung perfusion of lung transplants’ (manuscript in preparation)

8.2 Presentations at international conferences

8.2.1 Oral presentations

‘Preemptive inhibition of cathepsin C in candidates for transplantation improves early graft functions’, 35nd Winter School on Proteinases and Their Inhibitors. Italy, 2018

‘Preemptive inhibition of cathepsin C in candidates for transplantation alleviates early primary graft dysfunction after lung translantation’, 2nd Cathepsin C Symposium. France, 2019

8.2.2 Poster presentation

‘Preemptive inhibition of cathepsin C in candidates for transplantation improves early graft functions. German French Retreat, France, 2018

9. Curriculum vitae

Personal information

Salome Raffaella Tosca Sofia Rehm

Born 09.02.1990 in Gräfelfing

Education

since 07/2016	PhD Biology, Ludwig-Maximilian University, Munich, Prof. Dr. Elisabeth Weiß PD Dr. Dieter Jenne, Helmholtz-Zentrum Munich
04/2014 – 04/2016	Master of Science Biology (1,2), University of Regensburg Modules: Neurobiology, Immunology, Molecular Human Biolog Master thesis (1,0): Molecular analysis of endothelial TGF- β signalling pathway in the murine retina following oxygen-induced retinopathy
10/2013 – 12/2013	Internship “Dementia Research Unit”, University of New South Wales, Sydney
10/2009 – 07/2013	Bachelor of Science Biology (2,3), University of Regensburg Bachelor thesis at the Department of Behavioural and Molecular Biology, Bachelor thesis (1,3): “Introducing a novel model to study female aggression: Role of anxiety and oxytocin
09/2000- 06/2009	Kurt Huber Gymnasium, Gräfelfing, Abitur

10. Acknowledgement

Most of all I would like to thank my supervisor **PD Dr. Dieter Jenne** for his great guidance, his continual support and for always having an open ear for me. Thank you, for all the time you took to teach me how great science is done. I truly enjoyed and learned a lot through our scientific discussion and I benefited a lot from your vast knowledge and experience.

I am also very grateful to **Prof. Dr. Elisabeth Weiß**, my doctoral thesis supervisor at the faculty of biology at the Ludwig-Maximilians-Universität München, for her valuable suggestions and support during the years. I also want to thank the external expert of my thesis advisory board committee, namely **Prof. Dr. Boris Turk** for his time and his continuous interest in my work.

Many thanks go to our collaboration partners, most of all to **Carmela Morrone** and **Dr. Natalia Smirnova** for their contributions to my lung transplantation projects.

I want to acknowledge the financial support by the **European Union's H2020-PHC-2015** program RELENT (668036).

I dearly want to thank all the members of the Jenne group **Dr. Jessica Götzfried** and especially **Stefanie Weiß** who accompanied me through the whole time, for their support in scientific questions, a great atmosphere in the lab and a lot of fun.

I also benefited greatly from my fellow PhD students and colleagues. Most of all I want to thank **Kristina Arendt** and **Laura Mattner** for the great time together in the lab and outside.

Last but not least, I want to thank my family and my boyfriend for their continuous support and for always being there for me.

Eidesstattliche Erklärung

Ich versichere hiermit an Eides statt, dass die vorgelegte Dissertation von mir selbständig und ohne unerlaubte Hilfe angefertigt ist.

München, den 08.08.2019

Salome Rehm

Erklärung

Hiermit erkläre ich,

- dass die Dissertation nicht ganz oder in wesentlichen Teilen einer anderen Prüfungskommission vorgelegt worden ist.
- dass ich mich anderweitig einer Doktorprüfung ohne Erfolg **nicht** unterzogen habe.

München, den 08.08.2019

Salome Rehm